การเคลื่อนตัวของดินเนื่องจากการขุดค้ำยันในชั้นดินกรุงเทพ

นาย วูที ฮอง

GROUND RESPONSE DUE TO SHEET PILE BRACED EXCAVATION IN BANGKOK SUBSOILS

Mr. Vuthy Horng

Thesis Title   GROUND RESPONSE DUE TO SHEET PILE BRACED
                  EXCAVATION IN BANGKOK SUBSOILS
By   Mr. Vuthy Horng
Field of Study   Civil Engineering
Thesis Advisor   Associate Prof. Wanchai Teparaksa, Dr. Eng.

Accepted by the Faculty of Engineering, Chulalongkorn University in Partial
Fulfillment of Requirements for Master's Degree.

....Dean of the Faculty of Engineering
(Professor Direk Lavansiri, Ph.D.)

THESIS COMMITTEE:

....Chairman
(Associate Professor Boonsom Lerdhirunwong, Dr.Ing.)

....Thesis Advisor
(Associate Professor Wanchai Teparaksa, Dr.Eng.)

....Member
(Assistant Professor Tirawat Boonyatee, Dr. Eng.)

วูที ฮอง : การเคลื่อนตัวของดินเนื่องจากการขุดค้ำยันในชั้นดินกรุงเทพ. (GROUND RESPONSE DUE TO SHEET PILE BRACED EXCAVATION IN BANGKOK SUBSOILS) อ. ที่ปรึกษา: รองศาสตราจารย์ ดร.วันชัย เทพรักษ์, 138 หน้า. ISBN 974-17-5411-6.

ระบบค้ำยันเข็มพืดมีการใช้อย่างแพร่หลายสำหรับงานขุดดินลึกน้อยกว่า 9 -10 ม. ใน ดินเหนียวอ่อนกรุงเทพ พฤติกรรมของระบบค้ำยันเข็มพืดในงานขุดโดยทั่วไปจะประเมินจาก การเคลื่อนตัวด้านข้างของกำแพงเข็มพืดภายใต้แรงดันดินด้านข้าง งานวิจัยนี้ทำการตรวจสอบ พฤติกรรมและประสิทธิภาพของงานขุดดินด้วยระบบค้ำยันเข็มพืดในกรุงเทพมหานคร สำหรับ งานขุดดินลึก 6.90 ม. โดยมีค้ำยัน 3 ชั้นอยู่ที่ระดับ -1.00 ม, -3.25 ม. และ -5.30 ม. และได้มีการ ติดตั้ง Inclinometer ยึดติดกับเข็มพืดยาว 16 ม. จำนวน 3 จุด ผลการตรวจวัดการเคลื่อนตัวของ กำแพงเข็มพืดพบว่า ในช่วงเริ่มต้นของการขุดดินกำแพงเข็มพืดมีพฤติกรรมแบบคานยื่น ในขณะที่ขั้นตอนหลังจากติดตั้งค้ำยันและที่ขั้นตอนสุดท้ายของงานขุดพฤติกรรมของเข็มพืดมี ลักษณะโป่งออกเนื่องจากระบบค้ำยัน จากการควบคุมการติดตั้งระบบค้ำยันทันทีภายหลังการ ขุด สามารถควบคุมให้การเคลื่อนมากที่สุดของกำแพงเข็มพืดเกิดขึ้นที่ระดับความลึกไม่เกิน ระดับขุดดิน

การวิเคราะห์กลับด้วยวิธีไฟไนต์อิลิเมนต์โดยใช้ทฤษฎีการพังทลายของดินแบบ Mohr-Coulomb พบว่าความสัมพันธ์ที่เหมาะสมของอัตราส่วนโมดูลัสของดิน (Eu) และค่า กำลังรับแรงเฉือนของดินแบบไม่ระบายน้ำ (Su) ในขั้นตอนสุดท้ายของงานขุด มีค่าประมาณ 150-250 และ 2000 สำหรับดินเหนียวอ่อนและดินเหนียวแข็ง ตามลำดับ นอกจากนั้นยังพบว่า ดินเหนียวกรุงเทพมีพฤติกรรมของโมดูลัสแบบไม่เป็นเส้นตรง (Non-linear Young's Modulus)โดยขึ้นกับ shear strain ของเข็มพืด ผลการศึกษาในงานวิจัยนี้ได้เสนอให้มีการ ปรับปรุงขอบเขตของความสัมพันธ์ระหว่างอัตราส่วนการเคลื่อนตัวสูงสุดต่อความลึกกับค่า ความปลอดภัยต่อการเกิดการบวมขึ้นของดิน (Heave) ที่ได้จากผลที่เคยทำการศึกษางานขุดดิน ด้วยระบบค้ำยันเข็มพืดในชั้นดินกรุงเทพ

ภาควิชา...............วิศวกรรมโยธา...............	ลายมือชื่อนิสิต..
สาขาวิชา..............วิศวกรรมโยธา...............	ลายมือชื่ออาจารย์ที่ปรึกษา................................
ปีการศึกษา.........2548........	

VUTHY HORNG: GROUND RESPONSE DUE TO SHEET PILE BRACED EXCAVATION IN BANGKOK SUBSOILS. THESIS ADVISER: ASSOC. PROF. WANCHAI TEPARAKSA (DR. ENG.), 138pp. ISBN 974-17-5411-6

The sheet pile bracing system is the most common used for excavation in Bangkok soft marine clay in case of the excavation depth is less than 9-10 m. The lateral sheet pile wall movement caused by lateral earth pressure is often used to evaluate the performance and behavior of sheet pile braced excavation. This research aims to verify the behavior and performance of sheet pile braced excavation of the project in Bangkok city for 6.90-m depth of excavation with three bracing layers at -1.00 m, -3.25 m, and -5.30 m. Three inclinometers were installed fixed to the sheet piles of 16-m depth. The mode of the first excavation shows the sheet pile cantilevered mode, while the later stages of excavation, the mode is shifted to a bulging mode. The maximum lateral sheet pile movements occur around the depth at which excavations are undertaken due to the strict control of installation of struts after excavation.

The back analysis by means of Finite Element Method (FEM) based on Mohr-Coulomb failure envelope shows that the appropriate ratio of Young's modulus (E_u) and undrained shear strength of soil at the final excavation stage are in the order of 150-250 and 2000 for soft clay and stiff to very stiff silty clay. The behavior of Bangkok clay shows the nonlinear stress-strain-strength behavior depending on the order of shear strain of sheet pile wall. Based on case histories of sheet pile excavation work in Bangkok subsoil, the modified boundary of relationship between maximum deflection ratio and factor of safety against basal heave is proposed.

Department...Civil Engineering......Student's signature......................................
Field of Study...Civil Engineering...Adviser's signature....Wanchai Tepn.....
Academic Year.........2005...................

ACKNOWLEDGEMENTS

TABLE OF CONTENTS

LISTS OF FIGURES

LISTS OF TABLES

CHAPTER I

INTRODUCTION

1.1 Generality

Many major cities in the newly industrialized countries, such as Bangkok, Singapore, are located in areas with recent sedimentary deposits. Due to economic development, urban planning, tourist and population increasing in the last few decades, many construction projects of high-rise building complex, infrastructures and other construction facilities are becoming one of the most important activities. During the recent years of the development, the land has become limited; its price has exponentially increased. Couple with the solution to the traffic congestion and for the beauty of the city, Bangkok Metropolitan Administration (BMA) requires both designers and constructors to find the way for the area of car parking in the buildings constructed. As a result, underground construction projects cannot be avoided.

Deep excavations in soft clay deposits are usually conducted for several purposes, namely basements for tall buildings and stations for subways. Owing to the poor characteristics of soft ground, e.g. low strength, high compressibility, nonhomogeneity, and anisotropy, etc., deep excavations in the soft ground require special attention in both design and construction.

Soft Bangkok clay is so well-known for its poor characteristics and engineering properties that Bjerrum decided to include the soft clay in the Norwegian Geotechnical Institute's continuous research program on soft clays (Holmberg, 1977).

At the present times, four kinds of supporting systems have been used in Bangkok subsoil: 1. Sheet-pile walls, 2. Diaphragm wall with top-down construction technique, 3. Diaphragm wall with internal temporary bracing with bottom-up construction technique, and 4. Jet-grouted wall (Gravity wall).
At the beginning of the deep excavations in soft Bangkok clay in the 1970s, excavations were only carried down to depth less than 5m and only to construct one basement floor. Some of them were reported to meet so many problems and some others were unsuccessfully constructed (Sambhandharaksa, 1989).

1.2 Purpose

The sheet pile bracing system is widely used for deep excavation in the Bangkok soft clay. The popularity of the sheet pile bracing system is that: 1. the cost of its construction is relatively cheaper; 2. its construction does not require special procedures and equipments; 3. sheet piles are lightweight and reusable.

Due to the fact that braced steel sheet pile wall is a low stiffness earth retaining structures, braced sheet pile walls selected for excavation works at a great depth (more than 10m) in the Bangkok soft clay will result in large lateral movement and this lateral movement will result in large surface settlement and this settlement is the cause of damages to adjacent structures. Alternatively, to prevent or minimize such damages, the construction of diaphragm wall is introduced even though it is relatively expensive and difficult to construct. Instrumentations for diaphragm wall are more available than those of sheet pile bracing system, because instruments of diaphragm wall are cheaper compared to its system. For sheet pile bracing system, only few data are available. The researches on this aspect are relatively less dominant even though it can cause colossal damages to the adjacent structures.

It is, therefore, the purpose of this thesis to conduct further research on sheet pile braced excavation system. The objectives of this research are:

1-To conduct back analysis to determine the soil stiffness, Eu/Su.
2-To evaluate the performance of sheet pile bracing system by analyzing recorded data of excavation project in Bangkok City.
3-To investigate some factors affecting lateral deformation or movement of the braced cut.
4-To analyze and determine the field behaviors of sheet piles.
5-To plot some important graphs for design and analysis.

1.3 Scope of study

This research is involved in sheet pile bracing system in deep excavation in soft Bangkok clay. Two steps are done: First, inclinometer data in this research project was collected. Second, the analyses and comparisons were conducted based on numerical methods (Finite Element Method) in 2-D PLAXIS program.

CHAPTER II

LITERATURE REVIEW

This chapter thoroughly demonstrates the theoretical developments for deep excavation and some recent researches in theses, journals, proceedings, conferences, etc. The evolution of theories and applications of deep excavations in Bangkok city is described as well.

2.1 Types of excavation and supporting system

2.1.1 Unsupported excavation

The excavations are needed for most structures in construction industries. The excavations can be done without supporting the surrounding material if the depth of the excavations is shallow and if there is adequate space to establish slopes at which the materials can stand. The steepness of the slopes is a function of several factors (Peck, 1969) such as, the type and characteristics of soil, the climatic and weather conditions, the depth of the excavation, and the length of time the excavation must remain open.

If the soft clay is below the base level of the excavation, flat slopes may be required to avoid the heave of the bottom. In case of stiff or hard clays, the clays are known to commonly possess or develop cracks near the ground surface. If these cracks become filled with water, the hydrostatic pressure greatly reduces the factor of safety of the slopes progressively so that the safety of the slopes is likely to decrease with time. The unsupported excavations are vulnerable to failure when a site subjects to heavy vibration, e.g. near heavy traffic zones.

For these reasons, bracing is often used to support the sides of excavations in clay, even though the clay would stand briefly to the necessary height without lateral support.

2.1.2 Sheeting and bracing for excavation

Several construction sites situate near the edges of the property lines or adjacent to other sites on which structures already exist. Under these circumstances, the sides of the excavations must be made supported; and the supporting excavations would be braced or unbraced according to the depth of our excavations.

When the depth is under about 3m sheet pile is usually cantilevered (Bowles, 1997). The sheet pile is called cantilever sheet pile wall. When the depth is deeper than 3m, bracings are needed. Such underground structures are called sheeting or bracing systems of excavations.

2.1.3 Types of sheeting wall and bracing

Until the late 1960s, two types of walls were used in excavations. The two walls are soldier beams and laggings and braced sheet piles with rakes (or rakers). We use rakes (or rakers or inclined struts) when the excavation is too wide for the use of struts extending across the entire width and if the soil in the base of excavation is firm enough to provide adequate support for the inclined members. An alternative to cross bracing and rakes is tieback. The resulting wall is termed an anchored sheet-pile wall or anchored bulkhead. Since the late 1960s there have several wall types, such as diaphragm wall, bored pile wall, jet-grouted wall, etc. In Bangkok, currently, the most common types are steel sheet piles with steel wales and steel struts and the diaphragm walls (Teparaksa, 1999).

2.1.4 Materials for sheet piling

Sheet piling materials is normally made of steel. However, it can be made of timber, reinforced concrete, or composite.

- Timber sheet piling

Timber sheet piling is sometimes used for free-standing walls of height H<3m. It is more often used for temporarily braced sheeting to prevent trench cave-ins during installation of deep water and sewer lines. If timber sheeting is used in permanent structures above water level, preservative treatment is necessary, and even so the useful life is seldom over 10 to 15 years (Bowles, 1997).

- Reinforced concrete sheet piling

These sheet piles are precast concrete members, usually with a tongue-and-groove joint. The relatively large sizes, coupled with the high unit weight (γ_c=24 kN/m^3) of concrete mean that the piles are quite heavy and may not be competitive with other pile types unless they are produced near the sites.

- Steel sheet piling

Steel sheet piling is the most common type used for walls because of several advantages over other materials:
1. It is resistant to the high driving stress developed in hard soil.
2. It is relatively lightweight.
3. It can be reused several times.
4. It has a long life above or below water if it is provided with modest protection.
5. It is easy to increase the pile length by either welding or bolting. If the full design length cannot be driven, it is easy to cut the excess length.

6. Joints are less apt to deform when wedged full with soil and small stones during driving.

7. A nearly impervious wall can be constructed by driving the sheeting with a removable plug in the open thumb-and-finger joint.

- Composite sheet pile walls

For corrosion protection, we might encase the upper part of steel sheet piling in concrete after it is driven, with the concrete extending from below the water line to the pile top.

2.2 Deep excavations in soft Bangkok clay

Internally braced excavation is the only supporting method in Bangkok clay. Struts are used, but anchorages have not been successfully used. Regulations also prevent the use of anchorages especially in the thick soft clay deposits. These days, there are two kinds of commonly used retaining structures for deep excavations in Bangkok: steel sheet piles and diaphragm walls.

2.2.1 Steel sheet piles in soft Bangkok clay

Sheet pile bracing system (flexible retaining structures) is commonly used for general basement excavation of about 9-m depth. This depth limitation is due to the induce of large lateral movement of sheet pile and that deformation will induce the damages to the nearby structures (Teparaksa, 1993). Due to its low cost, it is also used for more than 11m excavation, for example in the project of Baiyoke II, which is the highest skyscraper in Bangkok city. It is the 89-story building with 11.3-m deep excavation for construction of basement and mat foundation. The flexible wall sheet pile bracing system with effectively preloading strut system was first introduced by Dr. Wanchai Teparaksa of Chulalongkorn University for deep excavations in very soft Bangkok clay.

The sheet piles used in Bangkok are usually 16 to 18m long with 1-2m penetration into the underlying stiff clay and have 10-mm thickness. These sheet piles consist of steel section connected by interlocks. Jet-grouting is sometimes applied to reduce lateral deformation (Moh and Chung, 1994). The construction sequence and its serviceability were summarized by Srichaimongkol (1991).
For the depth exceeds 10 meters, the rigid retaining structures such as diaphragm walls, secant pile walls and Berlin walls are used.

2.2.2 Diaphragm walls in soft Bangkok clay

Diaphragm wall, 0.8m to 1m in thickness, is generally used for deep excavations in Bangkok with the depth between 12-35m. There are many diaphragm wall activities under construction, for example the first blue line subway project of Metropolitan Rapid Transit (MRT). This subway project

consists of 18 underground stations. Excavation depth for the underground stations is between 22-33m (Teparaksa, 1999).

Conventional method and top-down method have been used. The tips of the diaphragm walls are usually in the stiff clay or sand (18 to 36m). Strut spacing is about 5m and 2 to 4 (some 5) levels are used.

There are two reasons for the success of the fast developments for the using of diaphragm wall technique throughout the world: First, the service of deeper basement and optimization of the site dimension and the space availability. Second, the cost per square-meter of excavation decreases in terms of money-value (Salvi, 1991).

The flexural rigidity of the diaphragm wall (much higher than sheet pile) will minimize deformations while withstanding high bending moments.

2.3 Bangkok subsoil Conditions

The general Bangkok subsoil conditions reported by Teparaksa (1999) and based on Bangkok MRT project are presented in Figure 2.1.
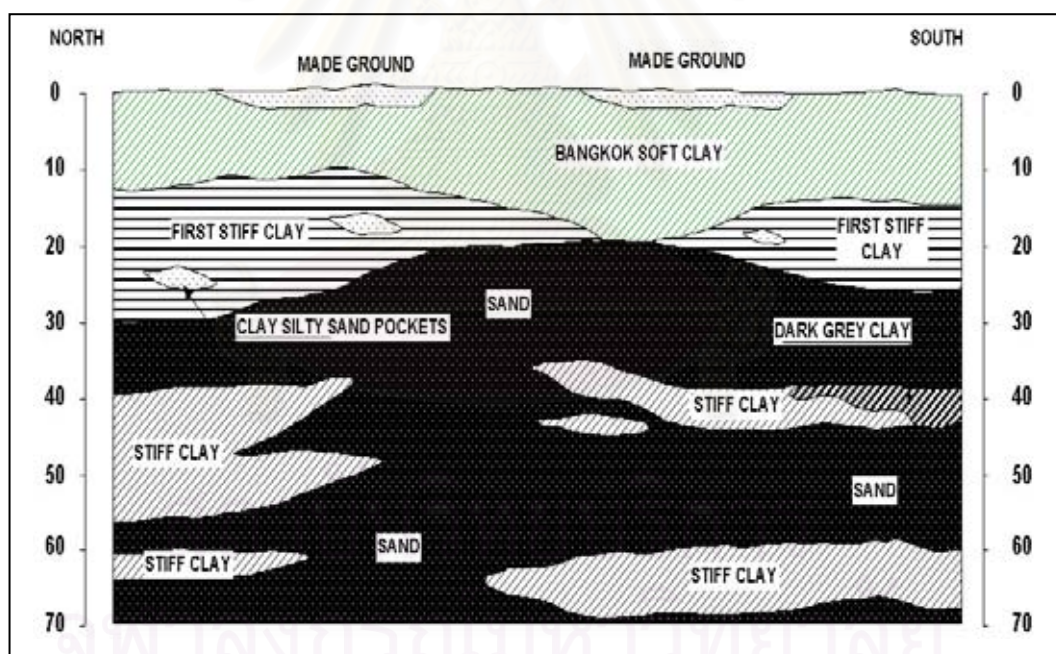
Figure 2.1 General subsoil profile (Teparaksa, 1999)

The Bangkok subsoils consist of the depth of 0-13m of soft marine clay on top. This clay is sensitive, anisotropic and creep (time-dependent stress-strain-strength behavior). These characteristics have made difficult the design and construction of deep basements, filled embankments and tunneling in soft clay. The first stiff to

stiff silty clay layer is encountered below soft clay and medium clay varying to 21m to 28m depth. This first stiff silty clay having low sensitivity and high stiffness is appropriate to be the bearing layer for underground structures. The first dense silty sand layer locating below stiff silty clay layer at 21-28 m depth contributes to variations in skin friction and mobilization of end bearing resistance of pile foundations constructed with different piling methods (dry and wet processes). The similar variations are also contributed by the second dense and coarse silty sand found at about 45-55 m depth.

The groundwater condition of the soft Bangkok clay is hydrostatic starting from 1 m below ground level. Deep well pumping from the aquifers has led to drainage of the soft clay and the first stiff clay. The piezometric level or the phreatic surface of the Bangkok aquifer is reduced and quite constant at about 23 m below ground surface as shown in Figure 2.2. This low piezometric level contributes to the increase in effective stress, causing ground subsidence.

However, the benefit of this low piezometric level is that it is easy to construct bored piles having pile tip in the first stiff clay using dry process and dry excavation for basement construction up to the silty clay level without any dewatering or pumping system (Teparaksa, 1999).
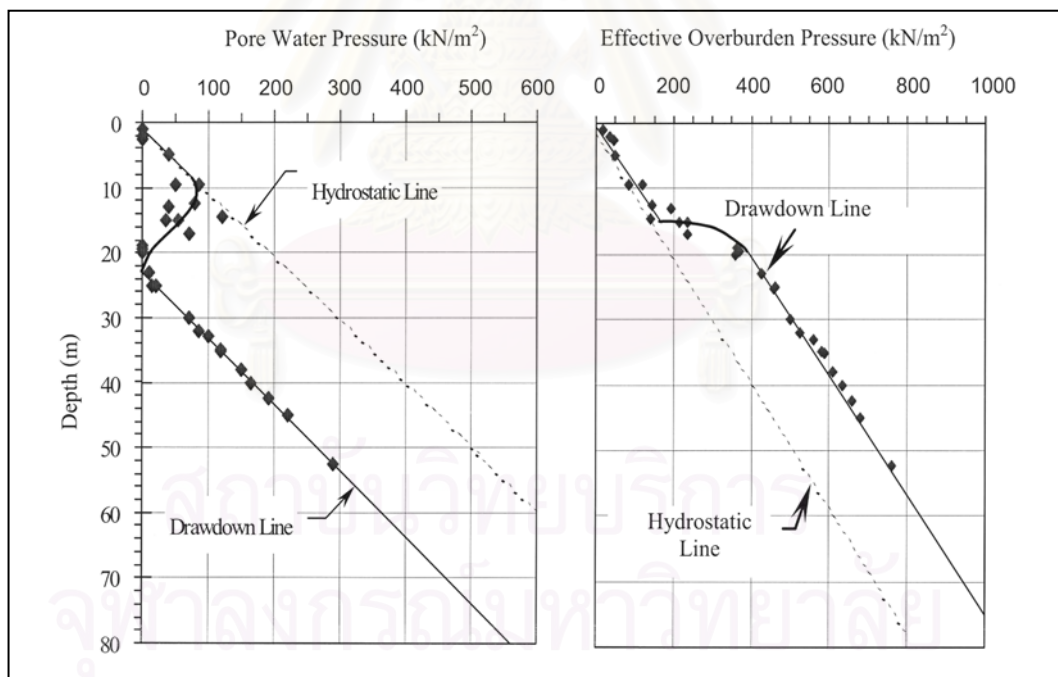
Figure 2.2 Piezometric level of Bangkok subsoils (Teparaksa, 1999)

2.4 Lateral earth pressure

The design of the sheet-pile wall bracing system requires a calculation of lateral earth pressure, which is a function of several factors such as 1) the type and amount of wall movement, 2) the shear strength parameters of the soil, 3) the unit weight of the soil, and 4) the drainage conditions of the backfill.

2.4.1 Lateral earth pressure at rest

At any depth z below the ground surface, the overburden stress is:

$$\sigma_o' = q + \gamma'z \qquad (1)$$

where   q = surcharge (force/unit area)
γ = unit weight of soil

If the wall is not allowed to move, the lateral earth pressure at depth z is:

$$\sigma_h = K_o\sigma_o' + u \qquad (2)$$

where   u = pore water pressure
K_o = coefficient of at-rest earth pressure

For sand, according to Jaky (1944), Ko can be calculated by:

$$K_o = 1 - \sin\phi' \qquad (3)$$

ϕ' = drained peak friction angle

According to Brooker and Ireland (1965), K_o for normally consolidated clays may be correlated with the plasticity index (PI) by the relationships:

$$K_o = 0.4 + 0.007 \times PI\ (\%) \qquad \text{for } 0 < PI < 40\%$$
$$K_o = 0.64 + 0.001 \times PI\ (\%) \qquad \text{for } 40 < PI < 80\%$$

For overconsolidated clays, K_o can be calculated by:

$$K_o(\text{overconsolidated}) \approx K_o(\text{normally consolidated}) \times \sqrt{OCR} \qquad (4)$$

where OCR = overconsolidated ratio

For soft Bangkok clay:
PI $\approx$ 36 – 40%
So $K_o = 0.4 + 0.007 \times (38) = 0.67$

2.4.2 Rankine active pressure

If a wall tends to move away from the soil, the soil pressure on the wall at any depth will decrease.

Using the plastic equilibrium (state at which every part of soil is on the verge of failure) and a Mohr's circle that touches the Mohr-Coulomb failure envelope, the Rankine active pressure, σ_a' is:

$$\sigma_a' = \sigma_o' \tan^2(45° - \phi'/2) - 2c'\tan(45° - \phi'/2) \tag{5}$$

$$\sigma_a' = \sigma_o' K_a - 2c'\sqrt{K_a} \tag{6}$$

where $K_a = \tan^2(45° - \phi'/2) =$ Coefficient of Rankine active earth pressure

$c' =$ cohesion

$\sigma_o' =$ overburden pressure

At z=0 m, the Rankine active pressure in equation (6) becomes, $\sigma_a' = -2c'\sqrt{K_a}$, indicating the tensile stress that decreases with depth and becomes zero at a depth $z = z_c$, or setting σ_a' in equation (6) equals zero,

$$\gamma z_c K_a - 2c'\sqrt{K_a} = 0$$

So

$$z_c = \frac{2c'}{\gamma\sqrt{K_a}} \tag{7}$$

$z_c =$ the depth of tensile crack

The total Rankine active force per unit length of the wall before the tensile crack is:

$$P_a = \int_0^H \sigma_a' dz \tag{8}$$

2.4.3 Rankine passive pressure

If the wall is pushed into the soil mass, the vertical stress at any depth z will stay the same, however, the horizontal stress will increase. From a Mohr's circle that the Mohr-Coulomb failure envelope, the Rankine passive pressure, σ_p', is:

$$\sigma_p' = \sigma_o' \tan^2(45° + \phi'/2) + 2c'\tan(45° + \phi'/2) \tag{9}$$

$$\sigma_p' = \sigma_o' K_p + 2c'\sqrt{K_p} \tag{10}$$

where $K_p = \tan^2(45 + \Phi'/2) =$ Coefficient of Rankine passive earth pressure

$c' =$ cohesion

$\sigma_o' =$ overburden pressure

The total Rankine passive force per unit length of the wall is:

$$P_p = \int_0^H \sigma_p' dz \tag{11}$$

2.5 Pressure envelope for braced excavation

2.5.1 Conventional method

No exact theoretical developments of strut-load magnitudes have been found since the beginning of soil mechanics history. Since it is not possible to predict which struts will experience the greatest loads, conventional method conservatively converts the strut loads to apparent pressure envelope (apparent pressure envelope is a fictitious pressure distribution for estimating the maximum strut loads in a system of bracing).

In the method, each strut is designed for the maximum load to which it may be subjected, and apparent pressure envelope can be drawn from the strut loads, which are measured from in the field.

Figure 2.3 shows the conventional method for obtaining the apparent pressure envelope from measured strut load.
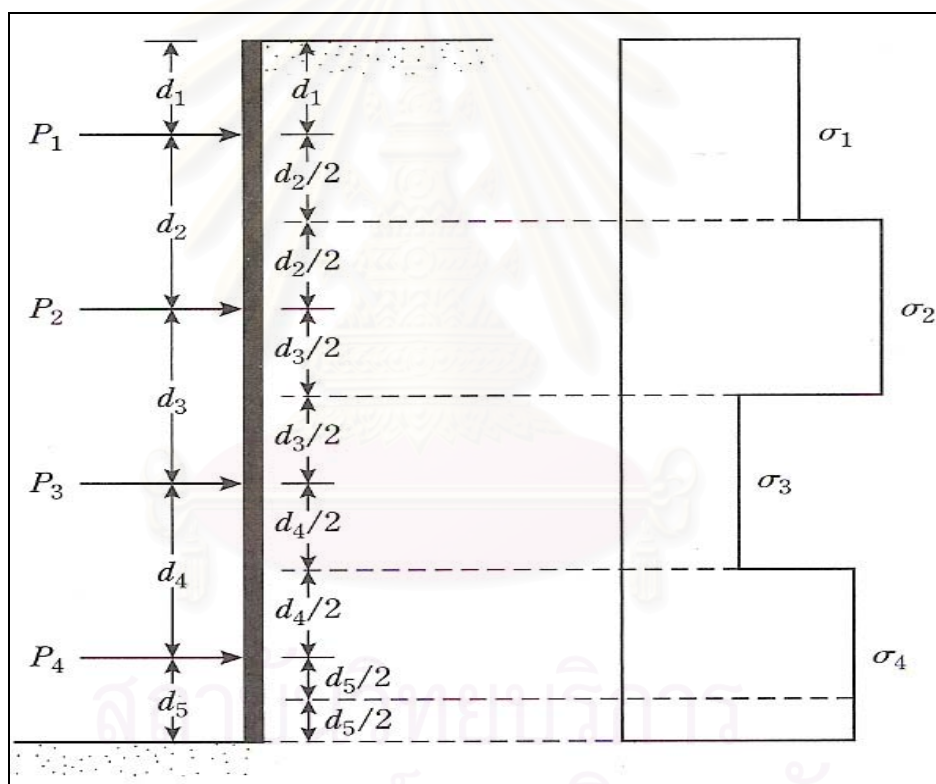
Figure 2.3 Procedure for calculating apparent pressure
diagram from measured strut load (Das, 2004)

In this figure P_1, P_2, P_3, P_4 . . . are the measured strut loads.
The horizontal pressure can then be calculated as follows:

$$\sigma_1 = \frac{P_1}{s(d_1 + \frac{d_2}{2})} \qquad , \qquad \sigma_2 = \frac{P_2}{s(\frac{d_2}{2} + \frac{d_3}{2})}$$

$$, \sigma_4 = \frac{P_4}{s(\frac{d_4}{2} + \frac{d_5}{2})} \quad , \qquad \sigma_3 = \frac{P_3}{s(\frac{d_3}{2} + \frac{d_4}{2})} \quad \ldots\ldots$$

where $\sigma_1, \sigma_2, \sigma_3, \sigma_4, \ldots\ldots$ = apparent pressure

$\quad$ s = center-to-center horizontal spacing of the struts

2.5.2 Peck's apparent pressure

$\quad$ Observing from the Berlin subway excavation, Munich subway excavation, and New York subway excavation, Peck (1969) used the conventional method described in section 2.5.1 to draw the envelope of apparent pressure diagrams as follows:

- Apparent pressure envelope for excavations in sand:

$$\sigma_a' = 0.65\gamma H K_a$$

where γ = unit weight of soil

$\quad$ H = depth of excavation

$\quad$ K_a = Rankine active pressure coefficient = $\tan^2(45° - \phi'/2)$

$\quad$ Φ' = effective friction angle of sand

Therefore, it is observe that the apparent earth pressure σ_a' for excavation in sand is equal to 65% of the Rankine active pressure.

This envelope is illustrated in figure 2.4.
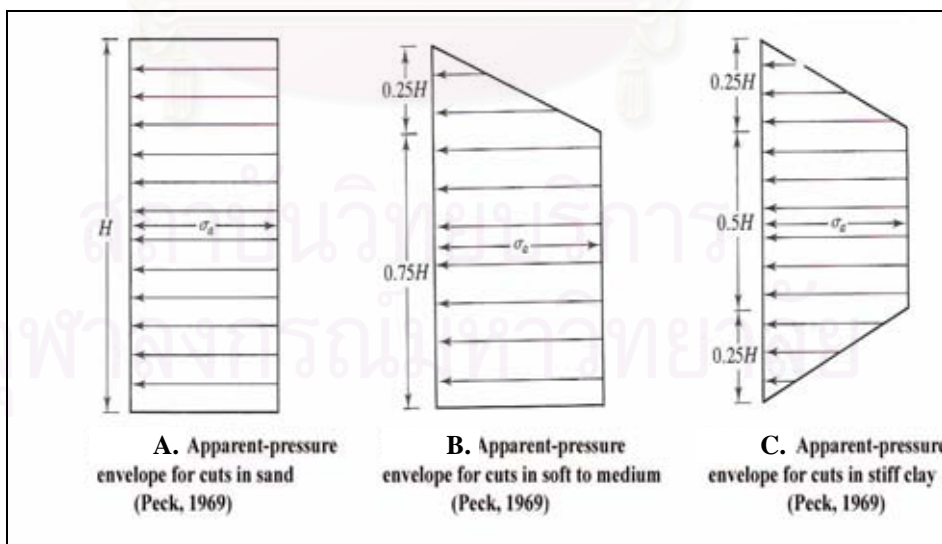
Figure 2.4 Apparent-pressure envelopes (Peck, 1969)

- Apparent pressure envelope for excavations in clay:

Peck (1969) also developed the method for designs of the envelope of apparent lateral pressure for excavations in clay by using the same procedures as those in sand. According to Peck, the apparent pressure envelope depends on the dimensionless number $\dfrac{\gamma H}{c}$, where c is the average undrained shear strength of the clay alongside the cut.

If $\dfrac{\gamma H}{c} \leq 4$, the magnitude of the apparent pressure envelope can be considered equal to 0.3γH. The behavior of the clay beside the excavation is essentially elastic and the load in the struts depends primarily on the deflection on the sheeting permitted during excavation and bracing. The lateral pressure in this case linearly increases from 0 to 0.3γH from the depth of uppermost excavation to 0.25H, then the pressure of 0.3γH remains constant until the depth of 0.75H, and then the pressure linearly decreases from 0.3γH to 0 from the depth of 0.75H to the lowermost excavation.
Figure 2.4(C) shows the case.

If dimensionless number $\dfrac{\gamma H}{c} > 4$, the magnitude of the apparent pressure envelope can be considered equal to ($\gamma H - 4c$). The increased value of $\dfrac{\gamma H}{c}$ is associated with inelastic behavior of the clay near the bottom of the excavation. Figure 2.4(B) shows this case. The diagrams of the lateral earth pressure may be used for values of $\dfrac{\gamma H}{c}$ as great as 10 or 12. On other hand, if the stability number $\dfrac{\gamma H}{c_b}$, where c_b is the undrained shear strength of soil below base level, is bigger than about 7 and base failure is imminent, the strut load may be much larger than indicated by the diagrams.

When several clay layers are encountered in the excavation, the average undrained cohesion can be calculated as:

$$c_{ave} = \frac{1}{H}(c_1 H_1 + c_2 H_2 + c_3 H_3 + ... + c_n H_n)$$

where c_1, c_2, c_3 … c_n = undrained shear strength in layers 1, 2, 3… n

The average unit weight is:

$$\gamma_{ave} = \frac{1}{H}(\gamma_1 H_1 + \gamma_2 H_2 + \gamma_3 H_3 + ... + \gamma_n H_n)$$

The apparent pressure envelopes above can be used with some assumptions as follows:

1). They applied to excavations having depths greater than about 6m.
2). Sand is assumed to be drained with zero pore-water pressure.
3). Clay is assumed to be undrained and pore-water is not considered.
4). The water table is assumed to be below the bottom of the excavation.

2.6 Bottom heave of an excavation in clay

When a braced excavation is constructed in soft clays, the clays may flow beneath the braced sheet pile walls into the excavation. The soil flow gives a rise in the base elevation that is generally termed as heave. In a braced excavation in soft clays, the weight of the soil surrounding the edge of the excavation acts like a surcharge on the soil at the level of the bottom of the cut and develops lateral forces in the subsoils. There are four noticeable researchers on this field: Terzaghi (1943), Bjerrum & Eide (1956), Teng (1981), and Chang (2000).

- Terzaghi method

Terzaghi (1943) analyzed the factor of safety (FS) of long braced excavations against bottom heave. The failure surface for the analysis in clay is illustrated in figure 2.5. The base of soil column efij adjoining the excavation is assumed to act as a footing. The sliding surface consists of a circular arc extending from the $45°$ isosceles plastic wedge fgh to the base of the footing and a vertical sliding plane ij extending to the ground surface. The factor of safety (FS) is defined as the ratio of the bearing capacity to the net vertical pressure at the base of the soil column fi.

Figure 2.5 Heaving in braced cuts in clay

In this figure:

B = width of excavation

H = depth of excavation

T = thickness of the clay below the base of excavation

q = uniform surcharge

c = cohesion

$B' = T$ or $\dfrac{B}{\sqrt{2}}$ (whichever is smaller)

$B'' = \sqrt{2}\, B'$

$Nc = 5.7$

$FS = \dfrac{q_u}{q}$

$q_u = c \times Nc$

$q = \gamma H + q(\text{surch\,arg}\,e) - \dfrac{c \times H}{B'}$

$$\boxed{FS = \dfrac{c \times Nc}{\gamma H - c \times H / B' + q}} \qquad (12)$$

For an excavation of limited length (L), a modification factor $(1+0.2B'/L)$ can be applied to Nc in equation (12):

$$\boxed{FS = \dfrac{c \times Nc \times (1+0.2B'/L)}{(\gamma + q/H - c/B')H}} \qquad (13)$$

- Teng method

In his analysis, he assumed that horizontal length $B_1 = D_1$ (figure 2.6) or $\dfrac{B}{\sqrt{2}}$ whichever is smaller. The net passive earth pressure is equal to $2Su_1$. He neglected the weight of soil below the line **be** on both sides. He also included the effects of surcharges, cracked-tensioned height, and effect of hard stratum. With the above assumptions, he used moment equilibrium about point **b** as follows:

$$H_{cr} = \dfrac{2Su_1}{\gamma}$$

where $Su_1 =$ undrained shear strength about the depth of excavation

$\gamma =$ unit weight above the depth of excavation

Figure 2.6 Heaving in excavation by Teng (1981)

$$S = Su_1 \left(H - \frac{2Su_1}{\gamma} \right)$$

$$\text{Resisting moment} = S \times B_1 + \left(Su_2 \times \frac{\pi}{2} B_1 \right)(B_1) + (2Su_2 \times B_1)\left(\frac{B_1}{2} \right)$$

$$\text{Acting moment} = \left[(q + \gamma H) \times B_1 \right] \times \left(\frac{B_1}{2} \right)$$

$$FS = \frac{Re\,sisting.Moment}{Acting.Moment}$$

$$FS = \frac{2Su_1 \left(H - \dfrac{2Su_1}{\gamma} \right) + 5.14Su_2 B_1}{(q + \gamma H) \times B_1} \tag{14}$$

If the soil above the line **bc** is granular, the shear resistance is:

$$S = \frac{1}{2} K_a \gamma H^2 \tan \phi$$

The formula FS above can be used if $\dfrac{H}{B} \leq 1$ and L is very long.

In case of square, rectangular, or circular excavation or in case of $\dfrac{H}{B} \geq 1$, Teng recommended using FS of Bjerrum & Eide (1956), that is:

$$FS = \frac{cN_c}{\gamma H + q} \qquad (15)$$

N_c = bearing capacity factor

- Method of Chang

Chang (2000) analyzed some cases records compiled by Bjerrum and Eide (1965) for the bottom cuts in clays in Oslo, Drammen, and Chicago. Chang suggested that the value of $\dfrac{c \times H}{B'}$ in the denominator of the FS of Terzaghi method should be put in the numerator and the ultimate bearing capacity at the base of a soil column with the width of B' should be equal to $5.14(1 + \dfrac{0.2 \times B''}{L})$.

Hence

$$FS = \frac{5.14c\left[1 + 0.2\left(\dfrac{B''}{L}\right)\right] + \dfrac{c \times H}{B'}}{\gamma H + q} \qquad (16)$$

- **Limit analysis by Chang**

Chang (2000) used the concept of plastic flow in the soil around a footing of Terzaghi and Peck (1948). The concept reveals that the mechanism beneath a surface footing is affected by the roughness of the contact surface of the footing. Chang used the upper bound limit analysis method of Chen (1975) for a direct analysis of the collapse height of the excavation, and subsequently the factor of safety against basal heave. The upper bound limit theorem, the rate of external work should be equal to the rate of internal energy dissipation in a system in a stability problem.

Figure 2.7 Limit Analysis Based on Sliding Mechanism (Chang, 2000)

Using the upper bound limit theorem for the figure 2.7, the critical height H_{cr} and FS are:

$$H_{cr} = \frac{5.14Su}{\left(\gamma - \dfrac{Su}{B'}\right)} \tag{17}$$

$$FS = \frac{5.14Su\left(1 + 0.2\dfrac{B''}{L}\right) + Su\left(\dfrac{H}{B''}\right)}{\gamma H + q_s} \tag{18}$$

where $B'' = \sqrt{2}T$, if $T \le \dfrac{B}{\sqrt{2}}$

$B'' = B$, if $T > \dfrac{B}{2}$

B = width of excavation
L = length of excavation
q_s = surcharge

2.7 Influence factors on wall movement in sheet pile wall

Deep excavations in soft clay can cause large lateral displacements and large settlements of the ground surrounding the excavation. Surrounding buildings can be damaged if the settlements are not well controlled. The magnitude of

ground movements depends on several influence factors such as soils' shear strength , ground water condition, excavation geometry, excavation sequence, duration of excavation, surcharge condition, existence of adjacent structures, construction method, type and method of installation of lateral support, spacing and stiffness of struts, strut preloading, depth and width of excavation, dewatering, the depth from the bottom of excavation to the hard stratum, the stability number $\dfrac{\gamma H}{c_b}$, depth of sheet pile embedment, workmanship, traffic loading, etc. There are more than ten factors that influence the wall displacement. Therefore, it is difficult to curb the displacement.

Some of the factors are described below.

2.7.1 Soil's properties

According to Peck (1969), the strength of the clay beneath the bottom of the cut at any given level of excavation has a decisive influence on the wall movement. His experience has demonstrated that if $\dfrac{\gamma H}{c_b}$, where c_b undrained shear strength below base level, is less than 6, movements of the sheet pile wall below the base level are small. If $\dfrac{\gamma H}{c_b}$ reaches about 8, the movements of even a well-designed bracing system become intolerably large. If $\dfrac{\gamma H}{c_b}$ is bigger than 8, the bracing system is likely to collapse because of large inward movements.

Vazari and Troughton (1992) showed that Young's modulus of the soil has a significant influence on the displacement. Decreasing Young's modulus from 10 to 5 kPa results in about 75% increase in displacement and increasing it from 10 to15 kPa results in about 40% reduction in displacement for the case of cantilevered wall with a 3.2-m excavation. Reducing friction angle Φ by a factor of 1.2 results in about 20% (at the top) to 40% (at the bottom) increase in the wall deflection.

Based on numerical experiment models, Potts and Fourie (1984) found that Ko value has an important effect on ground movement. Higher Ko value has larger movements calculated from limit equilibrium method.

Clough and Hansen (1981) showed that the importance of including clay anisotropy effects when estimating deformations for cases in which the factor of safety against the basal heave is less than 1.5.

2.7.2 Depth of embedment of sheet pile

Peck (1969) found that the portions of the sheet piles embedded below the bottom of the excavation reduce the inward movement associated with the last stages of excavations.
Mana and Clough (1981) analyzed field records on several excavation sites. They correlated the maximum lateral wall deflection (δ_{Hmax}) and the embedment. If the clay has N ($=\dfrac{\gamma H}{c_b}$) <6, the extension of the sheet pile below the excavation base has considerable effect to restrain lateral deflection. While the clay has N>8, the sheet pile embedment has small effect on lateral deflection.

2.7.3 Preloading (or prestressing)

To reduce the general movements of the bracing system as much as possible, Peck (1974) suggested that struts should be stressed as soon as they are installed. Prestressed loads about 40% and 70 % of the anticipated maximum strut load are usual.

O'Rourke (1981) reported that to close the contact struts and retaining system, hydraulic pressure is applied to the struts to induce rigid contact. The applied pressure may be 20 to 50% of apparent earth pressure.

Satabutr (1992) confirmed that preloading in eliminating deflection of retaining system but acute changes due to high preloading should be carefully studied, and that the behavior of preloading on flexible and rigid walls has different deformation characteristics.

For braced excavation in Bangkok subsoils, the lateral deflection shows an inward bulging shape to excavation side, however, the wall deflection was forced back due to applied preloading in the strut, and the maximum wall movement was reduced about 80% (Teparaksa, 1994). At the final excavation, higher preloading gains little benefits and may cause concentration of loads on some struts.
Although introduction of such large axial force to struts will require prudent planning and precise construction work, if the preloading method is adopted, it is possible to considerably prevent subsidence in the surrounding ground caused by the flexure of the earth holding walls, to increase rigidity of the steel earth holding works as a whole, to reduce the numbers of braces, etc. to be provided in the horizontal plane, and also to provide the larger working space. Owing to the advantages, efficiency in the excavation work as well as other related work will be increased.

2.7.4 Strut spacing

Peck (1974) stated that inward lateral movements increase with increasing vertical distance between struts. He further stated that if the movements are likely to be excessive, the distance between struts should be restricted and excavation should be permitted no deeper than necessary to permit installation of each of the struts. In plastic clays, he said, to keep the movements to a minimum, the vertical between struts should not exceed $\dfrac{2c}{\gamma}$, where c is the average shear strength of the clay for the depth of about B/2 below the level of the preceding strut, and B is the width of the excavation.

2.7.5 Time effect

Peck (1974) stated that if the excavation remains open for a long time, the stability might be reduced. He suggested that excavations should be done quickly with respect to the rate at which the water content of the clay can adjust to the new stress condition.

Som (1991) found that much problem could be avoided if the work is done fast and without any loss of continuity. Som studied the effect of time from the observed ground settlement data where cuts had been kept open at any depth for long period. The data gave the additional settlement that occurs as a function of time when a cut is left open at a particular level. From the data, he observed that the settlement increased rapidly with time, and, in 150 days, nearly 50% of additional settlement occurs which could be avoided if construction was done without any hold-up. Adequate planning and construction control are, therefore, necessary to ensure trouble free construction in the shortest possible time. Proper co-ordination, he said, between the excavation, placing of struts, and construction of underground structures is necessary to ensure that the different activities follow the desired sequence without undue loss of time at any stage.

2.7.6 Effect of hard stratum and wall stiffness

Peck (1974) found that if the bottom of the excavation is underlain at a shallow depth by a firm stratum, the tendency for a bearing capacity failure is greatly reduced. The lateral wall movement can also be decreased by driving piles around the boundary of the cut until they are firmly embedded in the underlying hard stratum. He further stated that large lateral movement occurs even if the pile sheeting is comparatively stiff and extends to a considerable distance below the bottom of the excavation, unless a firm base exists within the short distance below the bottom of the excavation.

Golberg et al. (1976) discussed the effects of the wall stiffness on resulting soil movements with comparable wall spacing; concrete walls are generally stiffer than soldier piles or sheet-pile walls. However, soldier piles and sheet pile walls

with closely spaced levels may be stiffer than concrete walls with widely spaced levels. By studying case histories, Goldberg et al. stated that deformations are a function of both soil strength and wall stiffness.

Mana and Clough (1981) also proposed that the movements depend upon wall and strut stiffness.

Wong and Broms (1989) stated that a hard stratum and wall stiffness can reduce appreciably the lateral deflections. From the conducting of the three series of analysis using two wall stiffnesses and four different thicknesses of the underlying clay layer, 17m, 22m, 33m, and 50m, Wong and Broms obtained the results for the final stage of the excavation (H=11m).

They found that the deflection ratio $\left(\dfrac{\delta_{H\max}}{H}\right)$ ranged from 0.18 at T=6 m to 1.18 at T=39m, where T is the thickness from the base level of excavation to the hard stratum. The reduction of the wall deflection when sheet pile was extended into the underlying hard stratum was found to be small. The reduction is less than 25%. The benefit is more pronounced for a stiff diaphragm wall when the thickness T is small. The reduction varies from 50% at T/B to about 15% at T/B=1.2, where B is the width of the excavation.

Akewanlop (1996) concluded that excavation with a rigid wall yielded a much lower movement than with a flexible wall. His observed magnitudes in Bangkok are $\left(\dfrac{\delta_{H\max}}{H}\right)$=0.2-0.7% for rigid walls regardless of the value of the factor of safety against basal heave and 0.5-1.5% for flexible walls for FS greater than 1.5.

Vazari and Troughton (1992) found that the rigidity of wall characterized by EI seems to play a smaller role in controlling movements than its appearance might suggest. For excavations in soft to medium clays, the effect of the wall stiffness is important. However, the decrease in movements is not directly proportional to the increase in wall stiffness.

Clough and Tsui (1974) reported that for an anchored excavation in soft to medium clays, an increase in wall stiffness of 32 times reduce the corresponding settlements by only 50%.

2.7.7 Effects of excavation depth and width

As stated by Peck (1974) that if $\dfrac{\gamma H}{c_b}$ is bigger than 8, movements of even a well-designed bracing system become intolerably large. In the stability number $\dfrac{\gamma H}{c_b}$, we notice that H becomes bigger then $\dfrac{\gamma H}{c_b}$ becomes bigger, and if H

becomes smaller then the stability number becomes smaller. As the depth of a braced excavation increases, according to the same author, the soil outside the excavation tends to settle and drag the piles down by negative skin friction. Peck continued that if the excavation is too wide, the bracing system may be supported by pile driven to suitable embedment or bearing below final excavation grade. The effect on the deflection ratio $\left(\dfrac{\delta_{Hmax}}{H} \right)$ with the depth of excavation has been investigated by Wong and Broms (1989). They found that for the three soil profiles with constant shear strength, the deflection ratio increased linearly with depth.

The effect on the deflection ratio with depth of excavation for five soil profiles was shown in figure 2.8.
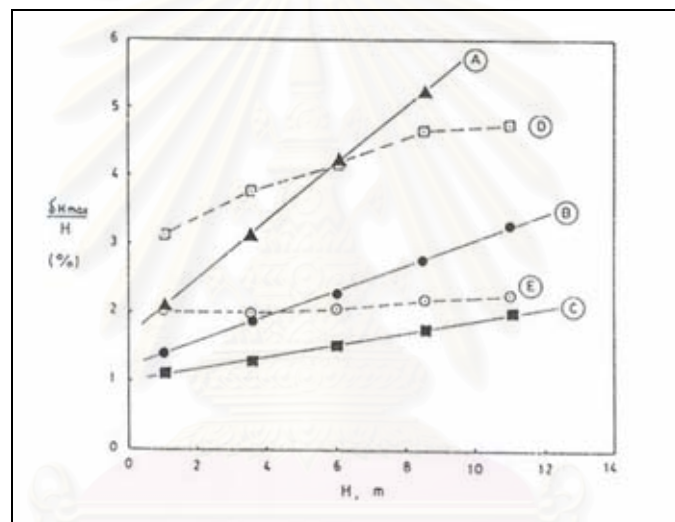
Figure 2.8 Variation of deflection ratio $\left(\delta_{Hmax} / H \right)$
with depth of excavation H (Wong and Broms, 1989)

For soil profile E, the deflection ratio is almost independent of the depth. It is conceivable that the deflection ratio for clay with high Cu/p' ratio may even decrease with increasing excavation depth.
If the clay deposit is very deep, their results indicated that the lateral deflection increases proportionally with the width of excavation. They compared this case with the settlement of a footing in clay where the settlement increases approximately linearly with the width of the footing at a given pressure.

2.7.8 Berm effect

Clough and Gordon (1977) studied the effect of berm size on settlements behind braced wall by using case history data and finite element analysis to

generate deformation on the system. Nondimensional parameters were used to obtain the relationship.

First, maximum settlement of the soil surface behind the wall was selected as the key index to the system performance. This parameter was nondimensionalized by dividing it by maximum excavation depth. The second nondimensional index to be used is percentage passive wedge remaining. This parameter is the ratio between the area occupied by a passive failure wedge in the berm and the area that would be occupied if the berm surface were horizontal, expressed as a percentage.

The final parameter is stability number N ($= \dfrac{\gamma H}{c_b}$). The result of analysis indicated that the value of the stability number is important in the selection of a berm size which can affect on maximum settlement.

For braced excavation in Bangkok subsoil, Teparaksa (1991) found that the effect of berm width is significant in reducing maximum lateral wall deflection, especially at the shallow excavation stage. However, the berm is not effective in deeper zone of excavation.

Phien-wej (1991) reported a large volume of void that left in the ground after sheet-pile extraction. In addition to the volume of the sheet pile itself, a large portion of void was created by removing thick slabs of clay being plugged on the U-shape face of the sheet pile. The plug is as thick as 150 mm. The problems of the clay plug was observed by Phien-wej in most of the past projects in Bangkok soils, and much larger ground movements were observed with longer sheet piles.

As mentioned above, they are too much influence factors for acceptably accurate designing of sheet pile bracing system against wall movements.
The effects of excavation scheme, construction method, construction procedures, workmanship, and so on, make our ability difficult to make a priori prediction of the behavior of braced excavations in clay.
So the designing depends on contractor's behavior of construction as well.

2.8 Relations between maximum lateral wall movement and factor of safety against basal heave

In sheet pile bracing systems, lateral movements of sheet pile walls cannot be avoided. Although lateral wall movement depends on several factors described earlier, the most important amount of the lateral wall movement is the elapsed time between the excavation and the placement of wales and struts and the factor of safety against the basal heave.
Mana and Clough (1981) analyzed the field records of several braced excavations in clay from the San Francisco, Oslo, Boston, Chicago, and Bowline Point (in New York) areas and observed that, under ordinary construction conditions, the maximum lateral wall movement, δ_{Hmax}, has definite relationship to the factor of safety against basal heave.

The factor of safety against basal heave was calculated by using the formula of Terzaghi (1943). The formula was described in section 2.6.

The figure correlating $\left(\dfrac{\delta_{H\max}}{H}\right)$ with the factor of safety against the basal heave is shown in figure 2.9.
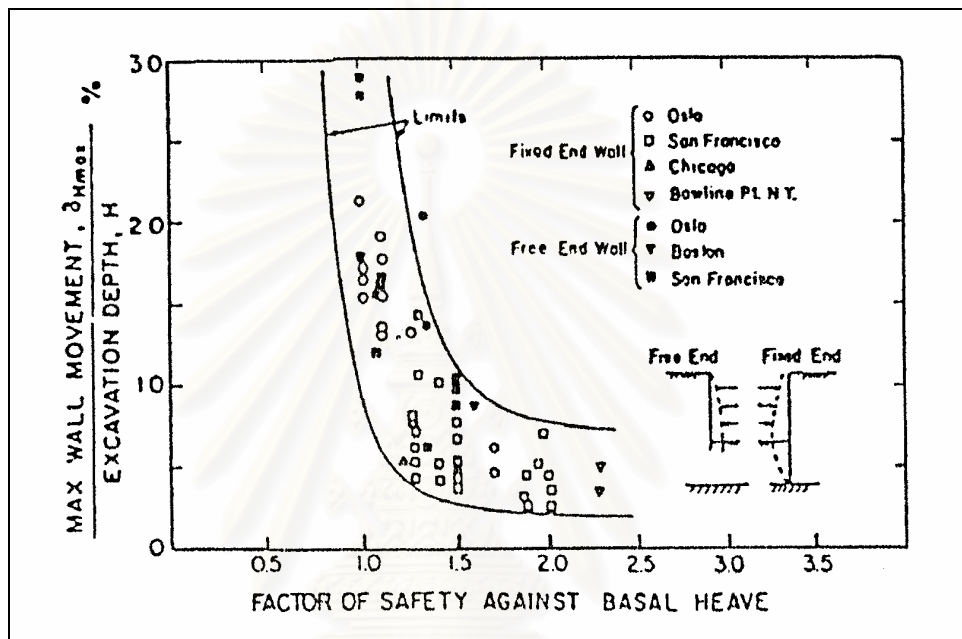
Figure 2.9 Correlation between $\left(\delta_{H\max}/H\right)$ and factor of safety against basal heave (Mana and Clough, 1981)

In this figure the dimensionless number $\left(\dfrac{\delta_{H\max}}{H}\right)$, where H is the depth of excavation, was correlated with the factor of safety against the basal heave calculated by Terzaghi. This figure shows that the lateral wall movement rapidly increases when the factor of safety is smaller than approximately 2. When the factor of safety is bigger than 2, the deflection ratio is roughly constant at a value of 0.5%. The fact that the dimensionless number $\left(\dfrac{\delta_{H\max}}{H}\right)$ is constant at higher factor of safety indicated that there exist large elastic properties of soil response. The rapid increase in lateral wall movement with lower factor of safety indicates the plastic properties of soil response.

Wong and Broms (1989) used five soil profiles with different undrained shear strengths (c_u) to correlate the deflection ratio $\left(\dfrac{\delta_{Hmax}}{H}\right)$ with the factor of safety proposed by Terzaghi (1943), the same manner as Peck.

$$FS = \frac{5.7 \times c_{u2}}{\gamma H - \dfrac{c_{u2} \times H}{0.7B}} \qquad (19)$$

where C_{u1} and C_{u2} = average undrained shear strengths of the clay above the bottom of excavation and down to a depth of 0.7B below the bottom of excavation, respectively. The correlation is shown in figure 2.10.
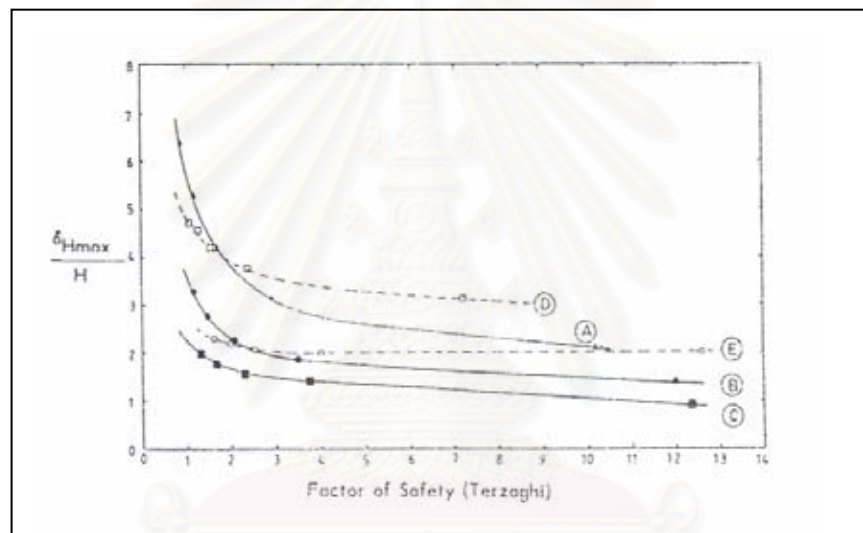
Figure 2.10 Variation of deflection ratio with factor of safety
against basal heave (Wong and Broms, 1989)

Wong and Broms found that the deflection ratio rapidly increases when FS<2.0. It is nearly constant when FS exceeds 2.0. However, at a given factor of safety the deflection ratio can varies within wide limits.

Teparaksa (1993) used the charts developed by Mana and Clough (1981) to study about lateral wall movements of the Baiyoke tower project. He found that the measurement was within or below the boundary proposed by Mana and Clough. The lower measurement, he suggested, might be due to the effect of 70% stage of preloading in the struts, which is higher than those proposed by Mana and Clough.

2.9 Relationship between system stiffness, factor of safety and maximum lateral wall movement

Relationship between system stiffness, factor of safety and maximum lateral wall movement was given by Clough (1982), as shown in figure 2.11. The stiffness parameters are expressed in a dimensionless term, $\dfrac{EI}{h_{ave} \cdot \gamma_w}$, where h_{ave} is the average vertical spacing of struts and γ_w is the unit of water.
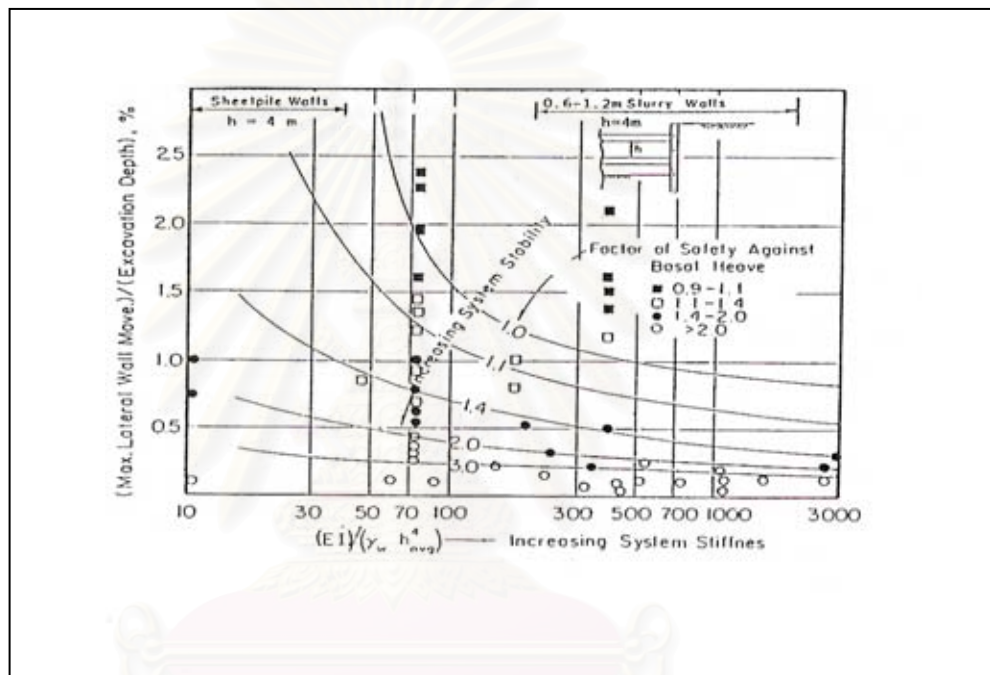
Figure 2.11 Relationship between system stiffness, factor of safety and maximum   lateral wall movement (Clough, 1982)

2.10 Relations between ground settlement and distance from the braced wall

The lateral wall movement, δ_H , will generally induce ground settlement, δ_v , around a braced excavation. Such settlement is generally referred to as ground loss. On the basis of several field observations, Peck (1969) provided curves for predicting ground settlement for various types of soils. The magnitude of ground loss varies extensively; however, the figure may be used as a general guide. The correlation of Peck is shown in figure 2.12.
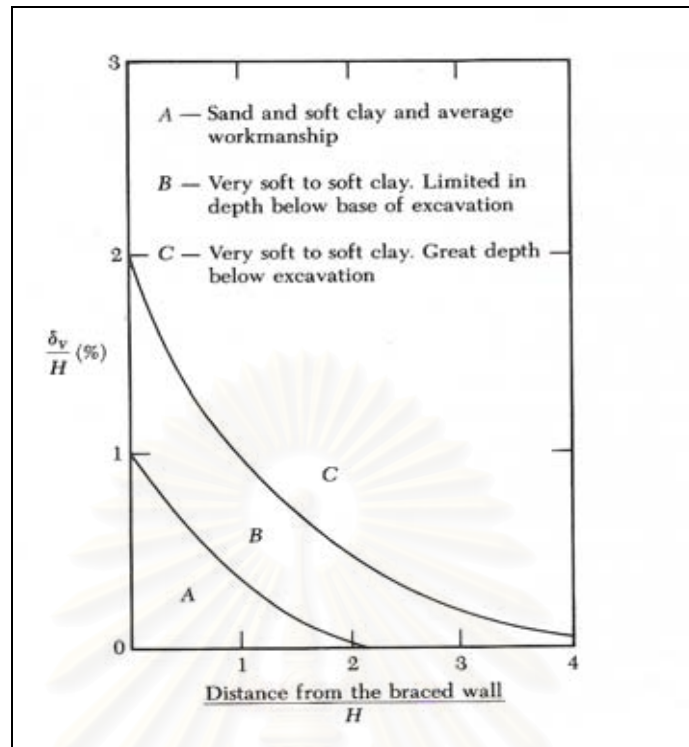
Figure 2.12 Variation of ground settlement
with distance (Peck, 1969)

It is observed from the figure that, in case of soils A and B, when the distance from excavation equals depth of excavation the settlement is less than 2% of the depth of excavation. In case of soil C, the settlement is more than 2% because there is effect from the long extension of the hard stratum below the base level of excavation.

Caspe (1966) presented a method of analysis that requires an estimate of the bulkhead deflection and Poisson's ratio. Using these values, Caspe back-computed one of the excavations in Chicago reported by Peck (1943) and obtained reasonable results. A calculation by the author indicates, however, that one could carry out the following steps and obtain results about equal good:
   1. Obtain the estimated lateral wall deflection profile.
   2. Numerically integrate the wall deflection to obtain the volume of soil in the displacement zone Vs. Use the trapezoidal formula, Simpson's one-third rule, or average end area.
Trapezoidal formula:

$$\int_{a}^{b} f(x)dx \approx \frac{h}{2}\left(f_1 + 2f_2 + 2f_3 + \ldots + 2f_n + f_{n+1}\right)$$

Simpson's one –third formula:

$$\int_{a}^{b} f(x)dx \approx \frac{h}{3}\left(f_1 + 4f_2 + 2f_3 + 4f_4 + 2f_5 \ldots + 4f_n + f_{n+1}\right)$$

3. Compute or estimate the lateral distance of the settlement influence. The method proposed by Caspe for the case of the base soil being clay as follows:

    a. Compute wall height to dredge line as H_w,

    b. Compute a distance below the dredge line, H_p

Soil type	Use $H_p \approx$
$\phi = 0$	B
$\phi - c$	$0.5\tan(45 + \dfrac{\phi}{2})$

Where B = width of excavation
From steps (a) and (b), we have:
$H_t = H_w + H_p$

    c. Compute the approximate distance D from the excavation over which ground loss occurs as:

$$D = H_t \tan(45° - \phi/2)$$

From the relation above, the maximum D is only H_t.

4. Compute the surface settlement at the edge of excavation wall as:

$$S_w = \frac{2V_s}{D}$$

5. Compute remaining ground settlements assuming a parabolic variation of S_i from D toward the wall as:

$$S_i = S_w \left(\frac{x}{D}\right)^2$$

Several factors complicate the foregoing calculations. One is the estimation of displacement below the excavation line. However, satisfactory results would probably be obtained by integrating the soil volume in the lateral displacement to the dredge line. The displacements below the dredge line are an attempt to account somewhat for soil heave (which also contributes to the ground loss) as well as lateral wall movement.

Many case studies showed that the method of Caspe well agreed with the method proposed by Peck (1969).

2.11 Relations between lateral wall movement and ground settlement

Analyzing the field data obtained from several excavations in the regions of Oslo, Chicago, and San Francisco, Mana and Clough (1981) provided a correlation between the maximum lateral wall movement of sheet piles, δ_{Hmax} and the maximum ground settlement, δ_{vmax}. The correlation is shown in figure 2.13.
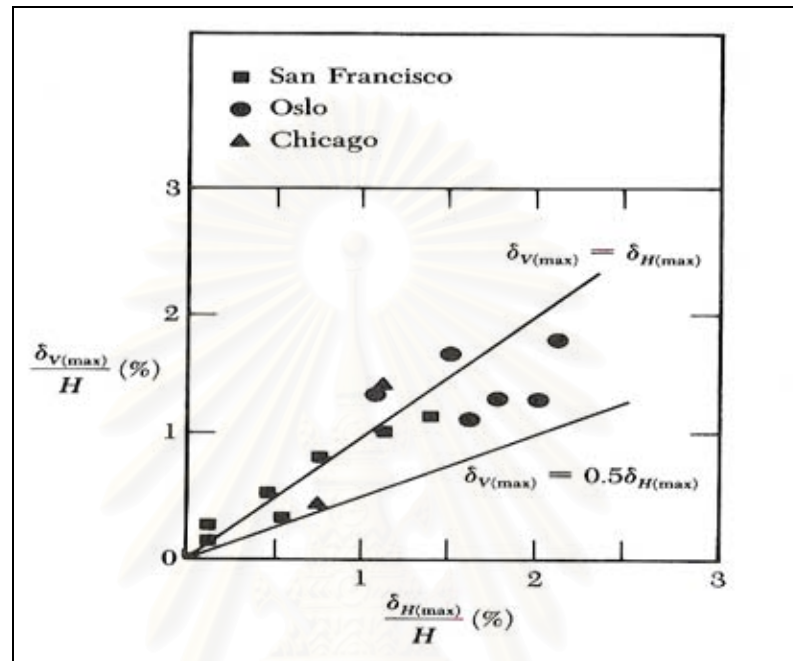
Figure 2.13 Variation of maximum lateral movement with
maximum ground settlement (Mana and Clough, 1981)

It can be seen from the figure that δ_{vmax} approximately equals from 0.5% to 1% times δ_{Hmax}.

It should notice that with poor construction effects, settlements in such conditions can easily exceed the lateral wall movements.

2.12 Computation of lateral wall movement by Wong and Broms

Wong and Broms (1989) proposed a method to estimate the maximum lateral wall movement for a braced excavation in soft clay. The following five assumptions have been made:

1. The clay thickness beneath the bottom of excavation to the hard stratum (T) exceeds half of the width of excavation (B/2);

2. The wall is flexible;

3. There are no net volume changes (undrained conditions) during the excavation. It has thus been assumed that the volumes that corresponds to the ground settlement (shaded area **a** is equal to the volumes associated the heave and

the lateral wall displacements above the bottom of excavation (shaded area b) as shown in figure 2.14 below.
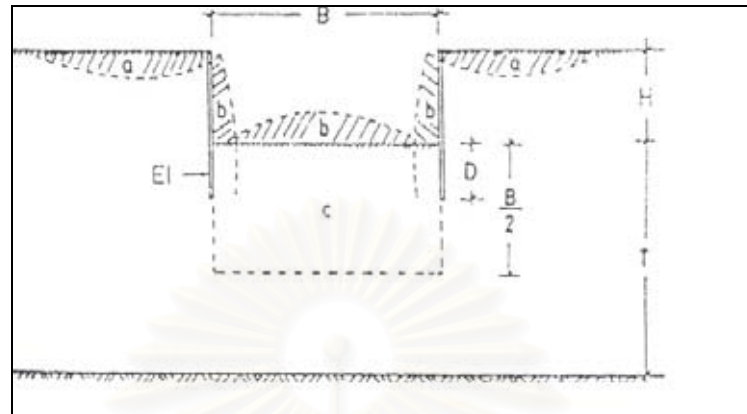
Figure 2.14 Movements around braced excavation
(Wong and Broms, 1989)

4. The lateral displacement of the soil is governed by the yielding of zone c, which extends down to a depth of B/2 as shown in figure 2.14.

5. The yielding is governed by the average stress level of the soil mass within the zone c and is proportional to $\left(\dfrac{\gamma H + q}{c_u \times N_c} \right)$, where q is the surcharge pressure and N_c is the bearing capacity pressure.

According to the assumptions made above, the method can be postulated that the behavior of the soil within the zone c governs the lateral wall movement. When the block c is subjected to a lateral pressure, the two sides will move inward (δ_H), forcing the soil to heave upward (δ_V) as shown in figure 2.14.
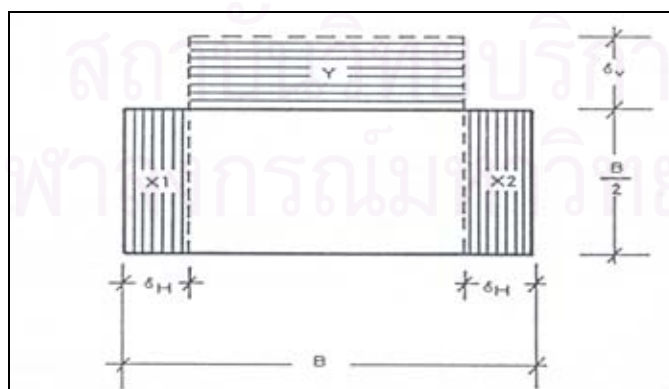
Figure 2.15 Idealized undrained deformation of
influence block (Wong and Broms, 1989)

Since the clay is assumed to be saturated, the volume of the block c does change. Therefore, the sums of the areas X_1 and X_2 will be equal to area Y. Then

$$2\delta_H \left(\frac{B}{2}\right) = \delta_V \left(B - 2\delta_H\right) \tag{20}$$

$$\Rightarrow \delta_H = \delta_V - \left(\frac{2\delta_H \delta_V}{B}\right)$$

The value of $(2\delta_V \delta_H / B)$ is small as compared with δ_V and δ_H.
Therefore, $\delta_H = \delta_V$ \hfill (21)

2.12.1 Tangent modulus method

The objective of this method is to derive a simple equation relating the average tangent stiffness of the soil to the average lateral displacement of the wall within the influence zone c. The thickness of the influence zone is B/2. The corresponding vertical strain increment ($\Delta\varepsilon_V$) can be expressed as follows:

$$\Delta\varepsilon_V = \frac{\delta_V}{B/2} \tag{22}$$

The vertical strain which depends on the tangent modulus E_t can then be computed as:

$$\Delta\varepsilon_v = \frac{\Delta\sigma_v}{E_t} = \frac{\Delta H \times \gamma}{E_t} \tag{23}$$

where $\Delta\sigma_V = $ the reduction of the total overburden pressure caused by excavation.
From equations (21), (22), and (23), we obtain:

$$\delta_H = \frac{\Delta H \times \gamma}{E_t} \times \frac{B}{2} \tag{24}$$

Equation (24) shows that the lateral wall displacement is directly proportional to the unloading γH and the width of excavation (B), and inversely proportional to the tangent modulus (E_t).

The tangent modulus E_t is related to the initial modulus (E_i), the stress level (S_L), and the failure ratio (R_f). From the hyperbolic formulation by Duncan et al. (1980):

$$E_t = \left(1 - S_L R_f\right)^2 E_i \tag{25}$$

where S_L = the average stress level of the soil within block c. It is an indicator of the extent of the plastic yielding within the block.

The failure ratio (R_f) governs the shape of the hyperbolic curve, which describes the nonlinear soil behavior. For undisturbed soft clays, $R_f = 0.7$.

E_i is the initial tangent modulus as shown in figure 2.16.
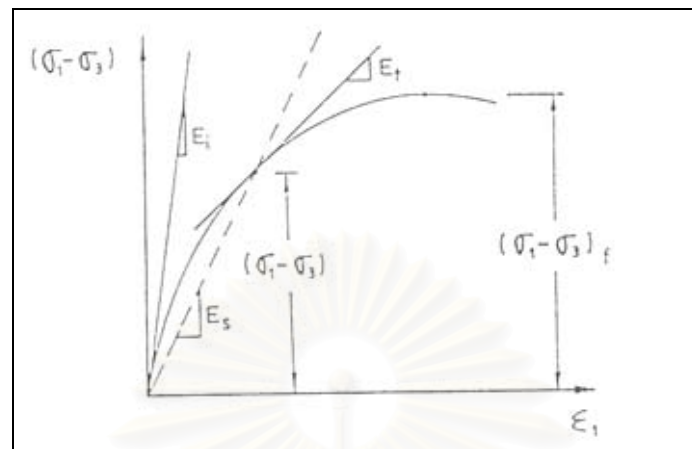
Figure 2.16 Determination of secant and tangent
moduli (Wong and Broms, 1989)

By making finite element analysis, Wong and Broms recommended to use
undrained modulus E_u instead of E_i.

With the tangent modulus method in equation (24), several analyses are required
to compute the deflections at the intermediate stages of the excavation. The total
wall displacement at the final depth is the sum of the incremental values. Wong
and Broms suggested that this drawback can be overcome by using the secant
modulus method.

2.12.2 Secant modulus method

In the secant modulus method, the total, rather than the incremental stress,
is used. The derivation of the basic equations is the same as those with the tangent
modulus method. The relative displacement can be expressed as:

$$\frac{\delta_H}{H} = \frac{\gamma}{E_s} \times \frac{B}{2} \qquad (26)$$

The secant modulus (Es) can be computed from the following equation:

$$E_S = E_u \left(1 - S_L R_f\right)$$

where S_L = stress level

R_f = failure ratio

E_u = undrained soil modulus

Wong and Broms plotted the maximum deflection ratio $\left(\dfrac{\delta_{Hmax}}{H}\right)$ from finite

element analysis with the deflection ratio in Equation (26) as shown in figure
2.17.
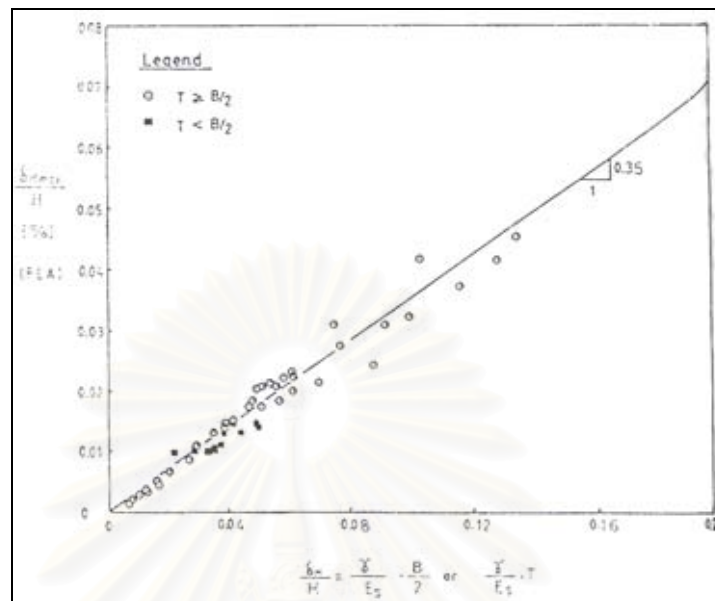
Figure 2.17 Comparison of maximum deflection ratio
from FEM analysis and average deflection ratio
(Wong and Broms, 1989)

From the figure 2.17, Wong and Broms modified equation (26) to be:

$$\delta_{H\max} = \frac{0.35\gamma H}{E_s} \times \frac{B}{2} \qquad (27)$$

It should note that the zone of influence has been assumed to extend down to a depth of B/2 below the bottom of excavation.
When T< B/2, Wong & Broms proposed to replace B/2 by T in equation (27).
Thus when T<B/2, Equation (27) becomes:

$$\delta_{H\max} = \frac{0.35\gamma \times H \times T}{E_s} \qquad (28)$$

To use equation (28), the average stress level (S_L) must be determined.

2.12.3 Average stress level

It has been assumed that $S_L = \dfrac{\gamma H + q}{c_u N_c}$. In this equation, c_u is the undrained shear strength of the soil within the zone of influence, q is the surcharge, and H is

the depth of excavation. The bearing capacity factor Nc, proposed by Bjerrum and Eide (1956), can be approximated as follows:

For $\dfrac{H}{B} \leq 2.5$, $Nc = 5\left(1 + \dfrac{0.2B}{L}\right)\left(1 + \dfrac{0.2H}{B}\right) \cdot \beta$

For $\dfrac{H}{B} \geq 2.5$, $Nc = 7.5\left(1 + \dfrac{0.2B}{L}\right) \cdot \beta$

Where β = a correction factor with respect to an underlying hard stratum (T<0.7B) proposed by Button (1953) is shown in figure 2.18.
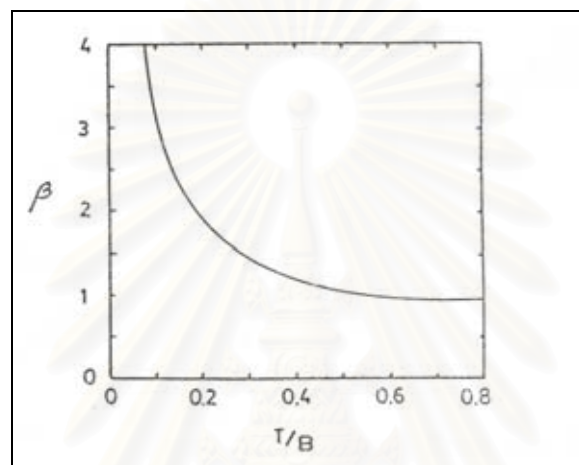
Figure 2.18 Correction factor for depth to
hard stratum (Wong and Broms, 1989)

2.13 Past investigations of deep excavations in Bangkok soft clay

The first useful state-of-the-art on ground movements in braced excavation was given by Peck (1969) who summarized data on settlements behind excavation from case histories and produced a useful chart for estimation of settlement. It should be noted that settlement data included in Peck's study were only of excavations with standard sections of steel sheet pile or soldier pile walls. Therefore, the chart is only applicable to excavations with a wall of light stiffness. As we know that the deep excavations in Bangkok soft clay have begun since the mid-1970s. In the periods, excavations were only carried down to depth shallow than 4-5 m to construct one basement floor. Later on, more researches and construction of deeper excavations have continued. Some important and noticeable researches on deep excavations are briefly illustrated as follows:

2.13.1 Amomsrivilai (1987)

Amomsrivilai (1987) analyzed the case study of single-strutted excavations supported by sheet-pile wall in Bangkok clays by finite element method. The program that the researcher used was developed from theories of

beam-on-elastic body with only one-dimensional element provided. The comparisons were made between various types of conventional methods, i.e. free-fixed earth method with Rowe's moment reduction factor, subgrade reaction method and the finite element analysis. The same researcher concluded that the finite element method was more accurate to simulate soil-structure interaction of the behavior of soil and supporting elements.

2.13.2 Chaiseri and Parkinson (1990)

Chaiseri and Parkinson (1990) reported the field monitoring and predicted deformations of diaphragm wall with "Top-Down" construction, which was, for the first time, introduced in Bangkok area. The well-achieved method of construction for deep basement was a combination of a diaphragm wall deeply embedded in the stiff clay, and the top-down construction method, which limits wall deflections as well as ground settlement to the low values. The type of excavation supporting system became the competitive solution to the conventional sheet pile method, because it provided excellent ground support during excavation and eliminate the effect of post excavation movements due to extraction of sheeting elements.

2.13.3 Heluin (1991)

Heluin (1991) analyzed the behavior of diaphragm walls constructed in Bangkok subsoils and the attempt to evaluate the elastic parameters of Young's modulus. The predictions of the soon-to-be-constructed project were also reported. The author's method of finite element method based on the elastic-plastic behavior followed the Mohr-Coulomb criteria. The wall was simulated as a vertical beam subjected to the soil pressure and initial state of stress after wall installation and before first excavation stage was assumed to correspond to Ko conditions.

The recommended values of Young's modulus for Bangkok subsoils were reported as follows:

Depths (m)	Young's modulus, E (MPa)
0.3 to 13.2	38
13.2 to 16.7	120
16.7 to rigid base	200

2.13.4 Noppadol Phien-wej (1991)

Nippadol Phien-wej conducted a research on a 5.1-m deep excavated pipe trench supported by a braced sheet pile wall of the 36-m long test section that was located along the route of a new water transmission line in the northern suburbs of Bangkok. In the research there were one inclinometer casing and 64 surface settlement gauges to monitor ground movements.

His results of the braced steel sheet pile behaviors are as follows:

1. The maximum short-term ground settlement caused by the trench excavation was in the order of 2.08 to 4.33% of excavation depth. The development of this large ground settlement was principally caused by the constraint imposed by the selected excavation method and procedures. Most of the ground movement developed during sheet pile pulling activities due to heavy surcharge from a crane and voids left in the ground below the sheet pile tip.

2. Approximate the same maximum ground settlement as lateral displacement toward the trench wall developed during the construction period. However, the settlements continued to increase by about 12%-30% during the three-week period after construction while the lateral ground movement remained relatively unchanged.

3. The variation of trench width and backfill compaction did not seem to help reduce the amount of ground movements at this excavation. It is because the ground movements were largely caused by construction related factors.

2.13.5 Sutabutr (1992)

In his thesis, Sutabutr used numerical analysis (FEM in CRISP program) to describe the behaviors of the soil mass during the excavation process. The deformation of retaining structures had been studied. His conclusions can be drawn as:

- Maximum settlements were observed at a depth ranging between 0.75 and 1.5 times the excavation depth.
- Sheet pile wall excavation resulted in higher settlements (about 263 mm) in the vicinity of the excavation, while diaphragm wall excavation with internal bracing resulted in low settlements (about 5.1 mm). From observations, he concluded that the diaphragm wall method of excavation is more suitable in congested areas. The performance of other methods of construction falls between these two extreme cases.
- He observed that the installation of foundation piles prior to excavation effectively limited ground movements.
- Linear preloading from the top pattern is more efficient than other patterns.
- The diaphragm wall by top-down construction method is the best for deep excavations in highly congested areas.
- The soil-structure mechanism was recommended to use the elasto-

perfectly plastic constitutive law.

- The lateral deformation (δ_H) and settlement (ρ) were related with the wall stiffness as given below:

$$\delta_H = 7.5 \times 10^2 (EI)^{-0.72}$$

$$\rho = 5.5 \times 10^5 (EI)^{-1.3}$$

2.13.6 Akewanlop (1996)

Akewanlop conducted a research on ground movements from braced excavation projects in Bangkok, used the FEM in CRISP program to investigate the movement characterization in soft soil, and reached conclusions that:

- In excavation with a rigid wall, $\delta_{H\max}$ occurring during the first stage of excavation could well be the largest value for the whole excavation. For a flexible wall, the largest value $\delta_{H\max}$ developed in the latter stage of excavation.

- Characteristics of wall movements of flexible sheet pile wall were different from those of rigid concrete diaphragm wall/contiguous bored pile. The former were mainly controlled by the soil and have relation with FS against basal heave. The latter were largely controlled by the rigid wall and thus were not much related to the FS value.

- Excavation with a rigid wall yielded a much lower lateral wall movements than with a flexible wall.

$\left(\dfrac{\delta_{H\max}}{H}\right)$ =0.2-0.7% for rigid wall regardless of the value of FS against basal heave.

$\left(\dfrac{\delta_{H\max}}{H}\right)$ =0.5-1.5% for flexible walls for $FS \geq 1.5$

- The length of the embedment has negligible effect on the magnitude of movement of braced excavation in Bangkok subsoils for the wall installed to the stiff clay layer or the first sand layer.

- The FEM analysis much overpredicted the movement in the cantilever mode.

2.13.7 Tanseng (1997)

Analyzing data from sheet pile wall and diaphragm wall projects, in soft Bangkok clay and using PLAXIS program for numerical analysis, Tanseng (1997) concluded that:

- Soil modulus for diaphragm wall is 500Su for soft to medium stiff clay and 2000Su for stiff clay. For sheet pile excavation, soil modulus is 150Su for soft to medium clay and 1000Su for stiff clay.

- The modulus obtained from the laboratory overpredict the value of deformation because strain that occurs in soil behind the wall is very small (less than 1%).

- The prediction of lateral wall movement both for sheet pile and diaphragm wall based on finite element method is very close to the field performance where the Mohr-Coulomb model (total stress analysis) is applied. However, the Modified Cam Clay model, the results of FEM analysis are very close to prediction only for soft clay.

- He recommended using the apparent earth pressure proposed by Terzaghi and Peck (1967) to design strut load.

- The relationship between field performance $\left(\dfrac{\delta_{Hmax}}{H}\right)$ and FS against basal heave for braced sheet pile wall shows a trend as proposed by Mana and Clough (1981).

The nondimensionalized wall movements $\left(\dfrac{\delta_{Hmax}}{H}\right)$ of diaphragm wall do not only depend on factor of safety against basal heave. Value of $\left(\dfrac{\delta_{Hmax}}{H}\right)$ ranges from 0.2-0.7%.

-Total force acting on wall based on finite element method is about 17% higher than measured values.

2.13.8 Gan Choon Hock (1997)

Hock collected deformation data from projects of deep excavations in Bangkok and used FEM in PLAXIS to verify the field performance. He reached conclusions that:

- A cantilever type of deformation was activated at the first cut. The amount of deformation is scattered with the quality of workmanship as well as the time of subsequent construction.

- The inclinometer tubes shall be arranged farther from geometry edges to prevent the movements constrained by the rigid structures.

- Deformations due to uneven excavation are excessively higher. Combination of the delay in bracing installation and possibly the sloughing of berm with time are the main contributions.

- Back-analysis modulus for soft Bangkok clay are as follows:
  Soft clay: Eu = 280Su-350Su
  Medium clay: Eu = 350Su-550Su
  Stiff clay: Eu = 800Su-1200Su

- Deformation was excessively calculated (5 mm) when surcharge was fully applied.

2.13.9 Wanchai (1993 & 1994)

Wanchai (1993) analyzed the data obtained from the sheet pile bracing system with fully effective preloading strut system, for the first time in Bangkok, for basement excavation of 11.3-m depth of the 89-story Baiyoke Tower II. He made conclusions that:

- Mode of sheet pile wall deflection is the rotation about the bottom or fixed end type.

- Traffic behind the sheet pile wall shows significant influence on the maximum surface settlement and maximum lateral wall movement.

- Berm width can reduce the maximum lateral wall deflection only at the first stage of excavation.

- The measured deflection ratio against basal heave tends to lower than those proposed by Mana & Clough (1981)

- The prediction of maximum wall movement by the simplified method proposed by Wong & Broms (1989) agrees well with the performance only at the final stage of excavation.

Based on the measurement of field performance with fully installation of the geotechnical instrumentations for deep excavations in soft Bangkok clay using sheet pile bracing system, Wanchai (1994) concluded that:

- Mode of sheet pile wall deflection is the rotation about the bottom or fixed end type.

- Traffic behind the sheet pile wall shows significant influence on the maximum surface settlement and maximum lateral wall movement.

- The efficient preloading system in the strut can reduce the horizontal wall displacement as well as vertical ground settlement.

- The variation of ground settlement with the distance is located in zone A and B of guide chart those proposed by Peck (1967).

2.13.10 Balasubramaniam, Bergado, Chai, and Sutabutr (1994)

The deformation characteristics of six excavations in Bangkok subsoil with different supporting systems had been analyzed by finite element method. The parametric studies were also performed on the factors, which influence the deformation of supported excavation. Based on these investigations, Balasubramaniam, Bergado, Chai, and Sutabutr drawn the following conclusions:

1. In general the computed deflections of the walls are in good agreements with the field data. The analysis provided a means of simulation of excavation sequence including the installation supporting elements and the preloading of the struts.

2. The deformation of the supported excavation is controlled by the stiffness of the retaining wall and bracing elements, and the method of excavation. Higher rigidity of diaphragm wall with top-down construction method reduced the lateral deflection of the wall with earth pressure distribution at retained side close to Ko condition. This system also increased the ability to withstand the surcharge loading on surrounding area of excavation. Comparing with the diaphragm wall,

steel sheet pile wall has larger deformation (more than 10 times larger) corresponding to earth pressure distribution at retained side less than Ko condition. A larger portion (40 to 80% of total value) of deformation occurred in the cantilever mode of deformation during the early stage of construction.

3. Parametric studies showed that preloading in struts as well as installing the barrette piles and foundation piles can improve the deformation characteristics of the excavation. When the stiffness of the wall (EI) is less than 750 MPa-m^4/m the stiffness has significant influence on the wall deflection. In addition, the embedment depth has greater control on the deformation behavior of the sheet pile walls but low sensitivity for braced diaphragm wall.

2.13.11 Wanchai (1999)

Wanchai (1999) investigated and compiled data from three different case studies of deep excavations in Bangkok subsoils with the aims to evaluate the soil stiffness parameters of the soft and stiff Bangkok clay for reinforced concrete diaphragm wall based on back-analysis method. The three deep excavation projects were: Thamasat University Project, Dindang Underpass Project, and Sathorn Complex Project.

His results showed that the soil stiffness in terms of Young's modulus was:

$$\frac{Eu}{Su} = 500 \quad \text{for soft Bangkok clay}$$

$$\frac{Eu}{Su} = 2000 \quad \text{for stiff Bangkok clay}$$

He noticed that these values also well corresponded to the results of self-boring pressuremeter tests of the first blue-line subway project in Bangkok.

2.14 Instrumentations for deep excavations

In sheet pile bracing systems constructed in Bangkok, three kinds of instrumentations are usually seen. Those are inclinometers, piezometers, and surface settlement points. The installation of these geotechnical instrumentations is mostly followed by the method proposed by Dunnicliff and Green (1988).

2.14.1 Surface settlement points

Surface settlement points are categorized as fixed borehole extensometers but are used for monitoring absolute deformation rather than relative deformation between a collar and a downhole anchor.

Typical applications are for monitoring settlement below embankments and surcharges, above soft ground tunnels or adjacent to braced excavations, and for monitoring uplift during grouting operations.

2.14.2 Inclinometers

Inclinometers fall within the category of transverse deformation gages. Inclinometers are defined as devices for monitoring deformation normal to the axis of a pipe by means of a probe passing along the pipe. Inclinometers are also referred to as slope inclinometers, probe inclinometers, and slope indicators.

Typical applications include the following:
1. Determining the zone of landslide movement.
2. Monitoring the extent and rate of horizontal movement of embankment dams, embankments on soft ground, and alongside open cut excavations or tunnels.
3. Monitoring the deflection of the bulkheads, piles, or retaining walls.

The inclinometers are installed in the steel casing that is weld to the sheet pile before driving. After driving sheet pile fixed with steel casing, cement-bentonite slurry is filled in the casing then inclinometer tube is installed in the casing.

Most inclinometer systems have four major components:
1. A permanent installed guide casing, made of plastic, aluminum alloy, fiberglass, or steel. When horizontal deformation measurements are required, the casing is installed in a near-vertical alignment. The guide casing usually has tracking grooves for controlling orientation for the probe.
2. A portable probe containing a gravity-sensing transducer.
3. A portable readout unit for power supply and indication of probe inclination.
4. A graduated electrical cable linking the probe to the readout unit.

2.15 Typical sheet pile bracing system

Normally Japanese sheet pile wall type FSP III of about 16-m long is used for work of about 6-8 m depth. However, for deeper excavation of about 8.5-10 m deep, sheet pile wall type FSP IV of 18-m long is adopted. The section and properties of sheet pile is shown in table 2.1.

Section	Dimensions			Section Area	Weight		Moment of Inertia		Section Modulus	
	W	h	t	Per pile	Per pile	Per wall width	Per pile	Per wall width	Per pile	Per wall width
	mm	mm	mm	cm^2	Kg/m	Kg/m^2	cm^4	cm^4/m	cm^3	cm^3/m
FSP III	400	125	13	76.42	60	150	2,220	16,800	223	1,340
FSP IV	400	170	15.5	96.99	76.1	190	4,670	38,600	362	2,270

Table 2.1 Some typical sheet-pile propertie

H-beam of W 300x300 mm x 94 kg/m section is generally used for the strut system of about 6-m horizontal strut spacing, wale system, and kingpost. However, for wider strut spacing and wider bracing depth H-beam of W 350x350 mm x 137 kg/m section is used. Typical section and properties of H beam is presented in table 2.2.

Section Index	Weight	Depth of Section (A)	Flange Width (B)	Thickness		Corner Radius (r)	Sectional Area	Moment of Inertia		Radius of gyration		Modulus of Section	
				Web (t_1)	Flange (t_2)			J_x	J_y	i_x	i_y	Z_x	Z_y
mm	Kg/m	mm	mm	mm	mm	mm	cm^2	cm^4	cm^4	cm	cm	cm^3	cm^3
350x350	159.0	356	352	14	22	20	202.00	47,600	16,000	15.30	8.90	2,670	909
	156.0	350	357	19	19	20	198.40	42,800	14,400	14.70	8.53	2,450	809
	137.0	350	350	12	19	20	173.90	40,300	13,600	15.20	8.84	2,300	776
	131.0	344	354	16	16	20	166.60	35,300	11,800	14.60	8.43	2,050	669
	115.0	344	348	10	16	20	146.00	33,300	11,200	15.10	8.78	1,940	646
	106.0	338	351	13	13	20	135.30	28,200	9,380	14.40	8.33	1,670	534
300x300	106.0	304	301	11	17	18	134.80	23,400	7,730	13.20	7.57	1,540	514
	106.0	300	305	15	15	18	134.80	21,500	7,100	12.60	7.26	1,440	466
	94.0	300	300	10	15	18	119.80	20,400	6,750	13.10	7.51	1,360	450
	87.0	298	299	9	14	18	110.80	18,800	6,240	13.00	7.51	1,270	417
	84.5	294	302	12	12	18	107.70	16,900	5,520	12.50	7.16	1,150	365

Table 2.2 Some typical strut propertie

2.16 Finite element method for deep excavations

The principal advantages of the finite element method are that the soil and the structure can be considered interactively and that both design loads and expected displacements can be correlated. Furthermore, complicated stratigraphy and unusual soil characteristics can be considered with greater facility than with classical methods. Construction sequence can be accounted for as well. The versatility of the finite element modeling for deep excavation has been conducted since the early 1970s.

Bjerrum (1972) illustrated the application of finite element method to analyze deep excavations at Vaterland 3 in Oslo. The upper 10 m of soil consists of medium stiff weathered clay, covering a deposit of normally consolidated soft clay of low plasticity. The initial value of Young's modulus was chosen 100 times the effective overburden stress. The value of the modulus assigned to each element was reduced as the degree of mobilized shear strength increased during the excavation process. The results of the analysis had reasonable agreement between computed and observed behavior.

Mana and Clough (1981) developed a finite element to estimate lateral wall movements and ground surface settlements which incorporated site geology, soil modulus, proximity of a firm stratum to the bottom of an excavation, and several aspects of construction, including preloading, wall stiffness and supporting spacing.

Wong and Broms (1989) used a nonlinear hyperbolic stress-strain to describe the behavior of the soil. The short-term undrained condition was simulated with a total stress analysis. The clay was assumed to be saturated with Poisson's ratio 0.49. The elastic modulus was based on a $Eu/Cu = 200$.

Wanchai (1999) used finite element method to study three cases of deep excavations in Bangkok. In the research, the two dimensional (2D) FEM method for plain strain condition simulating the soil-structure interaction was used to predict wall movements as well as the ground surface settlement. He compared the FEM results with the field performance to back-analyze to find the soil stiffness in terms of Young's modulus.

Due to the fast growth and development of high-capacity digital computers, there are, currently, many commercial finite element softwares such as CRISP, FLAC, and PLAXIS that can be utilized for deep excavations in a variety of soil conditions.

2.16.1 PLAXIS program

PLAXIS program (Brinkgreve and Vermer, 2001) is one of the commercial finite element softwares. Development of PLAXIS began in 1987 at

the Technical University of Deft as an initiative of Dutch Department of Public Works and Water Management. The initial brief was to develop an easy-to-use finite element code for the analyses for river embankments on the soft soils of the low land of Holland. In subsequent years, PLAXIS was extended to cover most other areas of geotechnical engineering. PLAXIS is a finite element package specifically intended for the analysis of the deformation and stability in geotechnical engineering projects. Geotechnical applications require advanced constitutive models for the simulation of the non-linear and time-dependent behaviors of soils. In addition, since soil is multi-phase material, special procedures are required to deal with hydrostatic and non-hydrostatic pore-pressure in the soil. Although the modeling of soil itself is an important issue, many geotechnical engineering projects involve the modeling of structures and the interaction between the structures and the soil. PLAXIS is equipped with special features to deal with the numerous aspects of geotechnical structures.

2.16.2 Elements in analysis

To analyze deep excavation in PLAXIS program, soil elements can be divided into several elements. For a 2D analysis (plane strain or axisymmetry) one may select either 6-node or 15-node triangular elements (figure 2.19).
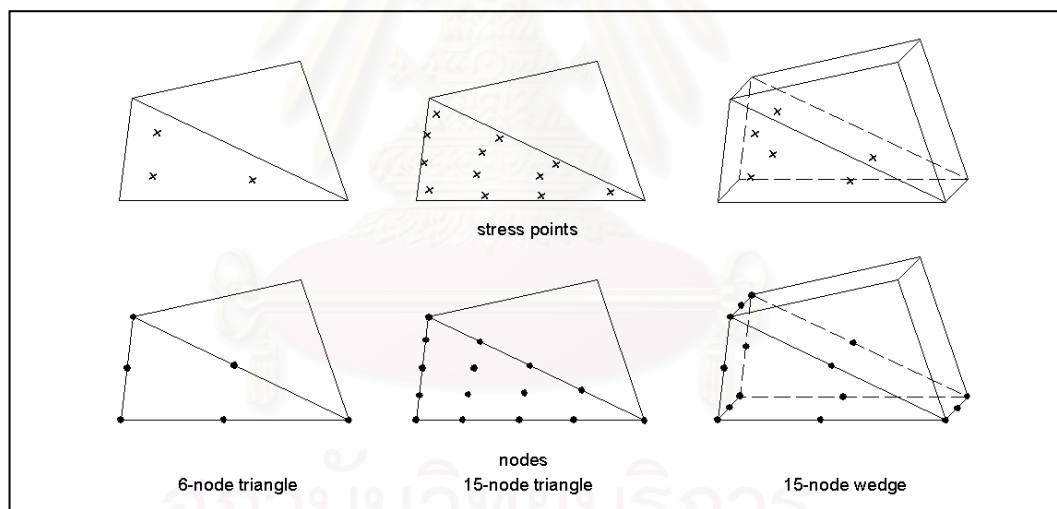
Figure 2.19 Nodes and stress points in soil elements
(Brinkgreve and Vermer, 2001)

The 6-node triangle is the default element for a 2D analysis. It provides a second order interpolation for displacements. The element stiffness matrix is evaluated by numerical integration using a total of three Gauss points (stress points). For the 15-node triangle the order of interpolation is four and the integration involves twelve stress points. For a 3D analysis (3D axisymmetry) only one element type is available, the 15-node wedge element. This element gives a second order interpolation for displacements and the integration involves six stress points.

The 15-node triangle is a very accurate 2D element which has been shown to produce high quality stress results for difficult problems, as for example in collapse calculations for incompressible soils. However, using 15-node triangles leads to relatively high memory consumption and slow calculation and operation performance. In previous PLAXIS versions the 15-node triangle was the default element type because the maximum number of elements was rather limited. In this 2001 version, however, the number of elements in a finite element mesh may be higher than allowed in previous versions. However, the accuracy of the results will in most cases be less than would be obtained using the same number of 15-node triangles. The accuracy of the 15-node wedge for a 3D analysis is comparable to the 6-node triangle in a 2D analysis.

A plane strain model is used for structures with a (more or less) uniform cross section and corresponding stress state and loading scheme over a certain length perpendicular to the cross section. Displacements perpendicular to the cross section are assumed to be zero.

An axisymmetric model is used for circular structures with a (more or less) uniform radial cross section and loading scheme around the central axis, where the deformation and stress state are assumed to be identical in any radial direction. The selection of plane strain or axisymmetry results in a two dimensional finite element model with only two translational degrees of freedom per node (x- and y-direction). A 3D-axisymmetry model is used for structures that are geometrically axisymmetric and loaded with a non-axisymmetric load, such as laterally loaded piles and circular foundations. The selection of 3D-axisymmetry results in a fully three dimensional finite element model with three translational degrees of freedom per node (x-, y- and z-direction).

2.16.3 Geometry

The generation of a finite element model begins with the creation of a geometry model, which is a representation of the problem of interest. A geometry model consists of points, lines and clusters. Points and lines are entered by the user, whereas clusters are generated by the program. In addition to these basic components, structural objects or special conditions can be assigned to the geometry model. It is recommended to start the creation of a geometry model by drawing the full geometry contour. In addition, one may specify material layers, structural objects, lines used for construction phases, loads and boundary conditions. The geometry model should not only include the initial situation, but also eventual construction stages that are considered in a later phase. After the geometry has been completed, one should compose data sets of material parameters and assign the data sets to the corresponding geometry components. When the full geometry is defined and all geometry components have their properties, the geometry model is complete and the mesh can be generated.

Beams in PLAXIS represent real plates in the out-of-plane direction and can therefore be used to model walls and plates. Beams are composed of beam elements with three degrees of freedom per node. Two translational degrees of

freedom (u_x and u_y) and one rotational degree of freedom (rotation in the x-y plane: ϕ_z). When 6-node soil elements are employed then each beam element is defined by 3 nodes whereas 5-node beam elements are used together with the 15-node soil elements.

The most important parameters are the flexural rigidity (bending stiffness) EI and the axial stiffness EA. From these two parameters an equivalent beam thickness d_{eq} is calculated from the equation:

$$d_{eq} = \sqrt{12\frac{EI}{EA}}$$

Bending moments and axial forces are evaluated from the stresses at the stress points. A 3-node beam element contains two pairs of stress points whereas a 5-node beam element contains four pairs of stress points. Within each pair, stress points are located at a distance $d_{eq}/\sqrt{3}$ above and below the beam centre-line.

2.16.4 Interface model

Interfaces are used to model the interaction between structures and the soil. A typical application of interfaces would be to model the interaction between a sheet pile wall and the soil, which is intermediate between smooth and fully rough. In this application interfaces are placed at both sides of the wall. The roughness of the interaction is modelled by choosing a suitable value for the strength reduction factor in the interface. This factor relates the interface strength (wall friction and adhesion) to the soil strength (friction angle and cohesion). Interfaces are composed of interface elements. Figure 2.20 shows how interface elements are connected to soil elements. When using 6-node soil elements, the corresponding interface elements are defined by three pairs of nodes, whereas for 15-node soil elements the corresponding interface elements are defined by five pairs of nodes.
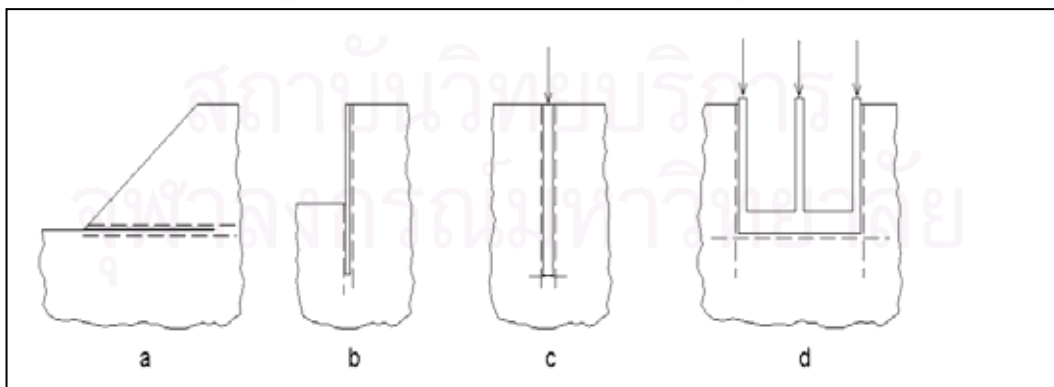
Figure 2.20 Examples in which interfaces are used
(Brinkgreve and Vermer, 2001)

In the figure, the interface elements are shown to have a finite thickness, but in the finite element formulation the coordinates of each node pair are identical, which means that the element has a zero thickness.

In PLAXIS program, the stiffness matrix for interface elements is obtained using Newton-Cotes integration points. The position of these integration points (or stress points) coincides with the position of the node pairs. Hence, for the 6-node interface elements a 3-point Newton-Cotes integration is used, whereas the 10-node interface elements use 5-point integration.

2.16.5 Material properties for analysis

In PLAXIS, soil properties and material properties of structures are stored in material data sets. There are four different types of material sets: Data sets for soil & interfaces, beams, geotextiles and anchors. All data sets are stored in a material data base. From the data base, the data sets can be assigned to the soil clusters or to the corresponding structural objects in the geometry model.

- Modeling of soil behavior

In PLAXIS, The non-linear stress-strain behavior can be modelled at several levels of sophistication. The well-known Mohr-Coulomb model can be considered as a first order approximation of real soil behaviour. This elastic perfectly-plastic model requires five basic input parameters, namely a Young's modulus, E, a Poisson's ratio, ν, a cohesion, c, a friction angle, φ, and a dilatancy angle, ψ. As geotechnical engineers tend to be familiar with the above five parameters and rarely have any data on other soil parameters, attention will be focused here on this basic soil model. In order to understand the five basic model parameters, typical stress-strain curves as obtained from standard drained triaxial tests are considered. The material has been compressed isotropically up to some confining stress σ_3. After this, the axial pressure σ_1 is increased while the radial stress is kept constant. In this second stage of loading soils tend to produce curves as shown in figure 2.21.

Figure 2.21(b) shows the test results put into an idealized form using the Mohr-Coulomb model.
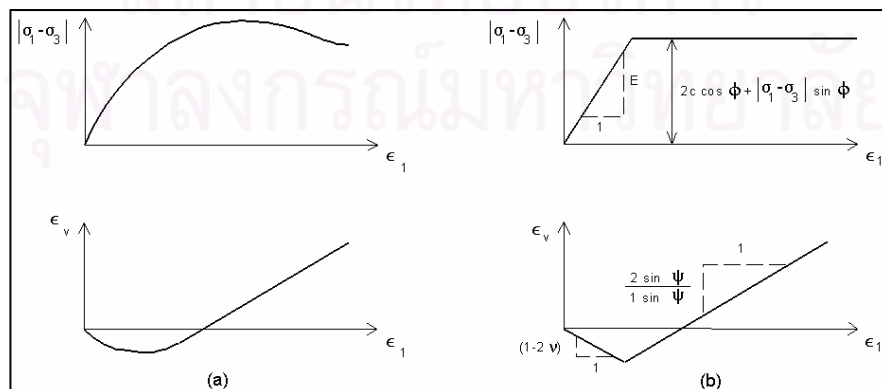
Figure 2.21 Results from standard drained triaxial tests and
elastic-plastic model (Brinkgreve and Vermer, 2001)

- Material model

To simulate the behavior of soil, PLAXIS uses several models such as: 1. Linear elastic model (represents Hook's law of isotropic linear elasticity), 2. Mohr-Coulomb model (a first approximation of soil behavior, in general, involves parameters (E, υ, c, φ, ψ), 3. Hardening soil model (elastoplastic type of hyperbolic model), 4. Soft soil model (Cam-clay type), and 5. Soft soil creep model (model of viscoplasticity).
Among the above models, Mohr-Coulomb model is the most preferred when the good soil data is not available.

- Mohr-Coulomb model (perfectly plastic)

Plasticity is associated with the development of irreversible strain. In order to evaluate whether or not plasticity occurs in a calculation, a yield function, f, is introduced as a function of stress and strain. A yield function can be often presented as a surface model with a fixed yield surface, i.e. a yield surface that is fully defined by model parameters and not affected by plastic straining. For stress states represented by points within the yield surface, the behavior is purely elastic and all strains are reversible.

- Elastic perfectly- plastic behavior

The basic principle of elastoplasticity is that strains and strain rates are decomposed into an elastic part and a plastic part:

$$\underline{\varepsilon} = \underline{\varepsilon}^e + \underline{\varepsilon}^p$$

$$\underline{\dot{\varepsilon}} = \underline{\dot{\varepsilon}}^e + \underline{\dot{\varepsilon}}^p$$

Hook's law is used to relate the stress rates to the elastic strain rates:

$$\underline{\dot{\sigma}}' = \underline{\underline{D}}^e \underline{\dot{\varepsilon}}^e = \underline{\underline{D}}^e (\underline{\dot{\varepsilon}} - \underline{\dot{\varepsilon}}^p)$$

In general, the plastic strain rates (Hill, 1950) are written as:

$$\underline{\dot{\varepsilon}}^p = \lambda \frac{\partial g}{\partial \underline{\sigma}'}$$

where g = plastic potential function
  λ = plastic multiplier

For purely elastic behavior, λ = 0 whereas in the case of plastic behavior λ is positive.

$$\lambda = 0 \text{ for:} \quad f < 0 \quad \text{or:} \quad \frac{\partial f}{\partial \underline{\sigma}'}^T \underline{\underline{D}}^e \underline{\dot{\varepsilon}} \leq 0 \quad \text{(Elasticity)}$$

$$\lambda > 0 \text{ for:} \quad f = 0 \quad \text{and:} \quad \frac{\partial f}{\partial \underline{\sigma}'}^T \underline{\underline{D}}^e \underline{\dot{\varepsilon}} > 0 \quad \text{(Plasticity)}$$

These equations may be used to obtain the following relationship between the effective stress rates and strain rates for elastoplasticity:

$$\underline{\dot{\sigma}}' = \left(\underline{\underline{D}}^e - \frac{\alpha}{d} \underline{\underline{D}}^e \frac{\partial g}{\partial \underline{\sigma}'} \frac{\partial f}{\partial \underline{\sigma}'}^T \underline{\underline{D}}^e \right) \underline{\dot{\varepsilon}}$$
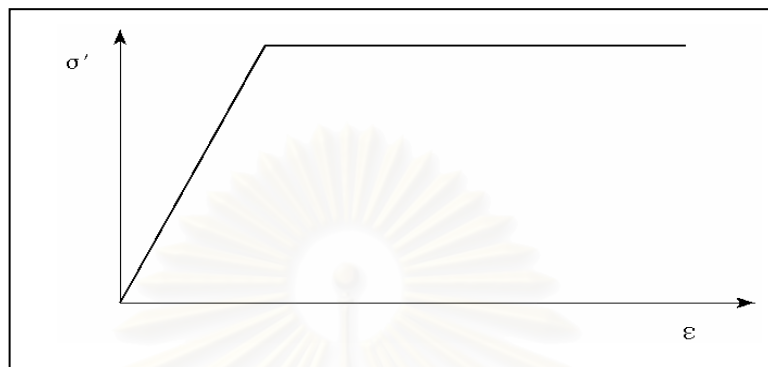
Figure 2.22 Basic idea of elastic perfectly plastic
model (Brinkgreve and Vermer, 2001)

- Formulation of the Mohr-Coulomb model

The full Mohr-Coulomb yield condition can be defined by three yield functions when formulated in terms of principal stresses:

$$f_1 = \frac{1}{2}|\sigma_2' - \sigma_3'| + \frac{1}{2}(\sigma_2' + \sigma_3')\sin\varphi - c\cos\varphi \leq 0$$

$$f_2 = \frac{1}{2}|\sigma_3' - \sigma_1'| + \frac{1}{2}(\sigma_3' + \sigma_1')\sin\varphi - c\cos\varphi \leq 0$$

$$f_3 = \frac{1}{2}|\sigma_1' - \sigma_2'| + \frac{1}{2}(\sigma_1' + \sigma_2')\sin\varphi - c\cos\varphi \leq 0$$

In addition to the yield functions, three plastic potential functions are defined for the Mohr-Coulomb model:

$$g_1 = \frac{1}{2}|\sigma_2' - \sigma_3'| + \frac{1}{2}(\sigma_2' + \sigma_3')\sin\psi$$

$$g_2 = \frac{1}{2}|\sigma_3' - \sigma_1'| + \frac{1}{2}(\sigma_3' + \sigma_1')\sin\psi$$

$$g_3 = \frac{1}{2}|\sigma_1' - \sigma_2'| + \frac{1}{2}(\sigma_1' + \sigma_2')\sin\psi$$

- Basic parameters of the Mohr-Coulomb model

The Mohr-Coulomb model requires a total of five parameters, which are generally familiar to most geotechnical engineers and which can be obtained from

basic tests on soil samples. These parameters with their standard units are listed below:

E : Young's modulus $[kN/m^2]$
ν : Poisson's ratio $[-]$
φ : Friction angle $[°]$
c : Cohesion $[kN/m^2]$
ψ : Dilatancy $[°]$

The alternative parameters of Young's modulus (E) and Poisson's ratio (ν) could be used for soil modeling in PLAXIS are shear modulus (G) and oedometer modulus (E_{oed}). Actually, the relationship between G, E_{oed} and E are given by equations below.

$$G = \frac{E}{2.(1+\nu)}$$

$$E_{oed} = \frac{(1-\nu).E}{(1-2.\nu).(1+\nu)}$$

So far it is known that the subsoil stiffness is not a constant value, but it depend on strain levels. Mair (1993) reported the changes of soil stiffness with different working shear strain levels for various structural systems (Figure 2.23). The typical working range of retaining wall is in the order of 0.01%-1%.
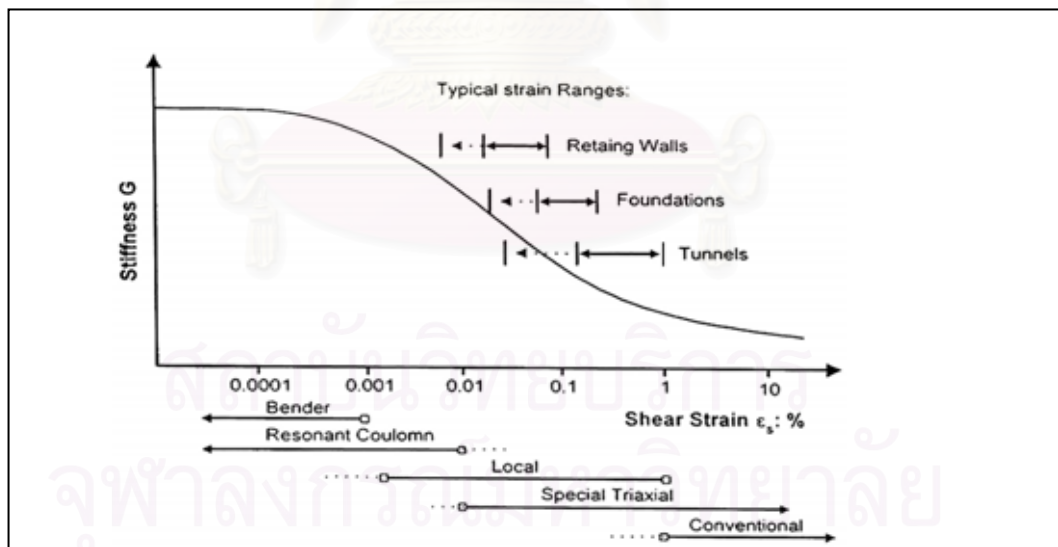
Figure 2.23 Typical shear modulus and shear strains for
different geotechnical works (Mair, 1993)

Teparaksa (2005) presented the correlation between soil stiffness in terms of G/S_u and shear strain for soft and stiff Bangkok clay as shown in figure 2.24. This correlation was developed from seven tests of Self Boring Pressuremeter tests during the design of the first MRT blue line in Bangkok city (Teparaksa, 1999).

| Soft Clay | Stiff Clay |
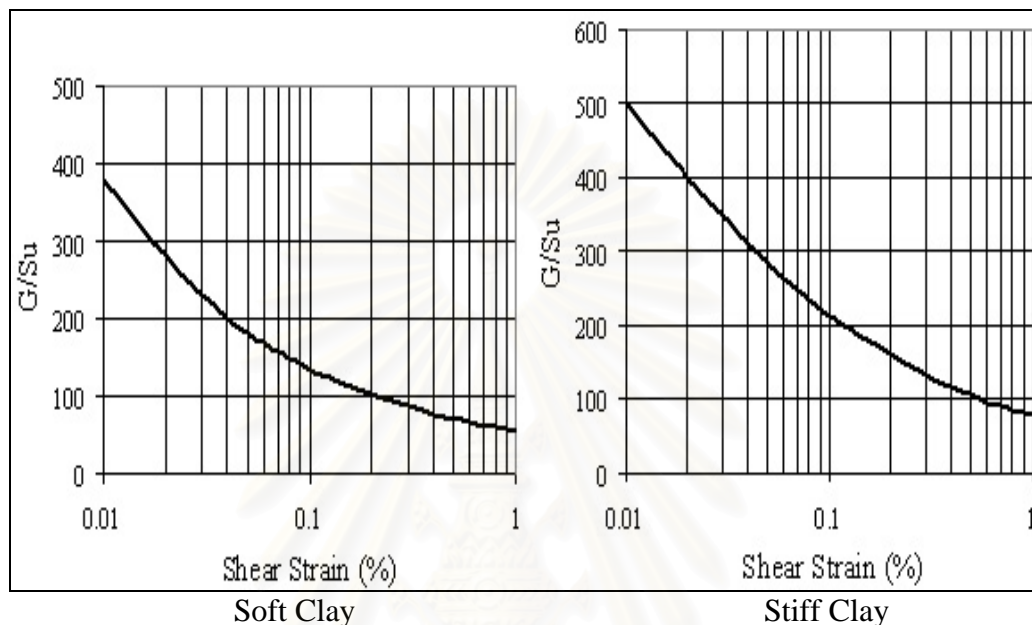
Figure 2.24 Shear modulus of Bangkok clays (Teparaksa, 1999)

2.16.6 Undrained analysis with effective parameters

All materials models implemented in PLAXIS are based on a relation between the effective stress rate, $\dot{\sigma}$ and the strain rate, $\dot{\varepsilon}$.

$$\dot{\sigma}' = M\dot{\varepsilon}$$

where M is a material stiffness matrix

Soil is considered multiphase, that is, soil has soil skeleton, water and/or air. Therefore there are two kinds of stress in the total stress level of soil: effective stress (caused by soil skeleton) and pore pressure (caused by water). Relationship between total stress, effective stress, and pore water pressure were well defined by Terzaghi (1925).

In PLAXIS it is possible to specify undrained behavior in an effective stress analysis using effective model parameters.

In this option the undrained behavior such as the effective parameters G and ν should be converted into undrained parameters E_u and ν_u according to equation:

$$E_u = 2.G.(1+\nu_u)$$

Fully incompressible behavior is obtained for $\nu_u = 0.5$. However, taking $\nu_u = 0.5$ leads to singularity of the stiffness matrix. In order to avoid numerical problems

caused by an extremely low compressibility, ν_u is taken as 0.495, which makes the undrained soil body slightly compressible.

Such an analysis requires effective soil parameters and is therefore highly convenient when such parameters are available. For soft soil projects, accurate data on effective parameters may not always be available. Instead, in situ tests and laboratory tests may have been performed to obtain undrained soil parameters. In such situations, measured undrained Young's modulus can be easily converted into effective Young's modulus by:

$$E' = \frac{2\ (1+\nu')}{3}\ E_u$$

Undrained shear strengths, however, cannot easily be used to determine the effective strength parameters φ and c. For such cases, PLAXIS offers the possibility of an undrained analysis with direct input of the undrained shear strength.

2.16.7 Undrained analysis with undrained parameters

In case that undrained analysis is chosen in PLAXIS, a total stress analysis will be performed without distinction between effective stress and pore pressure. Non-porous option can be selected to simulate undrained behavior. Undrained elastic properties $E = E_u$ and $\upsilon = \upsilon_u = 0.495$ in combination with the undrained strength properties $c = c_u$ and $\varphi = \varphi_u = 0^\circ$ are directly inserted.

2.16.8 Method of stress analysis in PLAXIS

PLAXIS program can be simulated in undrained or fully drained conditions for two-dimensional plane strain and axisymmetry problems. The staged construction of excavation can be simulated by adding or removing elements. In most case, the required time to complete excavation work in short, hence undrained behavior of clay can be assumed in analysis. PLAXIS provides two types of undrained analysis: undrained analysis with effective stress parameters and undrained analysis with total stress parameters.
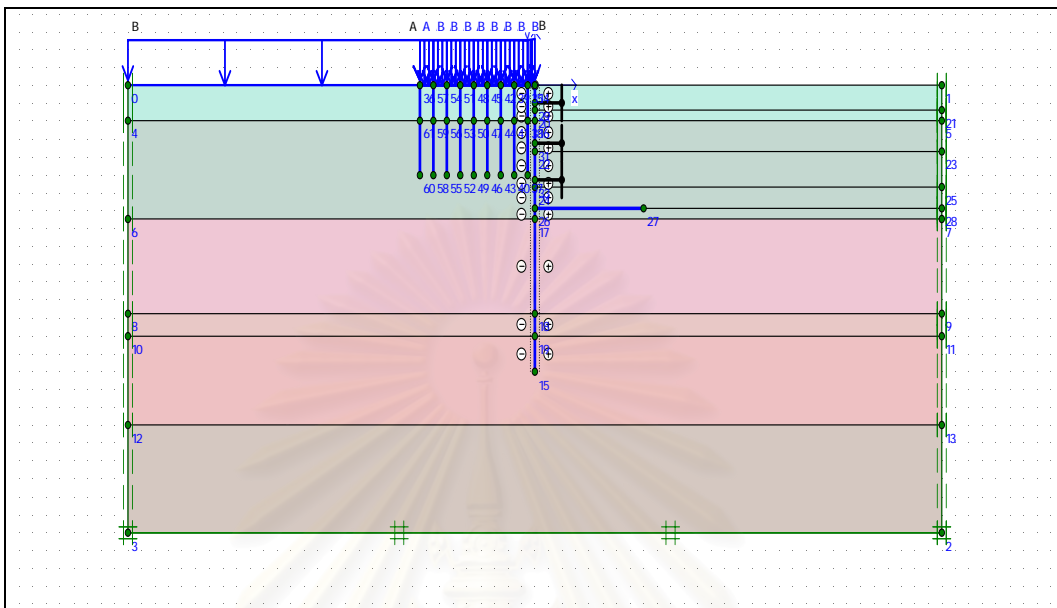
Figure 2.25 PLAXIS simulation of this research project

CHAPTER III

METHODOLOGY

3.1 Site description and monitoring instruments

This research project situates in Silom region, Bangkok. Condominium of eight floors and one basement was constructed. The basement is used for underground vehicle parking. The geometry of the project is rectangular with the length of 50.78 m and the width of 22.50 m (area=$1140\,\text{m}^2$). The building of three to four stories is at one side along the length of excavation and another building of two to three stories at another side. Along the rear side of the excavation is the small road and along the back side is canal.

Three inclinometers were installed fixed to the sheet pile wall. The depth of the inclinometers is equal to the depth of sheet piles. Inclinometer No 01 located 12 m and inclinometer No 02 located 30 m from the front side of the excavation and both inclinometers were installed on the right side of the excavation where three to four-story old buildings exist. Inclinometer No 03 located 25m from the front side and on the left hand side of the excavation where one to two-story old buildings exist. Reading was conducted at various stage of construction to observe the horizontal movements of the wall. The geometry of the project and the position of inclinometers are shown in figures 3.1, 3.2, and 3.3.

To construct the basement, excavation was conducted until the depth of -6.90 m below the road surface. Sheet pile bracing system was used in the deep excavation. The tip of the sheet piles was embedded in very stiff clay layer (16m below the ground surface).

There were three layers of struts in the bracing system. Struts of type W350x350x137 were used for all layers of strutting. The first, second, and third strut layers have depths of -1.00 m, -3.25 m, and -5.30 m, respectively, below the ground surface. The horizontal spacing of the struts was approximate 6 m for all layers of strutting. Eight struts along the length and three struts along the width of excavation were used for each layer.

Wales of type W350×350×137 were provided between sheet piles and struts. The same types of wales were used for all three layers of strutting.

Kingposts of type W300×300×94 (tip at -19m below ground surface) were utilized to carry the excavation machines and trucks from platforms. The machine and truck loading were designed to be $2\,\text{t}/\text{m}^2$ and transferred all their loading to the platforms and kingposts.

Ten rows (6-m spacing) and three rows (6-m spacing) of the kingposts were used along the length and the width of the excavation, respectively.

Totally thirty kingposts were used in the project. The arrangement of the kingposts is shown in figure 3.2.
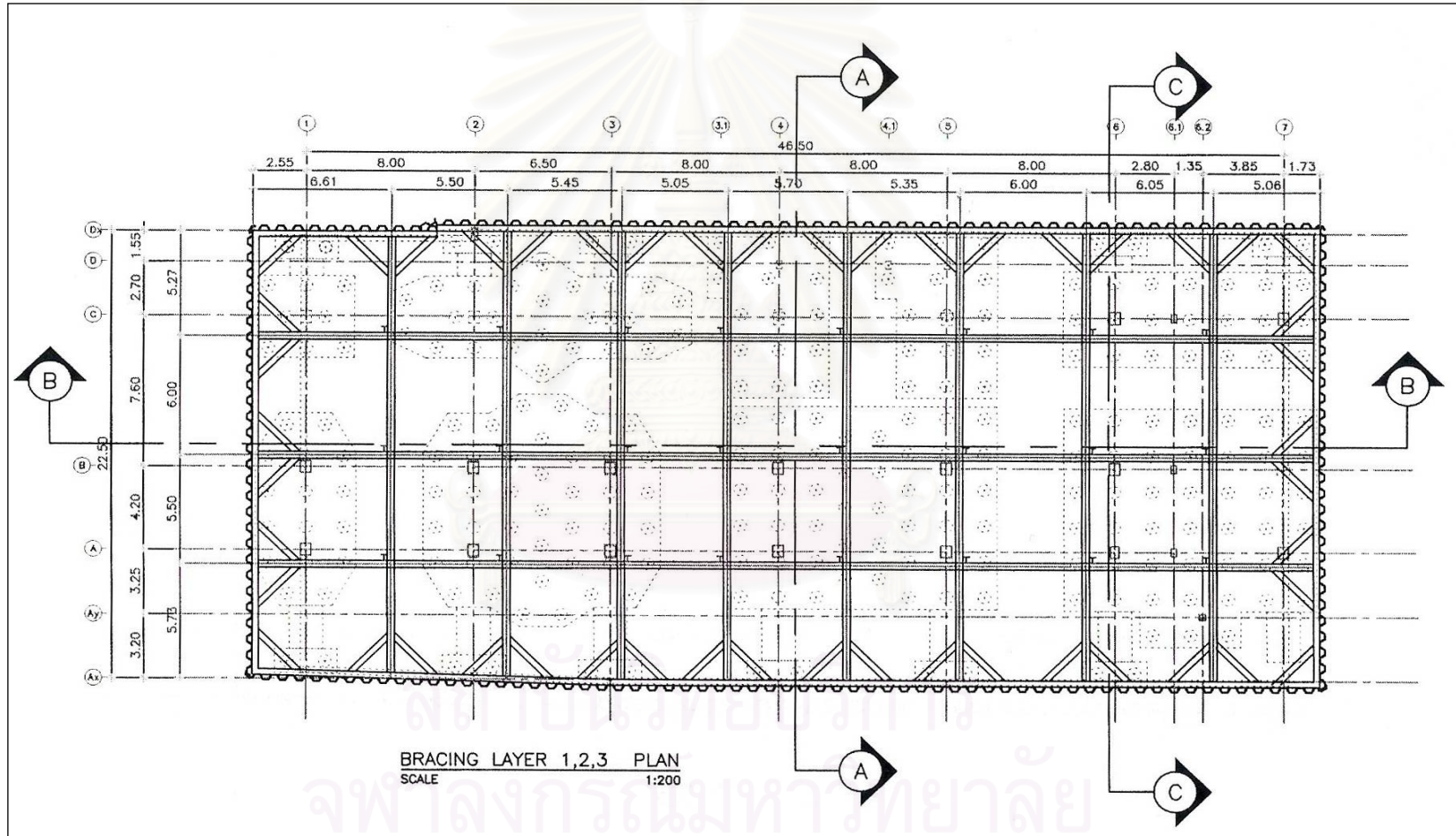
Figure 3.1 Layout of project (plane view)
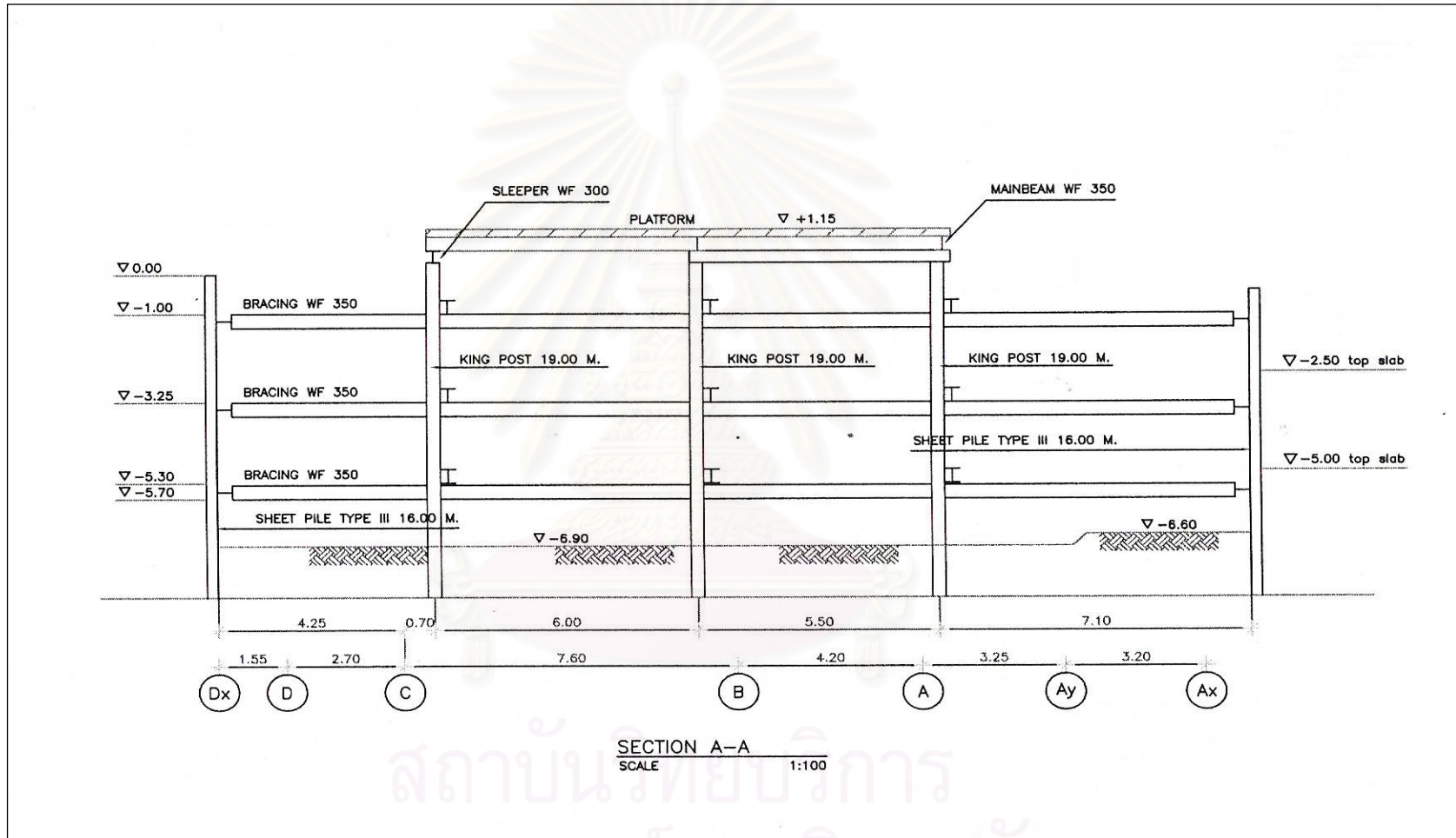
Figure 3.2 Layout of project (cross section)
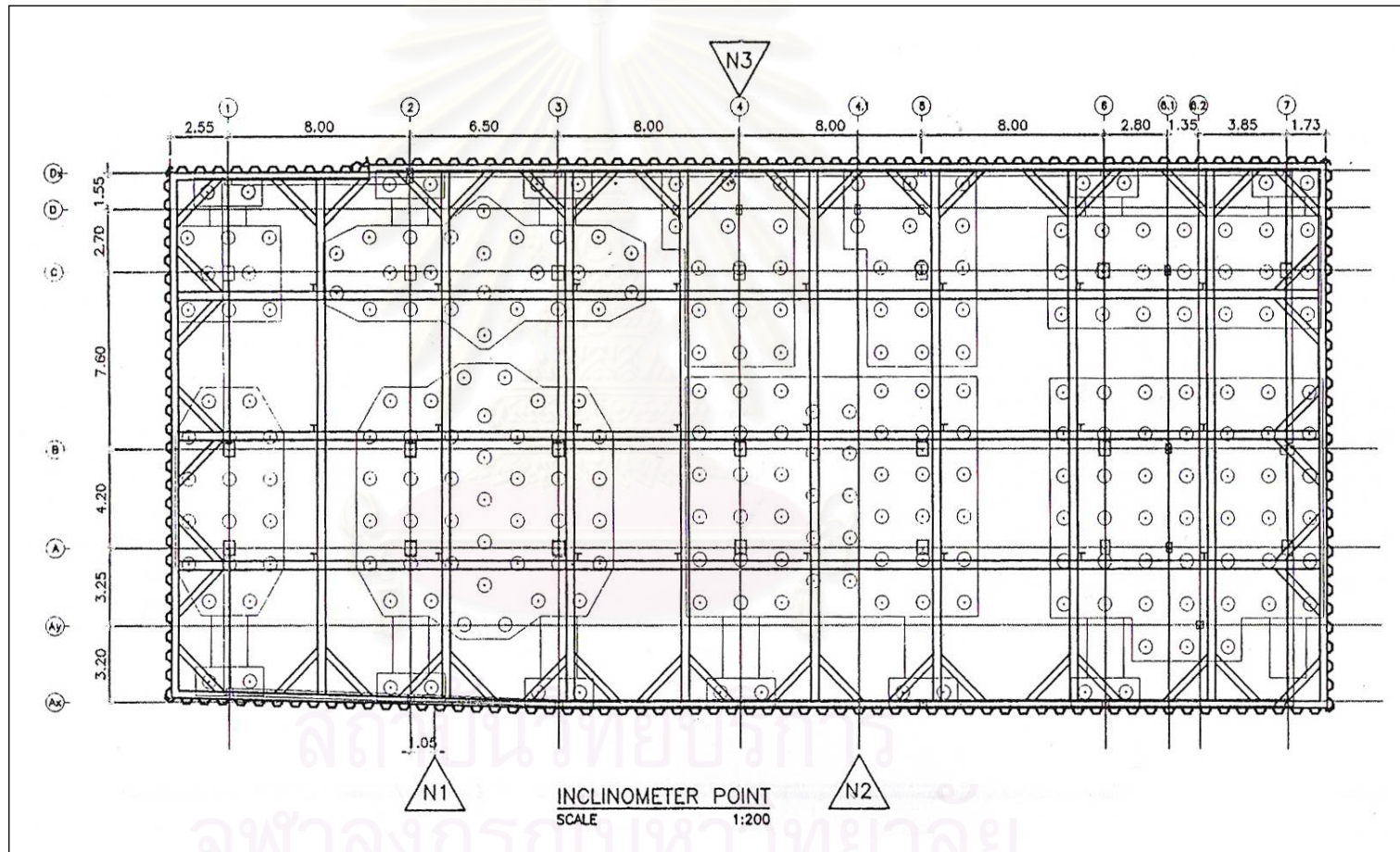
Figure 3.3 Position of inclinometers (plane view)
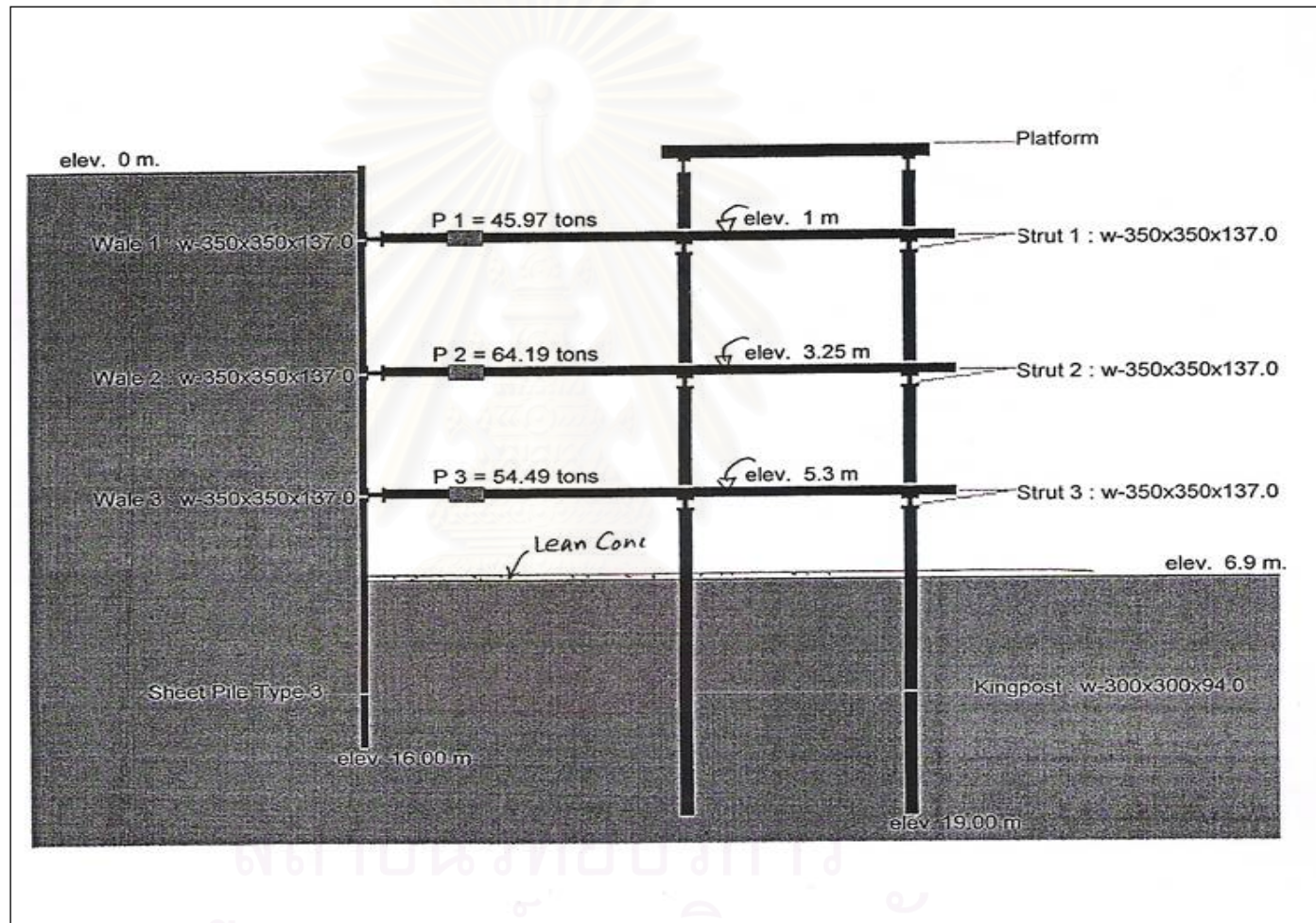
Figure 3.4 Typical cross section of bracing system
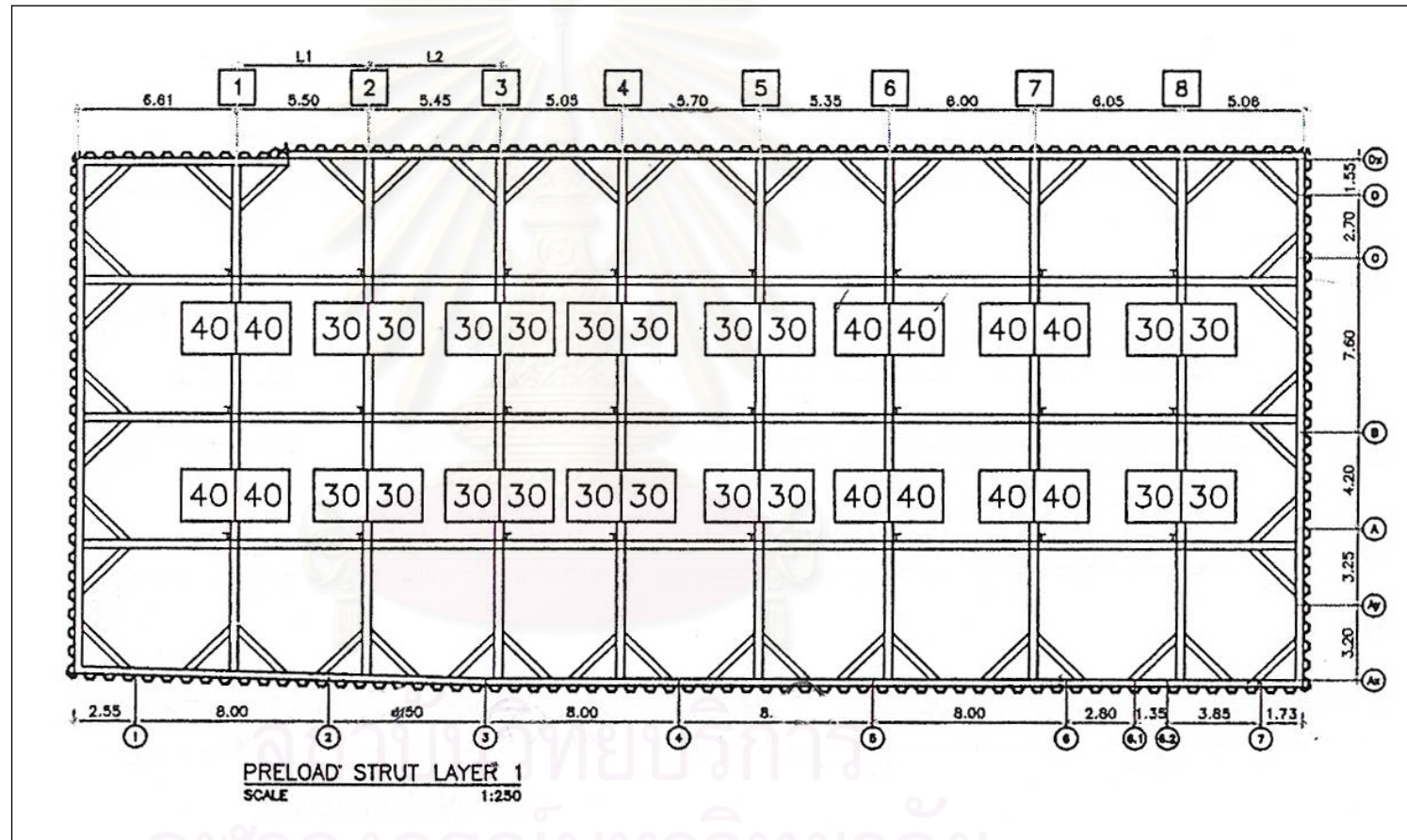
Figure 3.5 Layout of strut layer 01
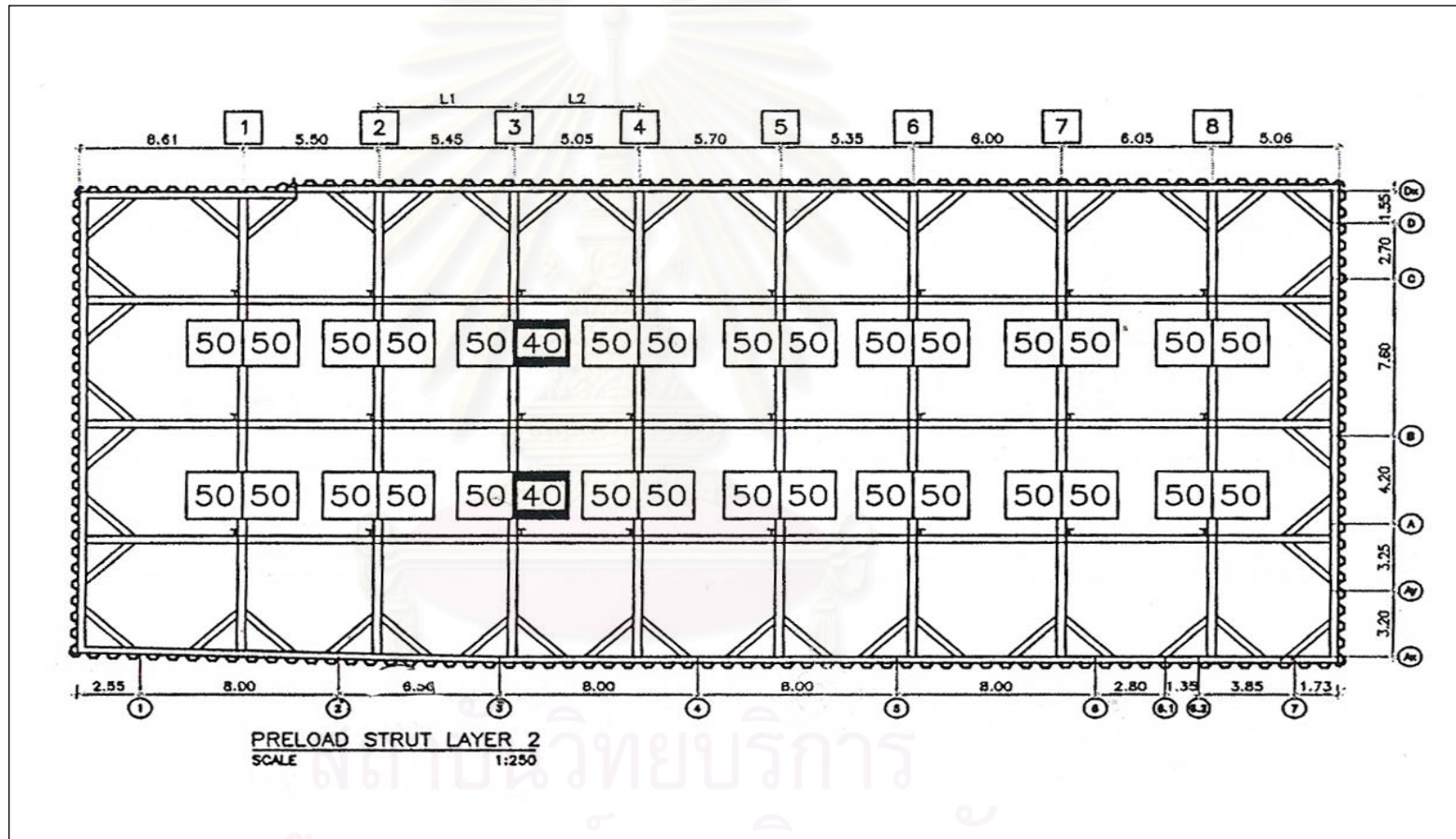
Figure 3.6 Layout of strut layer 02
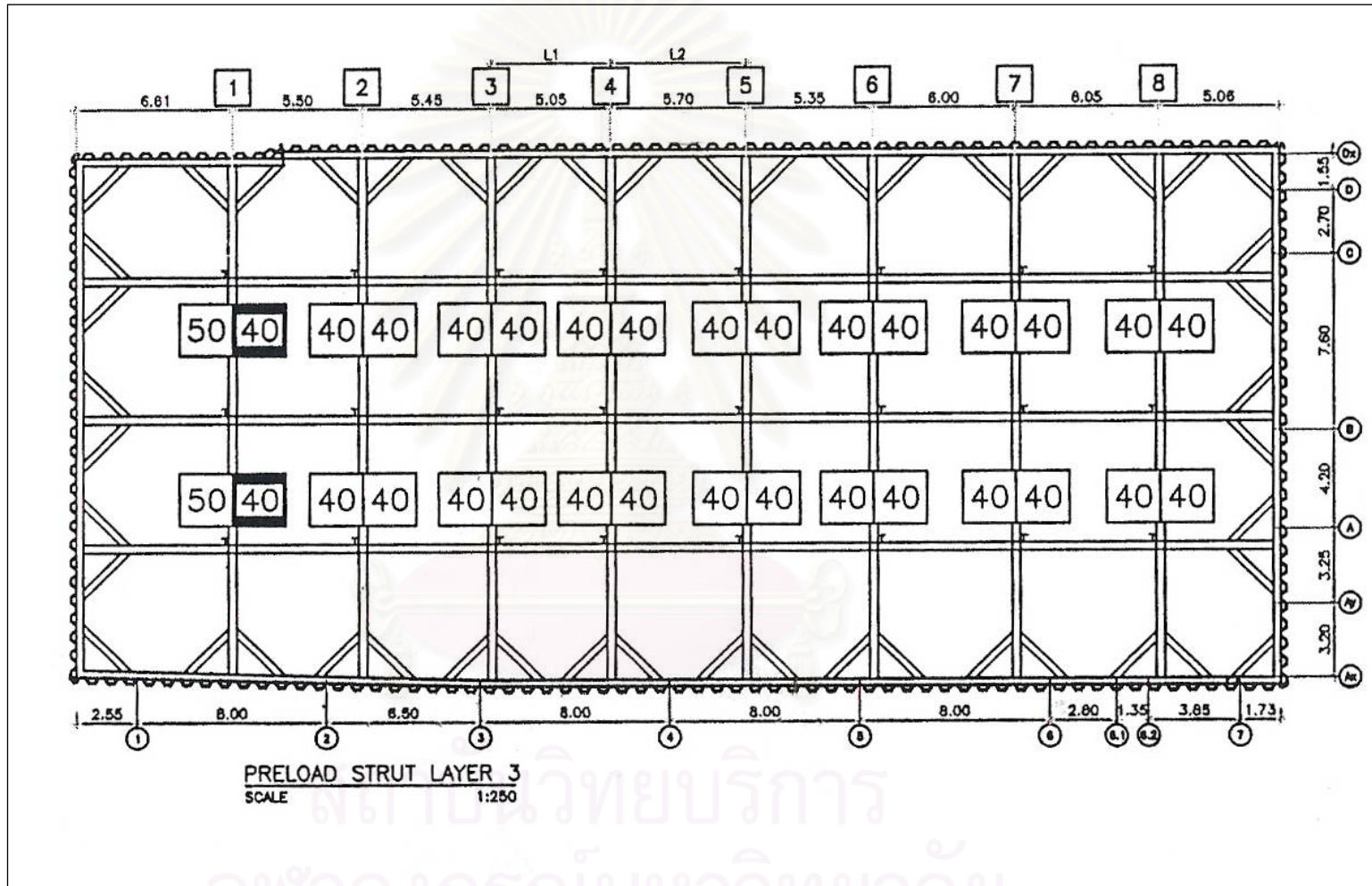
Figure 3.7 Layout of strut layer 03

3.2 Structural properties and excavations in the project

At the final depth of excavation, -6.1m and -6.90m below the ground surface, lean concrete was cast immediately after excavation reached the final depth. Its thickness was 15 mm and it was 8m from the sheet pile walls. The concrete's compressive strength is $f_c' = 240$ksc. The old residential building of three to four stories that located about 0.5 m from the sheet pile walls was very sensitive to the excavation works and behavior. So in this research, building properties and its surcharge were also included the analysis. In the simulation of building surcharge, each floor of building induced 1 t/m^2 to the excavation. The timber piles of 5m long were also included in the research analysis. The properties of lean concrete, concrete floor, and timber piles are summarized in the tables 3.1 to 3.5.

Preloading or prestressing of struts was also designed for the excavation work. Preloading by two hydraulic jacks for each strut was applied immediately after completion of each strut installation. Preloading was applied at both end of strut at the same time with the order of loading step.

The preloading in struts layer 01, 02, and 03 were designed at 30%, 50%, and 40%, respectively, of the apparent earth pressure diagram proposed by Terzaghi and Peck (1967). The magnitudes of the strut preloading of the three layers are shown in figures 3.5, 3.6, and 3.7.

The structural properties and excavation works are summarized below:

- Sheet piles:
  - Type: FSP III
  - Length: 16 m
- Wales:
  - Wales at layer 1: Type W 350x350x137.0
  - Wales at layer 2: Type W 350x350x137.0
  - Wales at layer 3: Type W 350x350x137.0
- Struts (8x3 numbers):
  - Layer 1: Type W 350x350x137.0 @ 6m
  - Layer 2: Type W 350x350x137.0 @ 6m
  - Layer 3: Type W 350x350x137.0 @ 6m
- Kingposts (10x3 numbers):
  - Type: W 300x300x94.0
  - Length: 19m
- Main-beam:
  - Type: WF 350
- Sleeper:
  - Type: WF 300
- Lean concrete:
  - Compressive strength: $f_c' = 240$ksc
  - Thickness: 0.15m
- Platform: At elevation 1.15m above road surface.

The depths excavated to install struts:
- Excavate to level -1.40m and install struts layer 01
- Excavate to level -3.70m and install struts layer 02
- Excavate to level -5.70m and install struts layer 03
- Excavate to level -6.90m and cast lean concrete.

Strut levels:
- Struts layer 01: -1.00m
- Struts layer 02: -3.25m
- Struts layer 03: -5.30m

Table 3.1 Sheet pile properties

Parameter	Name	Value	Unit
Type of behavior	Material type	Elastic	-
Normal Stiffness	EA	382000	t/m
Flexural Stiffness	EI	3360	t.m^2/m
Equivalent thickness	$d= \sqrt{12EA / EI}$	0.325	m
Weight	w	0.15	t/m/m
Poisson's ratio	υ	0.2	-

Table 3.2 Strut properties

Parameter	Name	Value	Unit
Type of behavior	Material type	Elastic	-
Normal Stiffness	EA	347800	t
Spacing out-of-plane	Ls	6	m
Max force	Fmax	1.10^15	t

Table 3.3 Lean Concrete properties

Parameter	Name	Value	Unit
Type of behavior	Material type	Elastic	-
Normal Stiffness	EA	279400	t/m
Flexural Stiffness	EI	524	t.m^2/m
Equivalent thickness	d	0.15	m
Weight	w	0.36	t/m/m
Poisson's ratio	υ	0.15	-

Table 3.4 Concrete properties of building floor

Parameter	Name	Value	Unit
Type of behavior	Material type	Elastic	-
Normal Stiffness	EA	763500	t/m
Flexural Stiffness	EI	5730	t.m^2/m
Equivalent thickness	d	0.3	m
Weight	w	1.2	t/m/m
Poisson's ratio	υ	0.15	-

Table 3.5 Timber pile properties

Parameter	Name	Value	Unit
Type of behavior	Material type	Elastic	-
Normal Stiffness	EA	17100	t/m
Flexural Stiffness	EI	24.12	t.m^2/m
Equivalent thickness	d	0.13	m
Weight	w	0.011	t/m/m
Poisson's ratio	υ	0.3	-

3.3 Soil conditions

The unconfined compression test and standard penetration test (SPT) were carried out before excavation. Two boring logs BH-01 and BH-02 were investigated in the field before excavation process. The two boring logs were plotted together as shown in figure 3.8.

From the fig.3.8, the soil was classified as follows:

1) Weathered crust from depth of 0 m to 2.00 m with Su(UC) equals $2.15\,t/m^2$.

2) Soft clay layer 01 from depth of 2.00 m to 7.50 m with Su (UC) equals $1.40\,t/m^2$.

3) Soft clay layer 02 from depth 0f 7.50 m to 12.75 m with Su (UC) equals $2.23\,t/m^2$

4) Stiff silty clay from depth of 12.75 m to 14.00 m with SPT equals 13 blows/ft.

5) Very stiff silty clay from depth of 14.00m to 19.00m with SPT equals 20 blows/ft.
6) Very stiff to hard silty clay from depth of 19.00m to 21.45m with SPT equals 27 blows/ft.

The undrained shear strength from unconfined compression test does not simulate the strength in the field. It has lower values of undrained shear strength because of sample disturbance. As a result, in the case of weathered crust layer, soft clays layers 01 and 02, in which their undrained shear strength obtained from unconfined compression test was converted to undrained shear strength of field vane shear test (FVT) by the following relation:

$Su(UC) = \beta \, Su \, (FV)$
For Bangkok soft clay, $\beta = 0.75$

So $Su(FV) = \dfrac{Su(UC)}{0.75}$

In the case of the stiff to very stiff silty clay, in which SPT were conducted, the correlation between number of blows/ft and undrained shear strength was related:

$Su \text{ (undisturbed) } (t/m^2) = 0.685 \, N \text{ (for Bangkok clay)}$

The coefficient of lateral earth pressure, Ko, can be calculated by the relation:

$K_o = 0.65(OCR)^m$

OCR = overconsolidated ratio
m is a parameter that correlates with plasticity index (Ladd et al, 1977) as shown in figure 3.9.
PI = 27% in the project. From the figure 3.9, m=0.4.
OCR = 1.8 for weathered crust
OCR = 1.6 for soft clay
OCR = 2.0 for stiff clay
Table 3.6 shows the values of the coefficient of lateral earth pressure, Ko, for all the six layers of soil.
The reduction factor was calculated according to figure 3-10.
The overall soil classification and its parameters were summarized in the table 3.7.

Table 3.6 Values of Ko

Soil layers	Ko
Weathered Crust	0.82
Soft Clay layer 1	0.78
Soft Clay layer 2	0.78
Stiff Silty Clay	0.86
Very Stiff Silty Clay	0.86
Very Stiff to Hard Silty Clay	0.86
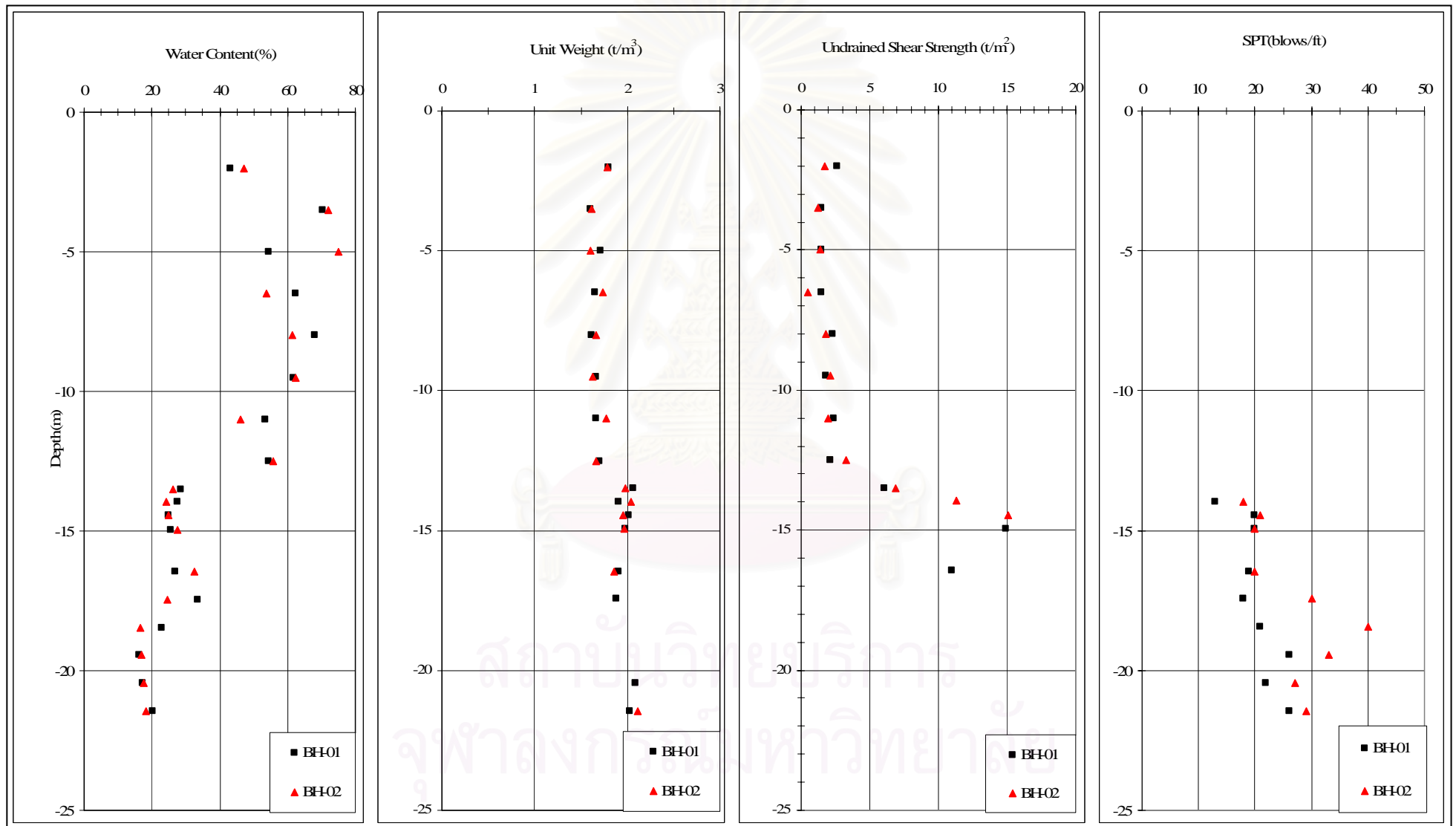
Figure 3.8 Subsoil condition for this research project
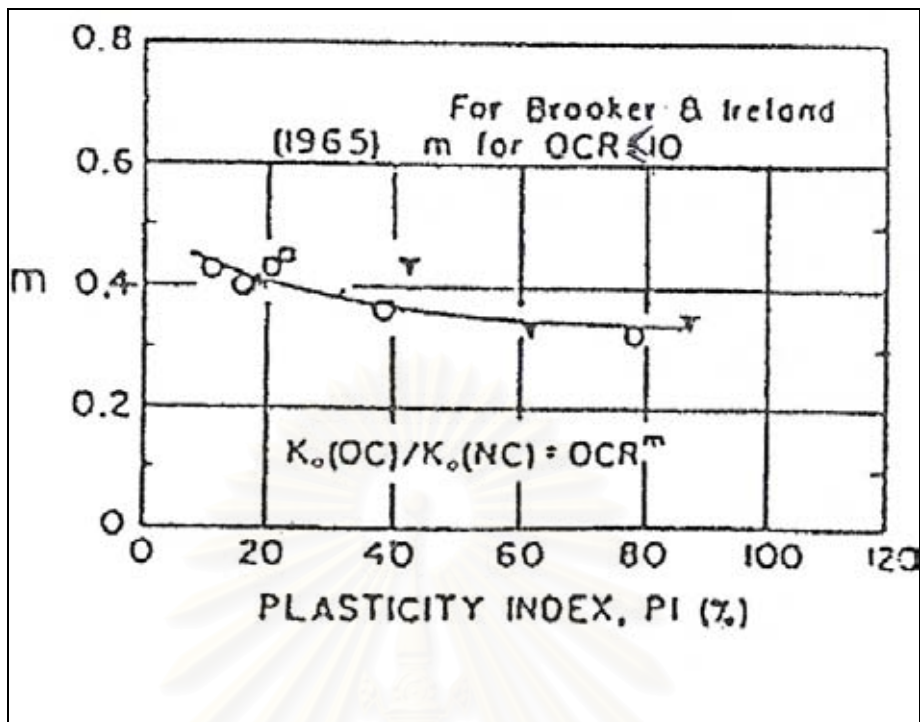
Figure 3.9 Parameter m and PI(%) (Brooker & Ireland, 1965)
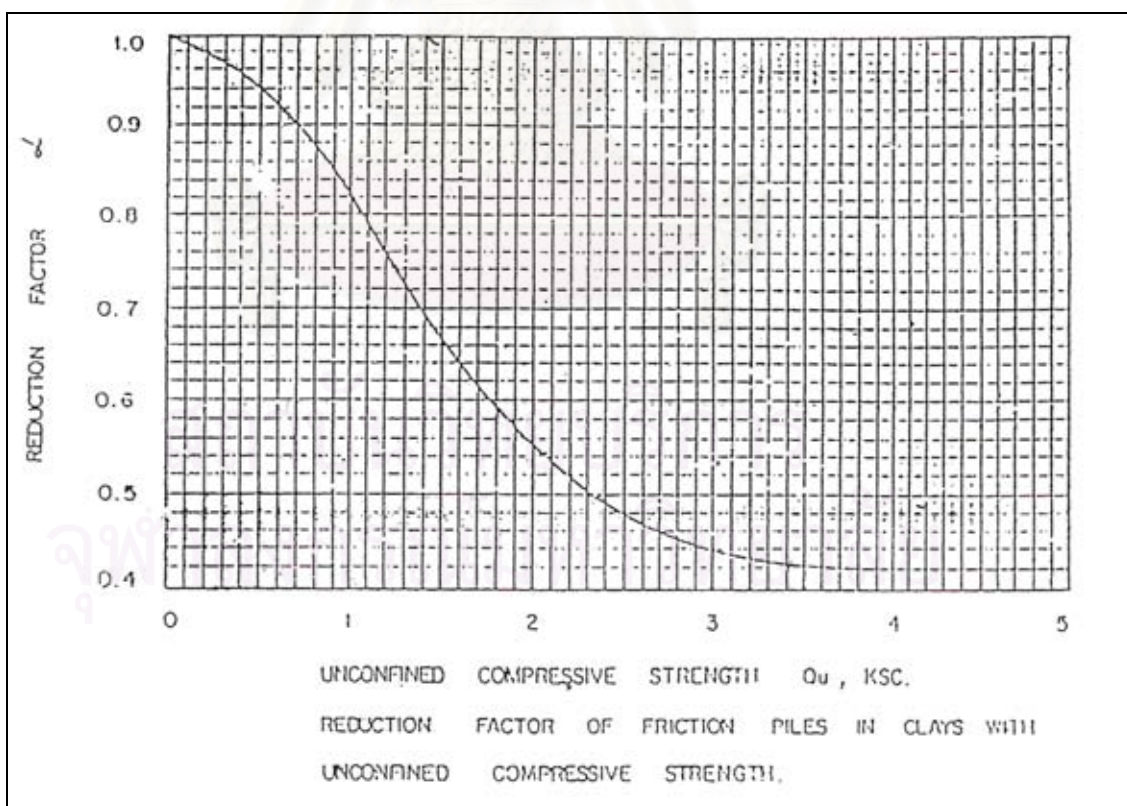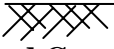
Figure 3.10 Reduction factor coefficient (Teparaksa, 1999)

Table 3.7 Summary of soil properties in this research project

Depth (m)	Wn(%)	$\gamma_t(t/m^3)$	$\gamma_d(t/m^3)$	Su(UC) (t/m²)	N(SPT) (blows/ft)	Su(FV) (t/m²)	Su (t/m²)	α
EL. 0.00 Weathered Crust	45	1.80	1.24	2.15	-	2.87	-	0.95
EL. -2.00 Soft Clay layer 01	62	1.65	1.02	1.4	-	1.87	-	0.96
EL. -7.50 Soft Clay layer 02	59	1.66	1.04	2.23	-	2.97	-	0.95
EL. -12.75 Stiff Silty Clay	26	2.00	1.59	-	13	-	8.90	0.60
EL. -14.00 Very Stiff Silty Clay	26	2.00	1.59	-	20	-	13.70	0.45
EL. -19.00 Very Stiff to Hard Silty Clay	17	2.00	1.71	-	27	-	18.50	0.45
EL. -21.45								

สถาบันวิทยบริการ
จุฬาลงกรณ์มหาวิทยาลัย

3.4 Sequential stages of construction

Construction sequences and workmanship are ones of the main parts of several influence factors in the deep excavation. These influence factors can considerably affect the shape and behavior of lateral sheet pile wall movements. The construction sequences and workmanship in the research project were summarized as follows:

1. Driving sheet piles (at –16 m) and driving kingposts and install platform.
2. - Excavation to -1.40m by excavating at the center area with installation of bracing system by keeping soil berm at both ends. Bracing layer 01 at -1.00m.
   - Excavate soil berm and extend the one line by one line bracing system to be fully braced.
   - Preload struts line by line.
3. - Excavate to -3.70m by excavating at the center area with installation of bracing system by keeping soil berm at both ends. Bracing layer 02 at -3.25m.
   - Excavate soil berm and extend the one line by one line bracing system to be fully braced.
   - Preload struts line by line.
4. - Excavate to -5.70m by excavating at the center area with installation of bracing system by keeping soil berm at both ends. Bracing layer 03 at -5.30m.
   - Excavate soil berm and extend the one line by one line bracing system to be fully braced.
   - Preload struts line by line.
5. Excavation to final depth and casting lean concrete
6. Remove bracing struts layer 03 and casting foundation, basement slab and extend reinforced concrete wall and then backfill sand between the RC wall and sheet pile walls.
7. Remove bracing struts layer 02 and casting foundation, basement slab and extend reinforced concrete wall and then backfill sand between the RC wall and sheet pile walls.
8. Remove bracing struts layer 01 and casting foundation, basement slab and extend reinforced concrete wall and then backfill sand between the RC wall and sheet pile walls.
9. Remove sheet pile walls and platform.

The important construction sequences are shown in figure 3.11 to 3.18.
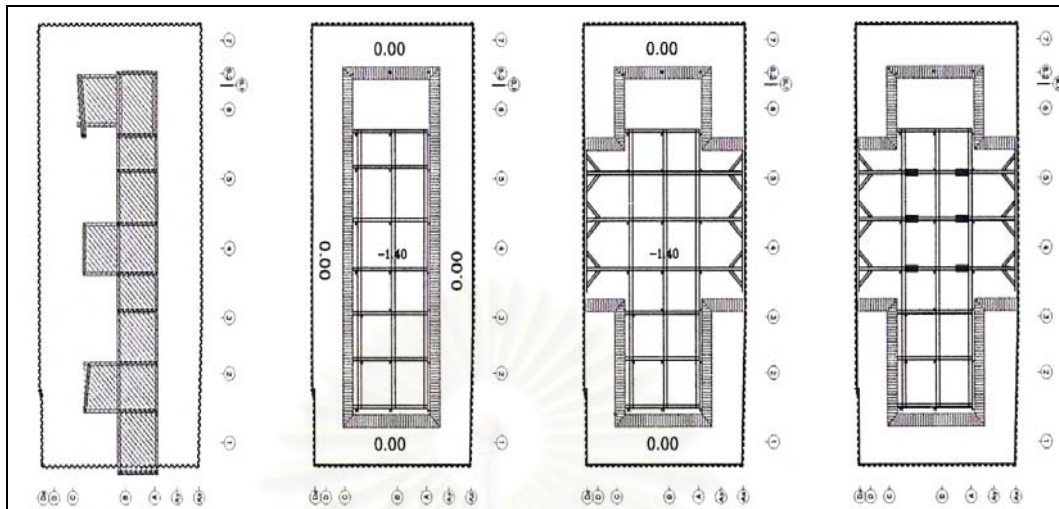
Figure 3.11 Excavation to -1.40m and install struts layer 01
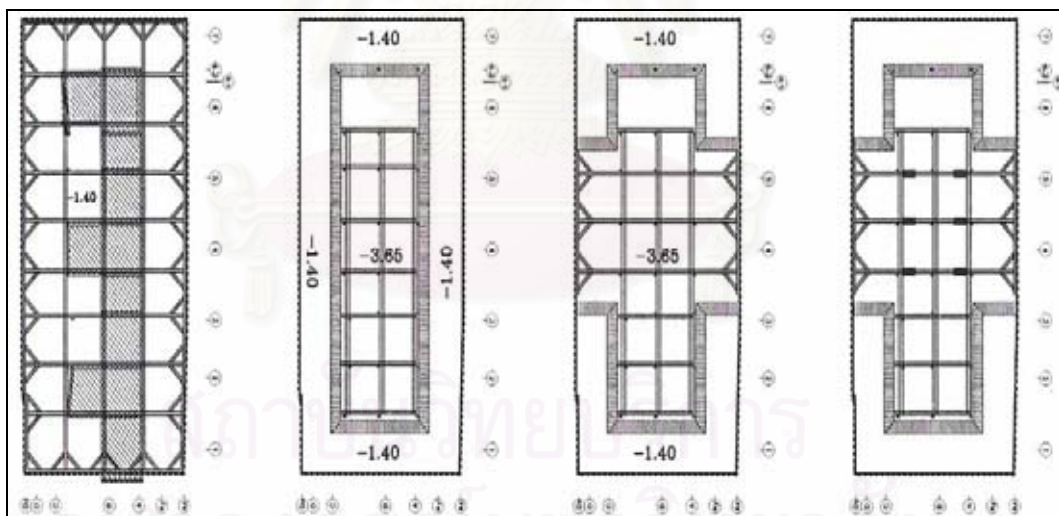
Figure 3.12 Excavation to -3.70m and install struts layer 02
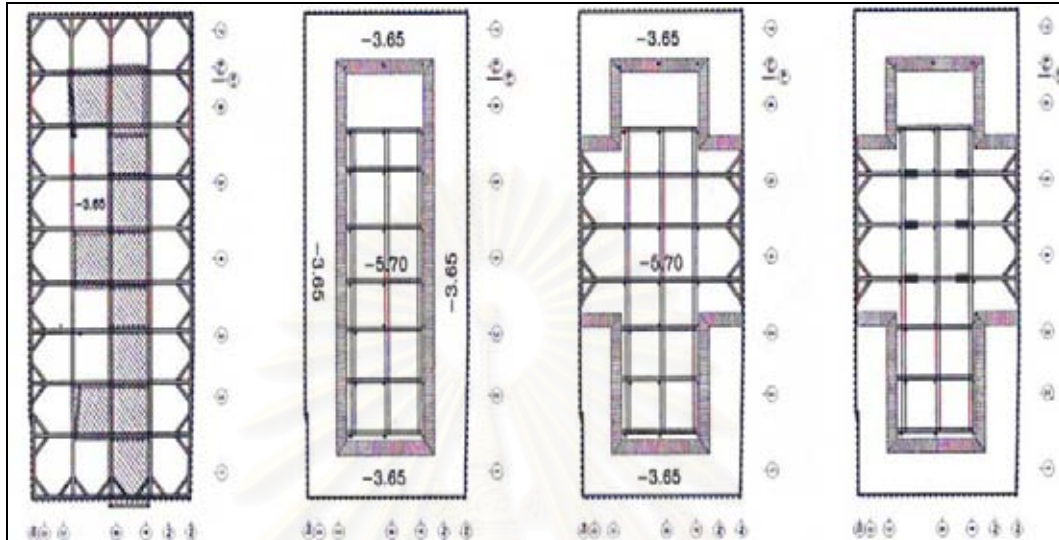
Figure 3.13 Excavation to -5.70m and install struts layer 03
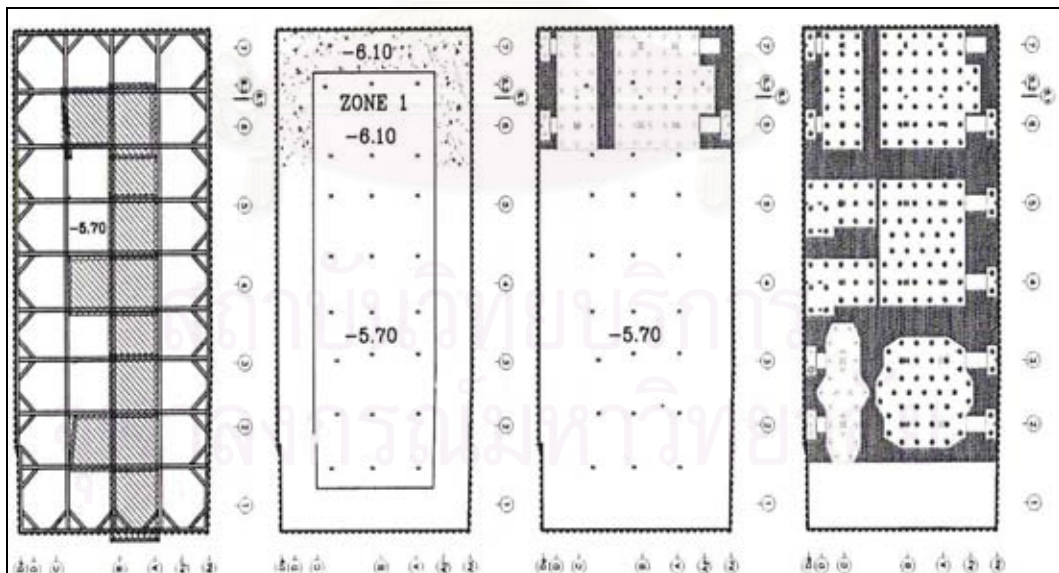
Figure 3.14 Final excavation and cast lean concrete
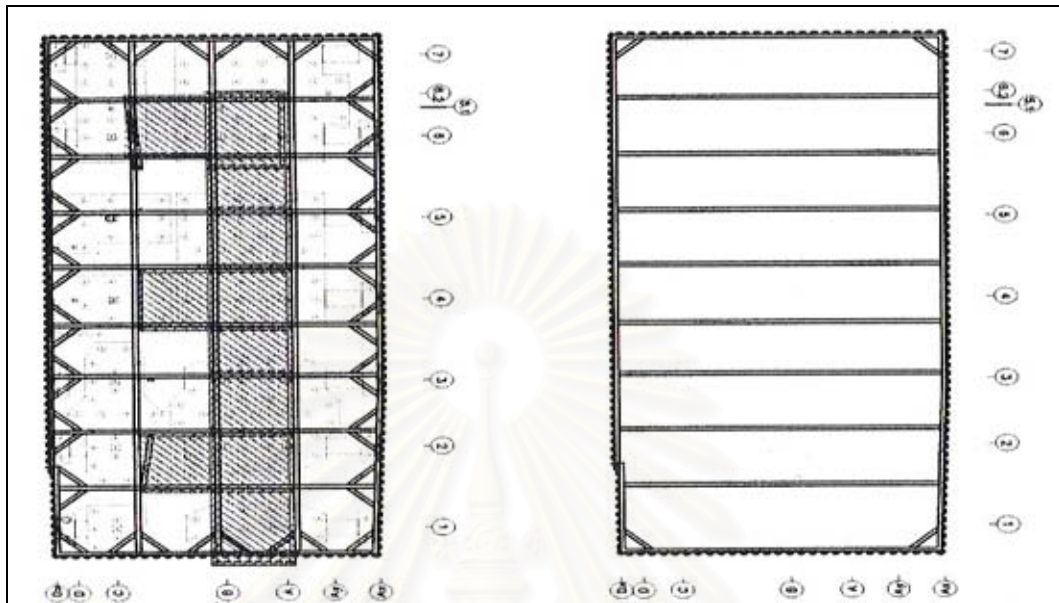
Figure 3.15 Remove struts layer 03
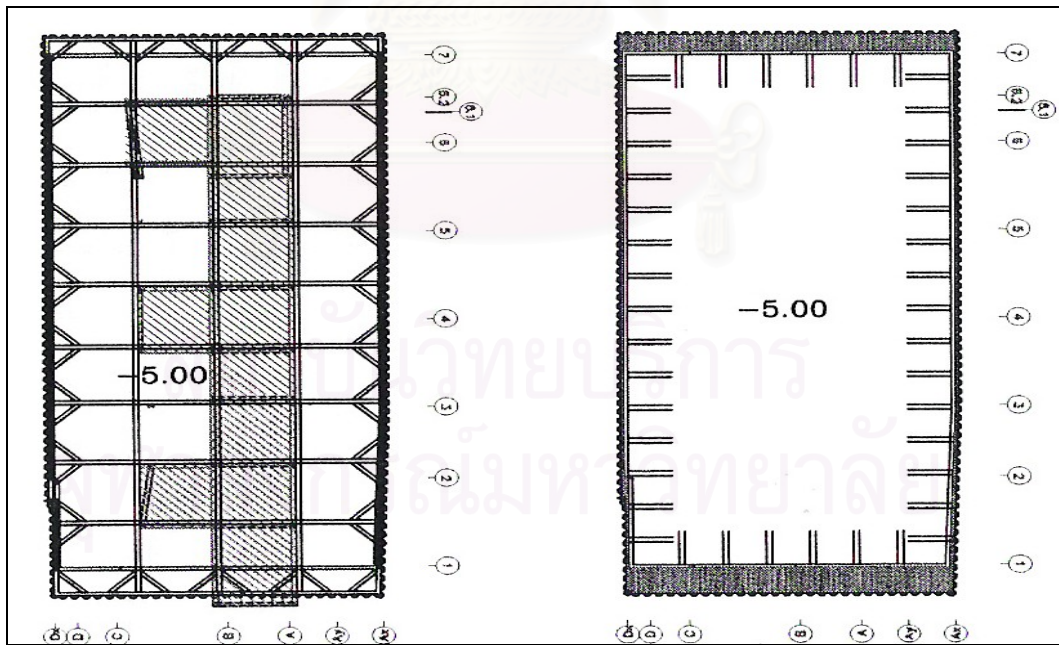
Figure 3.16 Remove struts layer 02
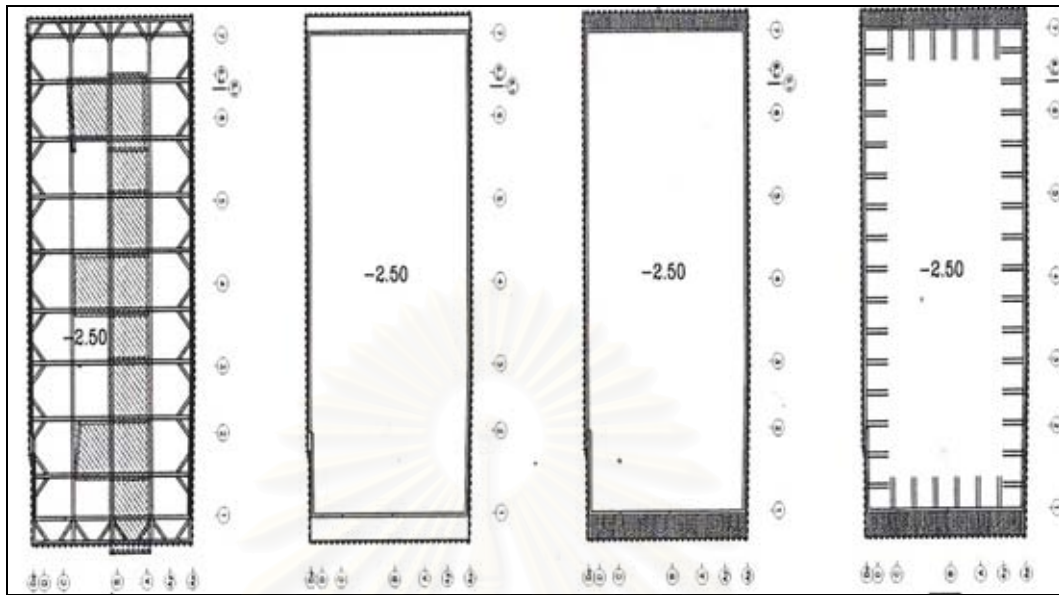
Figure 3.17 Remove struts layer 01
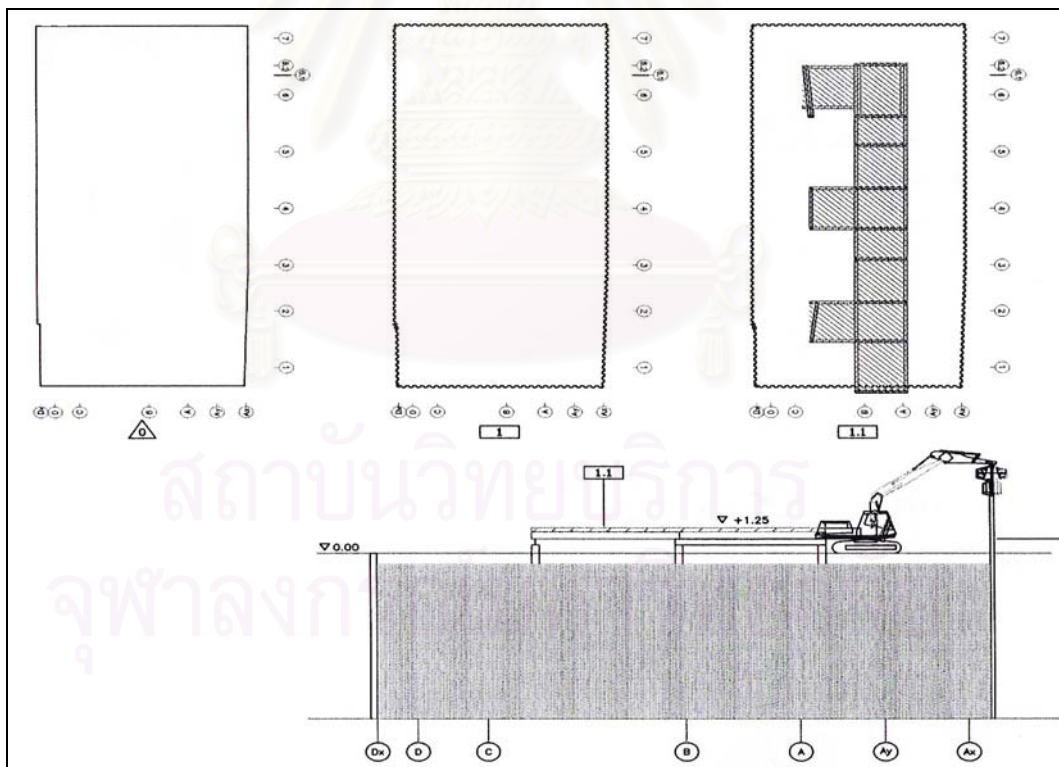
Figure 3.18 Remove sheet pile walls and platform

3.5 Data analysis and interpretation

The analysis and interpretation were divided into two parts: the first part was the analysis of field data of inclinometers by construction sequences and the second part was the analysis of field data by numerical analysis (FEM) in PLAXIS.

3.5.1 Analysis and interpretation of field data and its behavior

All the data from the three inclinometers were collected. But the data from inclinometer No 03 broke down in the field. The lateral sheet pile wall movements of inclinometers No 01 and No 02 were classified and were plotted against depth by sequential stages of construction as follows:
1. Excavation to -1.40m and installation of struts layer 01
2. Preloading of struts layer 01
3. Excavation to -3.70m and installation of struts layer 02
4. Preloading of struts layer 02
5. Excavation to -5.70m and installation of struts layer 03
6. Preloading of struts layer 03
7. Final excavation -6.90m and cast lean concrete.
8. Removing of struts layer 03
9. Removing of struts layer 02
10. Removing of struts layer 01

The plots of lateral wall movements δ_H (mm) of sheet pile against depth (m) for inclinometer No 01 and No 02 are shown in figures 3.19, 3.20, 3.21, and 3.22.
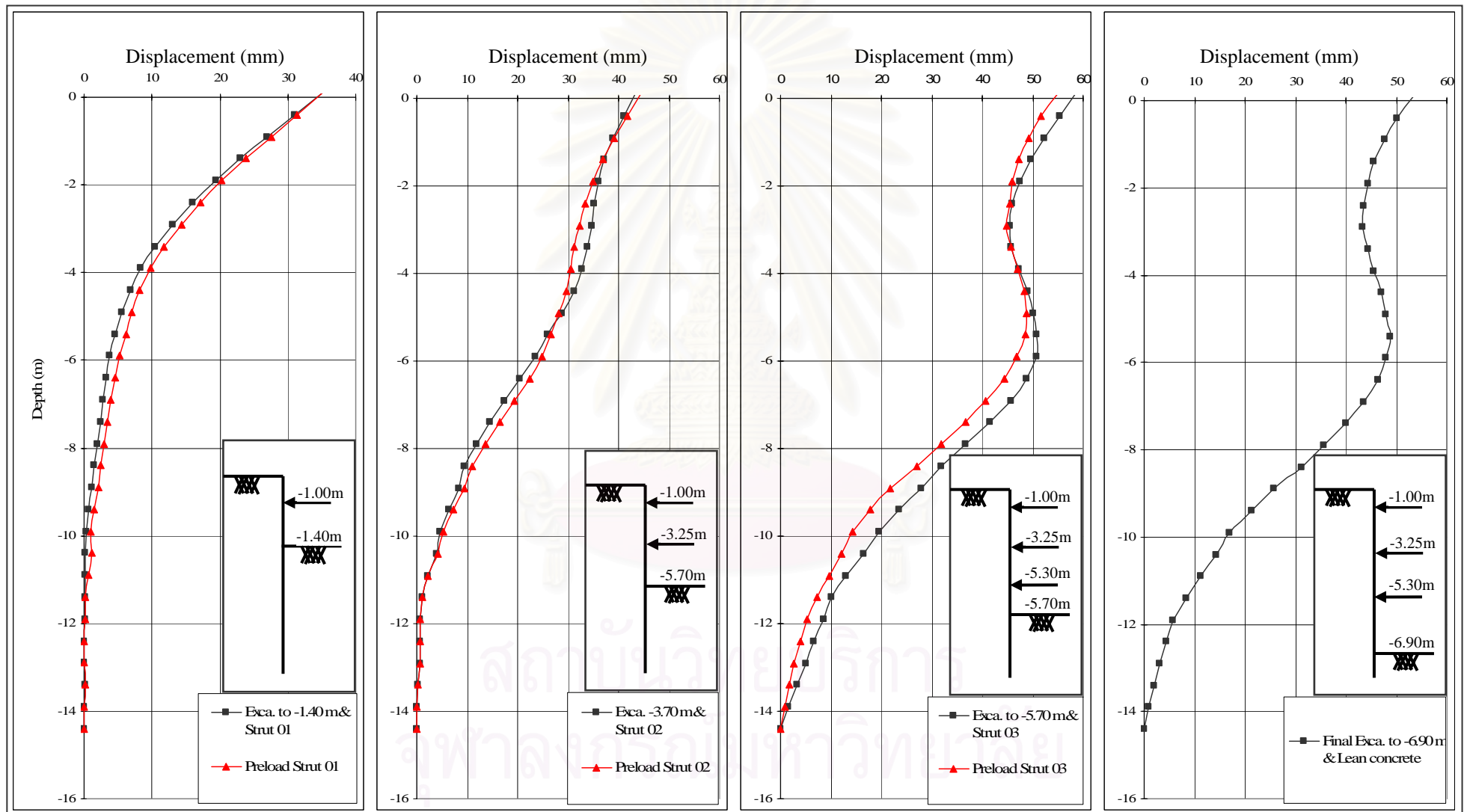
Figure 3.19 Lateral sheet pile wall movement of field inclinometer 01
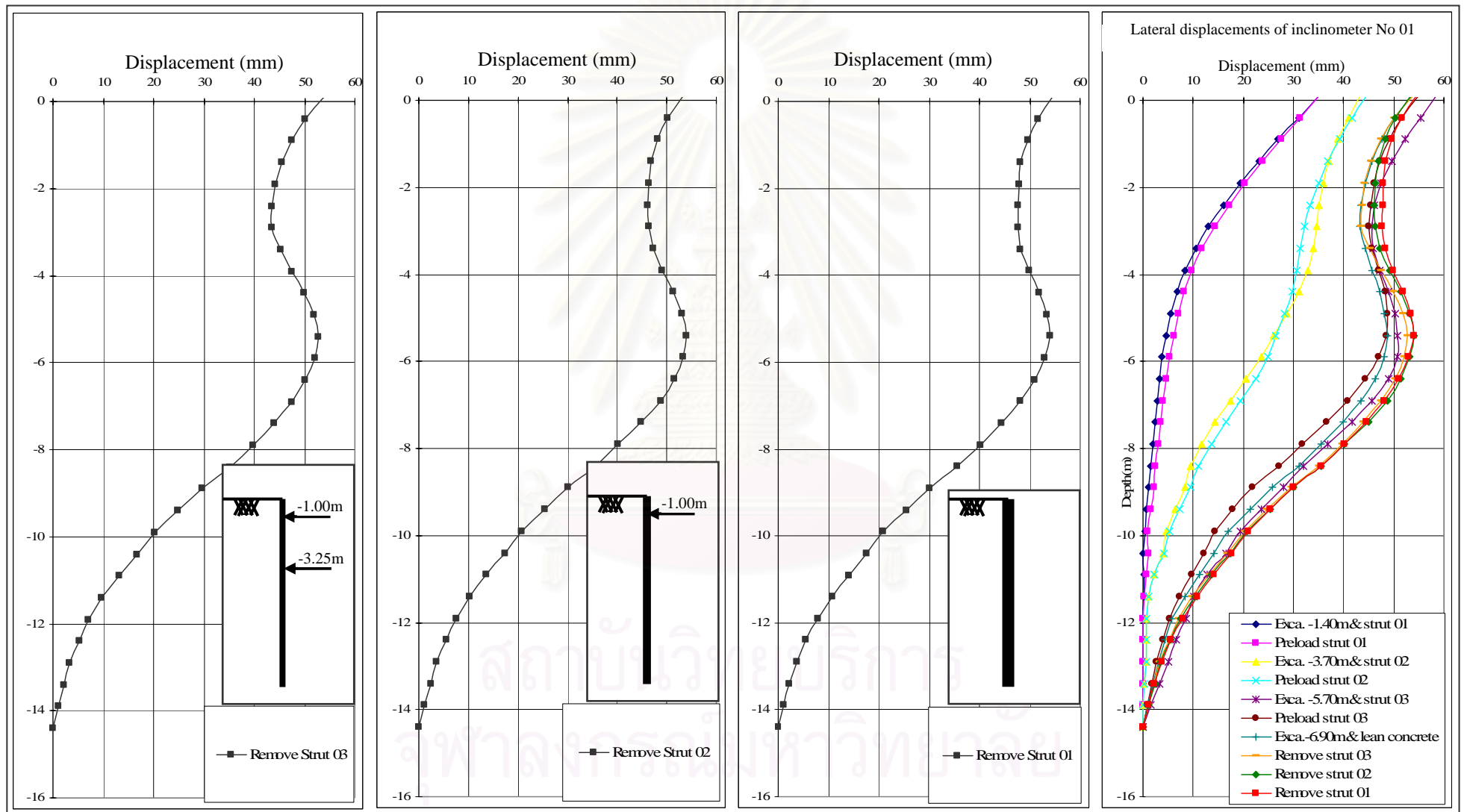
Figure 3.20 Lateral sheet pile wall movement of field inclinometer 01
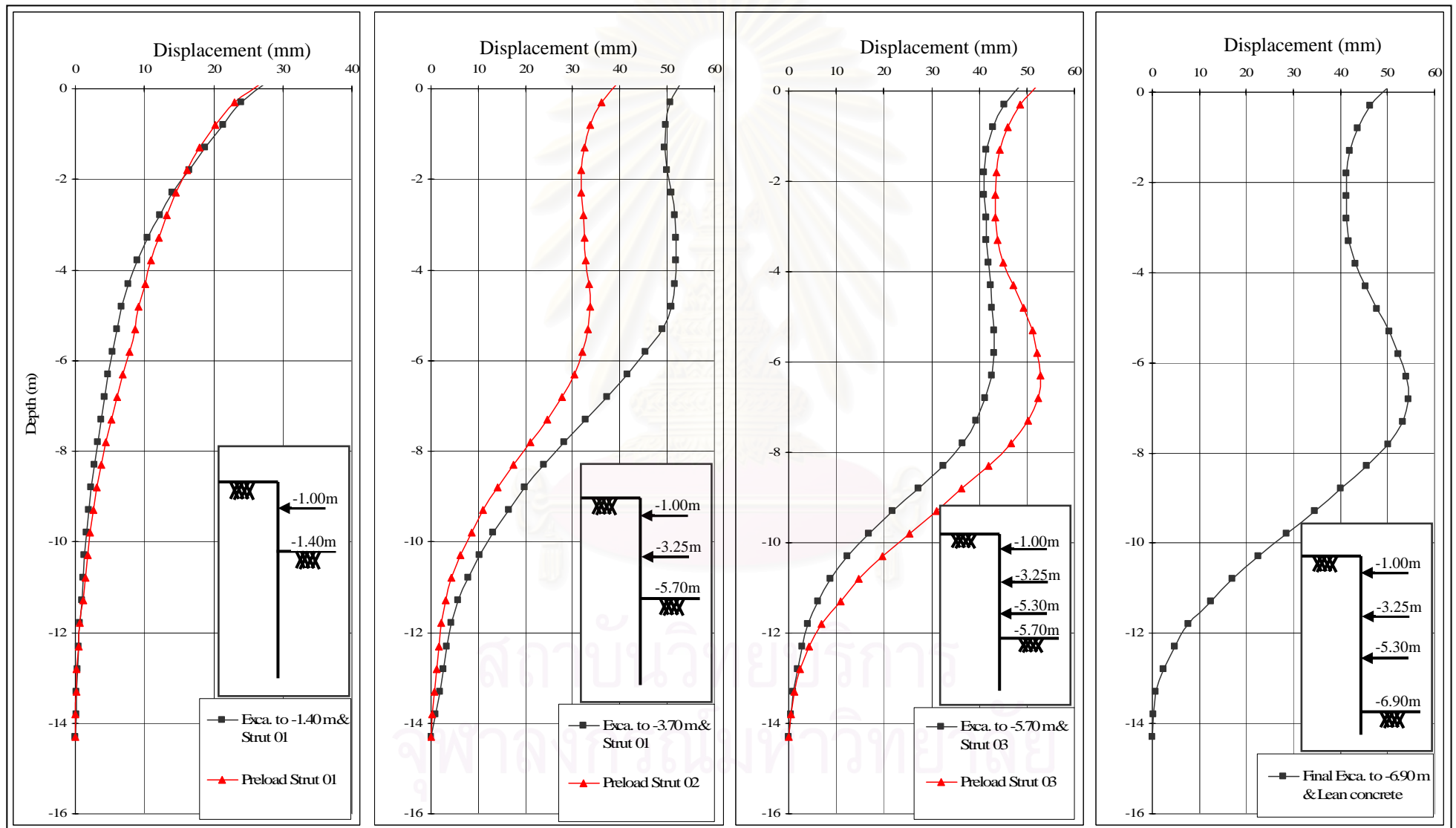
Figure 3.21 Lateral sheet pile wall movement of field inclinometer 02
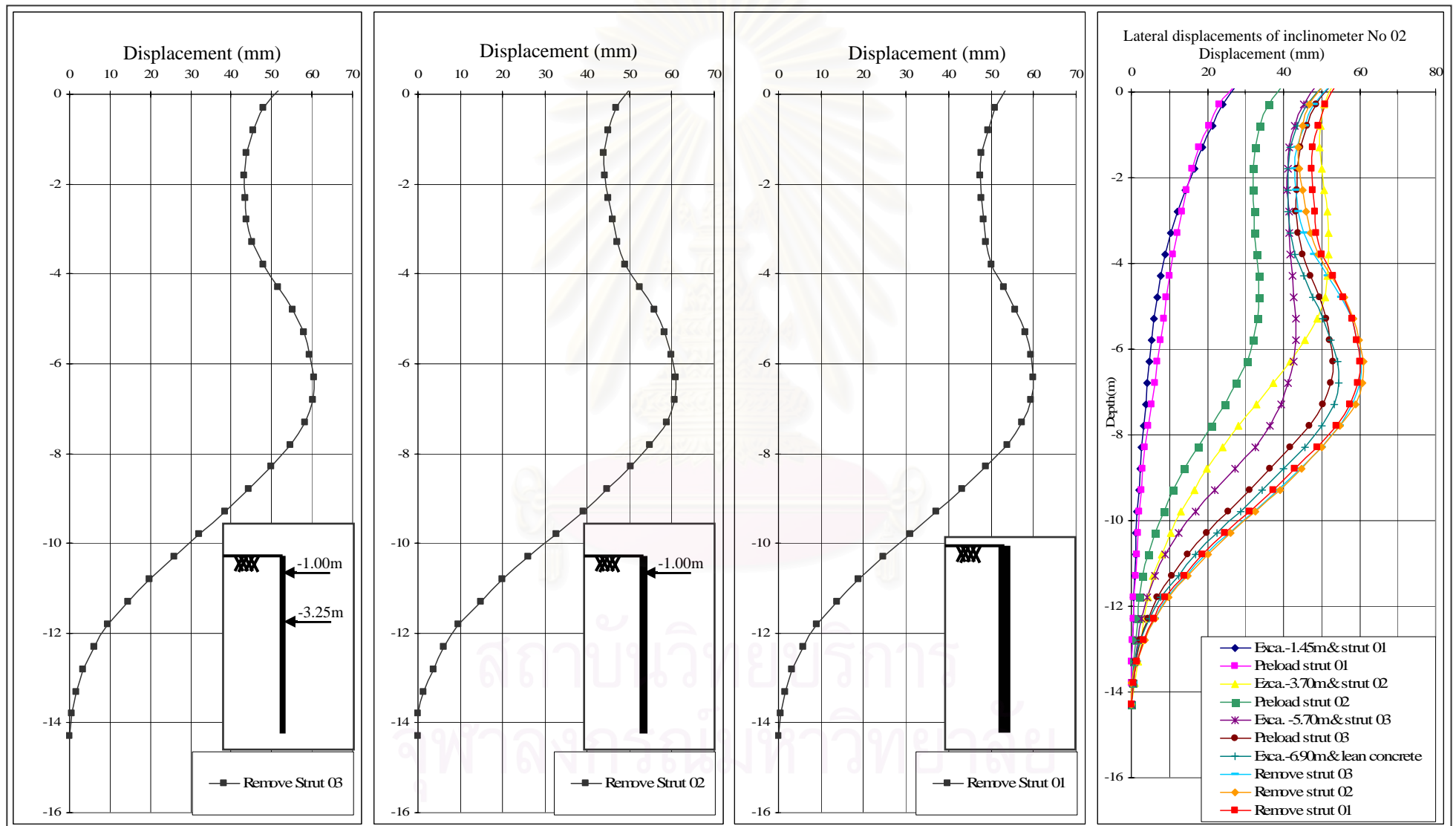
Figure 3.22 Lateral sheet pile wall movement of field inclinometer 02

From the figures 3.19, 3.20, 3.21, and 3.22, maximum lateral sheet pile wall movements can be found as follows.

Inclinometer No 01:

1. Excavation to -1.40m and installation of struts layer 01, $\delta_{H\,max} = 35mm$

2. Preloading of struts layer 01, $\delta_{H\,max} = 35mm$

3. Excavation to -3.70m and installation of struts layer 02, $\delta_{H\,max} = 43mm$

4. Preloading of struts layer 02, $\delta_{H\,max} = 44mm$

5. Excavation to -5.70m and installation of struts layer 03, $\delta_{H\,max} = 51mm$

6. Preloading of struts layer 03, $\delta_{H\,max} = 49mm$

7. Final excavation -6.90m and cast lean concrete, $\delta_{H\,max} = 49mm$

8. Removing of struts layer 03, $\delta_{H\,max} = 53mm$

9. Removing of struts layer 02, $\delta_{H\,max} = 54mm$

10. Removing of struts layer 01, $\delta_{H\,max} = 54mm$

Inclinometer No 2:

1. Excavation to -1.40m and installation of struts layer 01, $\delta_{H\,max} = 28mm$

2. Preloading of struts layer 01, $\delta_{H\,max} = 28mm$

3. Excavation to -3.70m and installation of struts layer 02, $\delta_{H\,max} = 52mm$

4. Preloading of struts layer 02, $\delta_{H\,max} = 34mm$

5. Excavation to -5.70m and installation of struts layer 03, $\delta_{H\,max} = 44mm$

6. Preloading of struts layer 03, $\delta_{H\,max} = 54mm$

7. Final excavation -6.90m and cast lean concrete, $\delta_{H\,max} = 55mm$

8. Removing of struts layer 03, $\delta_{H\,max} = 61mm$

9. Removing of struts layer 02, $\delta_{H\,max} = 62mm$

10. Removing of struts layer 01, $\delta_{H\,max} = 60mm$

Maximum sheet pile wall movements from inclinometer data for each stage of construction were normalized by dividing with corresponding depths of excavation $\left(\dfrac{\delta_{H\,max}}{H}\right)(\%)$. The nondimensional number, $\left(\dfrac{\delta_{H\,max}}{H}\right)$, was plotted with the factor of safety against basal heave that was proposed by Terzaghi and Peck (1967).

From Terzaghi and Peck (1967), the factor of safety was calculated as follows:

From Terzaghi and Peck (1967), the factor of safety was calculated as follows:

$$FS = \frac{5.7 \times S_{u2}(1 + 0.2B'/L)}{\left(\gamma + q/H - S_{u1}/B\right) \times H}$$

Where $B' = T$ or ($B/\sqrt{2}$), whichever smaller.

T= -16 m below ground surface.

The calculation of FS with depths of excavation was summarized in table 3.8.

Table 3.8 Calculation of FS with depths of excavation

Parameters / Depths(m)	B' (m)	$1 + 0.2B'/L$ (m)	γ (t/m^3)	S_{u1} (t/m^2)	S_{u2} (t/m^2)	FS
-1.40	14.60	1.06	1.80	2.87	2.87	2.77
-3.70	12.30	1.05	1.73	2.41	2.87	1.155
-5.70	10.30	1.04	1.70	2.22	2.87	0.889
-6.90	9.10	1.04	1.69	2.16	2.87	0.786

3.5.2 Finite Element Analysis in PLAXIS

Finite element analysis in PLAXIS (Brinkgreve & Vermeer, 2001) was used in this research. The finite element technique was utilized to back-analyze in-situ soil stiffness parameters Eu/Su for weathered crust, soft clays, stiff clay, and very stiff clay by considering sequential stages of construction, in which the author well observed and well documented, in this research project. The method of the back-analysis was conducted by using trial and error process. The values Eu/Su of all the six soil layers were iteratively adjusted in Finite Element Analysis to best fit the results of FEM lateral wall movements with field inclinometers.

The research project was modeled with undrained analysis with undrained parameters. Plane strain condition and 6-node triangular elements with very fine meshes were used in the analysis. Failure criteria of Mohr -coulomb model with undrained parameters were modeled for all soil layers. Poisson's ratio, $\nu = 0.495$, were inserted in the undrained analysis. Undrained shear strengths from correlated field vane tests and SPT in the field were used in the process. The piezometric drawdown from deep well pumping in Bangkok, the building surcharge and its

timber piles, and traffic loading were considered in the numerical analysis. The stages of construction and the values of strut preloading were carefully and well analyzed in this research. Figures 3.23 and 3.24 show finite element meshes of the research project.
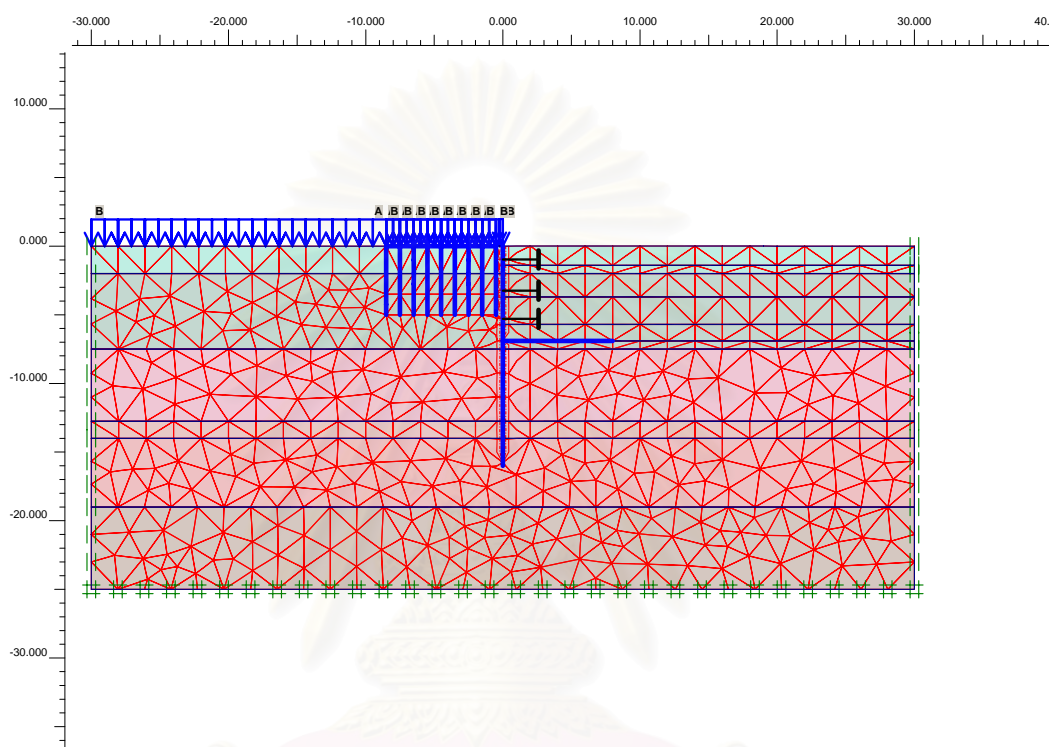
Figure 3.23 Finite Element mesh for the research project
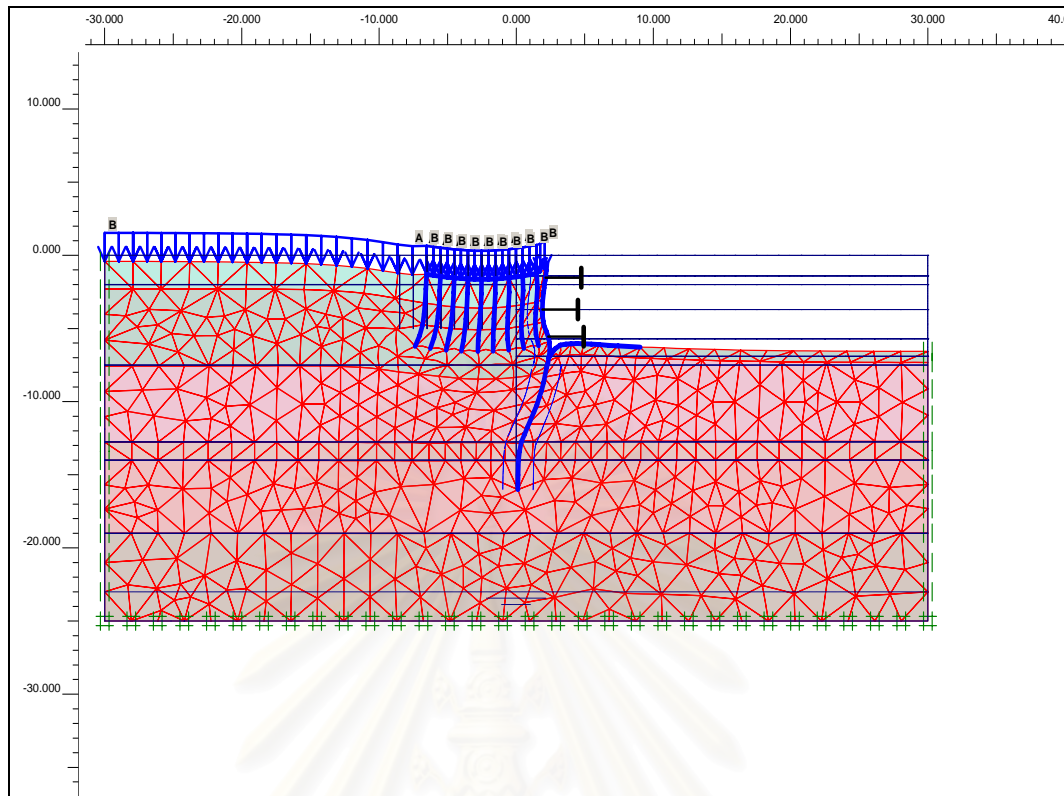
Figure 3.24 Finite Element mesh for the research project

CHAPTER IV

RESULTS AND DISCUSSIONS

4.1 Generality

The method of back-analysis of soil stiffness and its results are discussed in details in this chapter. A number of influence factors affecting the braced sheet-pile wall movements such as the factor of safety against basal heave, depths of excavation, time effect is shown. Data from five sheet pile case histories of excavation works in Bangkok were used to modify the relationship between $\delta_{H\max} / H$ and factor of safety against basal heave by Mana & Clough (1981) to well predict the behavior of sheet pile walls in Bangkok. Some results from observations of field behavior are also indicated in this research.

4.2 FEM analysis and results

Soil stiffness is very important for designing and analysis. Finite Element Method was used to conduct back-analysis of Bangkok soil stiffness Eu/Su by comparing FEM lateral wall movements with those from the field. The geotechnical engineers realize that the Young's modulus is dependent on the order of shear strain level.

Mair (1993) used the ideas to correlate the shear strain (ε_S) with shear modulus (G) as shown in figure 2.23. Mair conducted many kinds of experiments such as bender element, resonant column, conventional, and triaxial testings. Mair also determined typical strain range for different structures such as retaining walls, foundations, tunnels in the $\varepsilon_S - G$ graph.

From Self-Boring Pressuremeter tests during the design of the first MRT blue line in Bangkok city, Teparaksa (1999) presented the correlation between soil stiffness in terms of G/Su and shear strain as shown in figure 2.24.

Using Mair's and Teparaksa's frameworks, back-analysis to obtain the values of Eu/Su in the field can be searched.

In the back-analysis, PLAXIS was used to make trials and errors by varying the values of Eu/Su for all soil layers in PLAXIS so that the curves of lateral wall movements from FEM analysis well fit with the inclinometer data in the field.

The graphs of lateral wall movements from inclinometers No 01 and No 02 are shown together in figure 4.1.

Note that the first stage of construction (excavate – 1.40m and install struts layer 01) was observed to be unusual compared with some previous case histories. This led to the skepticism of first construction sequence in the field and workmanship. The latter stages of construction also reveal the doubt. Therefore, in addition to the varying values of soil stiffness Eu/Su, stages of construction were also made trials and errors. Many cases of FEM analysis by trials and errors were conducted.

The results showed that there existed no immediate strut installation after soil was excavated to level -1.40m or the strutting was too late after the excavation level. Earth lateral movement already moved inside the excavation side to some extent before the struts layer 01 were installed. Figure 4.2 shows the results of FEM stages of construction compared with the field data.

The ineffectiveness of struts-layer-01 installation led to a new arrangement of stages of construction to be analyzed in FEM as follows:

(1) Initial stress simulation (Initial stage of construction)
(2) Excavation to level -1.40 m (no struts layer 01) (First stage of construction)
(3) Excavation to level -3.70 m and installation of struts layer 01 & 02 at the same time (Second stage of construction)
(4) Preloading of struts layer 02 (Third stage of construction)
(5) Excavation to level -5.70 m and installation of struts layer 03(Fourth stage of construction)
(6) Preloading of struts layer 03 (Fifth stage of construction)
(7) Final depth of excavation to level -6.90 m and cast lean concrete (Sixth stage of construction)

In the project, the old four-story building lies less than 0.5m along one side of sheet pile walls. The timber piles of the building strongly affect the behavior and maximum lateral wall movements in some sequential stages of construction. Their effect will be shown in the analysis of each stage of construction. Figure 4.3 shows the effect of timber piles in FEM analysis.

The shear strain level lies between 0.01% to over 1% for sheet piles, in this research project, Eu/Su were varied between 100 and 2000 depending on soil type. In most sheet piles excavation projects in Bangkok, the shear strain level of stiff to very stiff clay layers are observed to be small, therefore, their values of Eu/Su are large. From Teparaksa's appropriate presentation (1999), Eu/Su for stiff to very stiff clays are in the order of 1000-2000. Iterations were done to their best-fitting with field data. The typical back-analysis graphs are shown in Figure 4.4 in which Eu/Su were varied 500, 750, 1000, 1200, 1500, and 2000 for stiff to very stiff clay. From this graph, the values of Eu/Su =2000 for stiff to very stiff clay layers for research excavation have the tendency to best fit the most with the field data. Therefore, the values Eu/Su for stiff to very stiff silty clays in field are equal to 2000.

For weathered crust and soft clay layers 01 and 02, inclinometer data showed large lateral deformation. Such high shear strain level leads to low values of Eu/Su. As a result, back-analysis of the weathered crust and the two layers of soft clay were conducted with the values of Eu/Su between 150 and 1500.

The stages of construction in the FEM analysis had been already fixed. The values Eu/Su for the three bottom clay layers: stiff silty clay, very stiff silty clay, and very stiff to hard silty clay had been analyzed and found that the best values Eu/Su are 2000 for the three layers.

Therefore, the remaining iterations were performed on the values Eu/Su for weathered clay, soft clay layer 01, and soft clay layer 02. The effect of the timber piles of the nearby building were also included and excluded by trials and errors in the FEM analysis for each construction sequence.
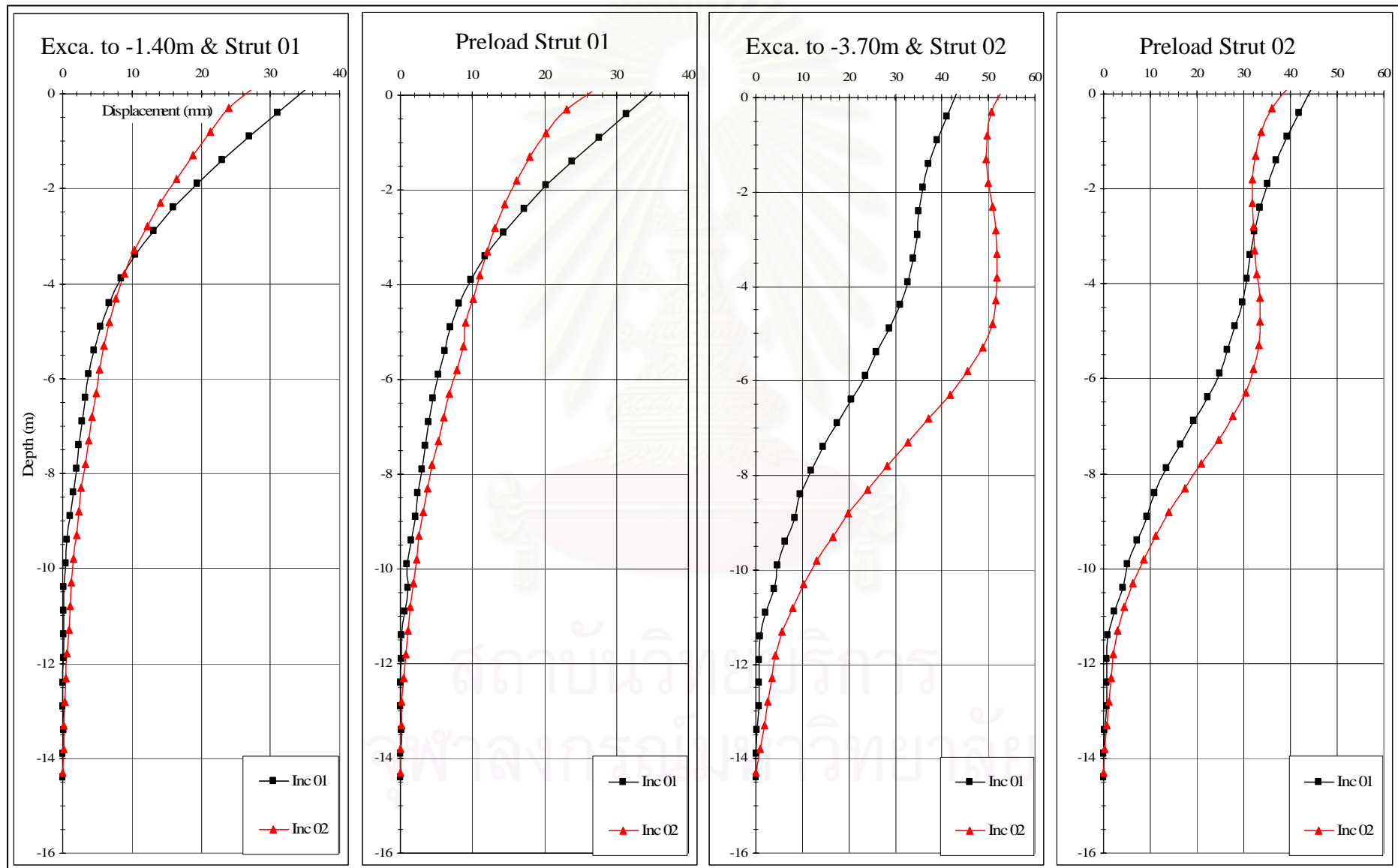
Figure 4.1 Lateral wall movements of inclinometers 01 & 02
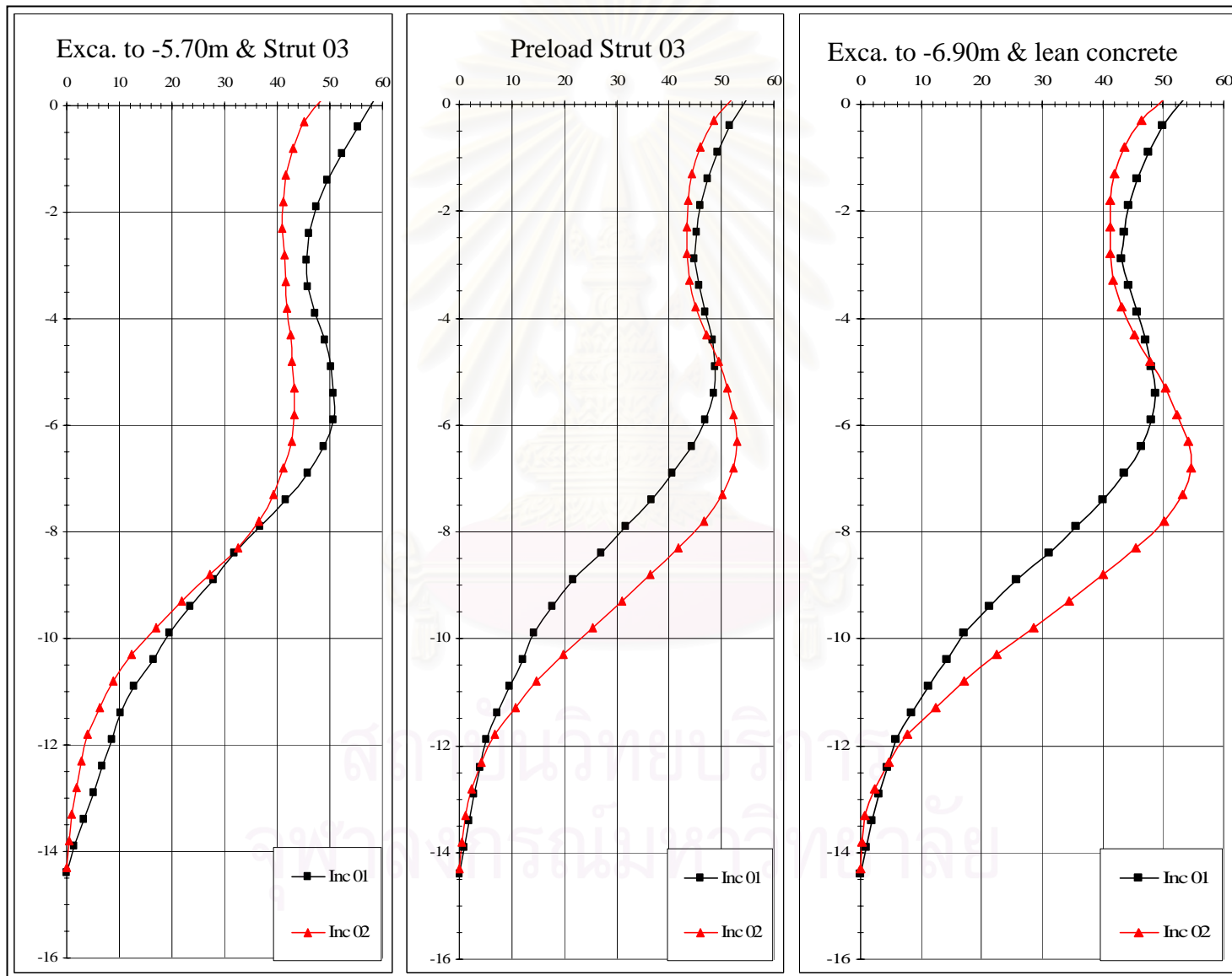
Figure 4.1 (con't) Lateral wall movements of inclinometers 01 & 02
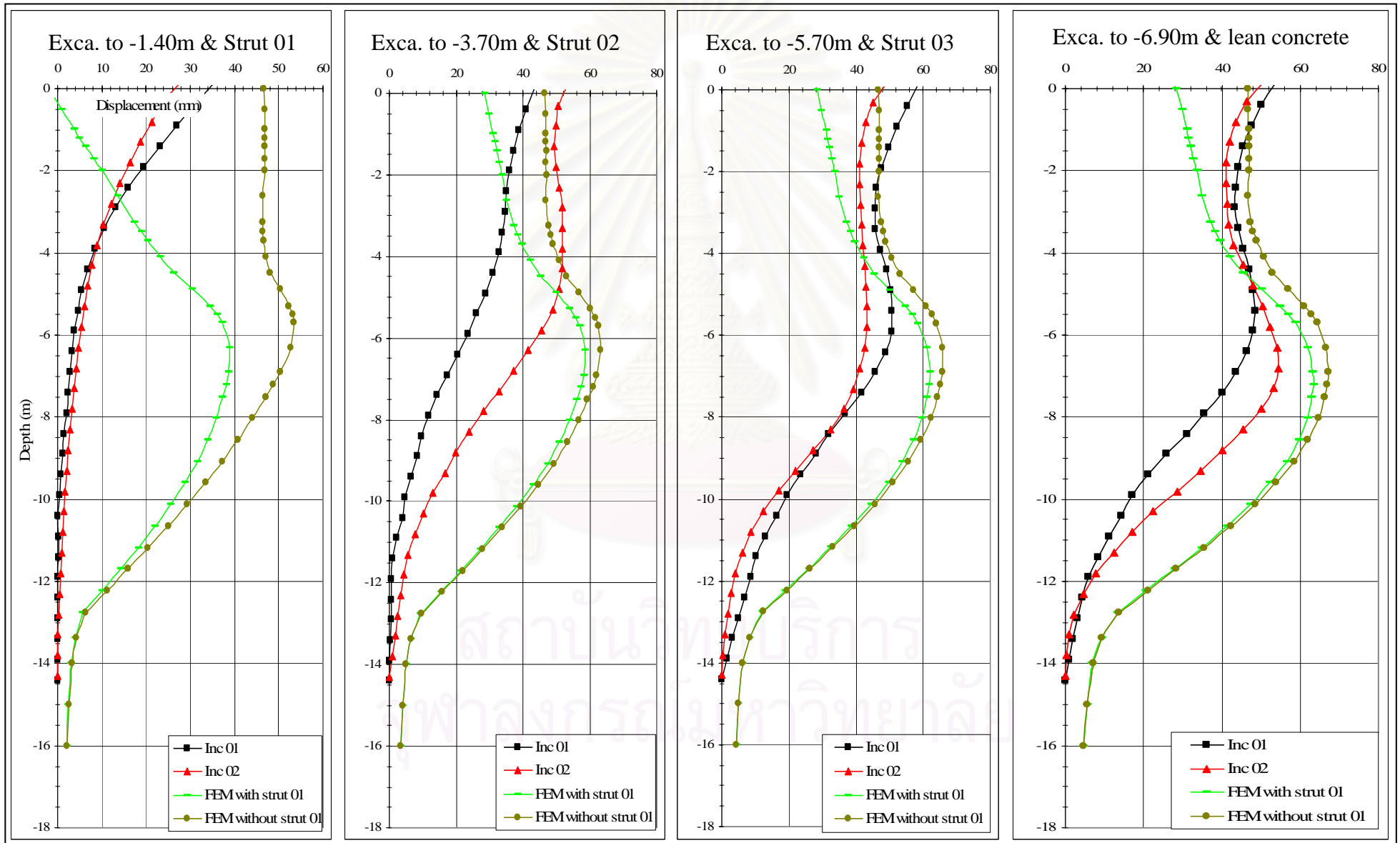
Figure 4.2 Stages of construction in FEM analysis
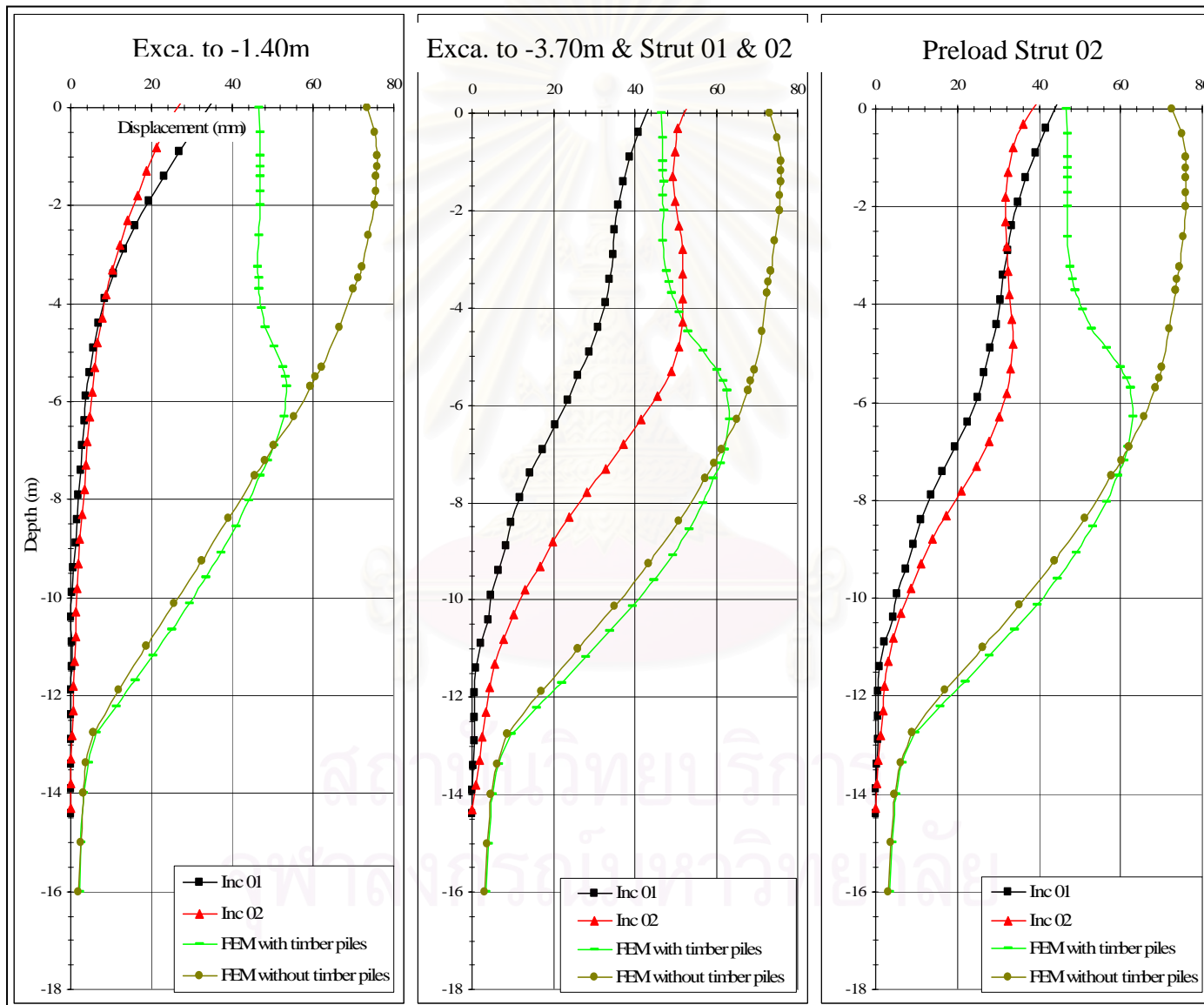
Figure 4.3 Effect of timber piles on lateral wall movements in FEM analysis
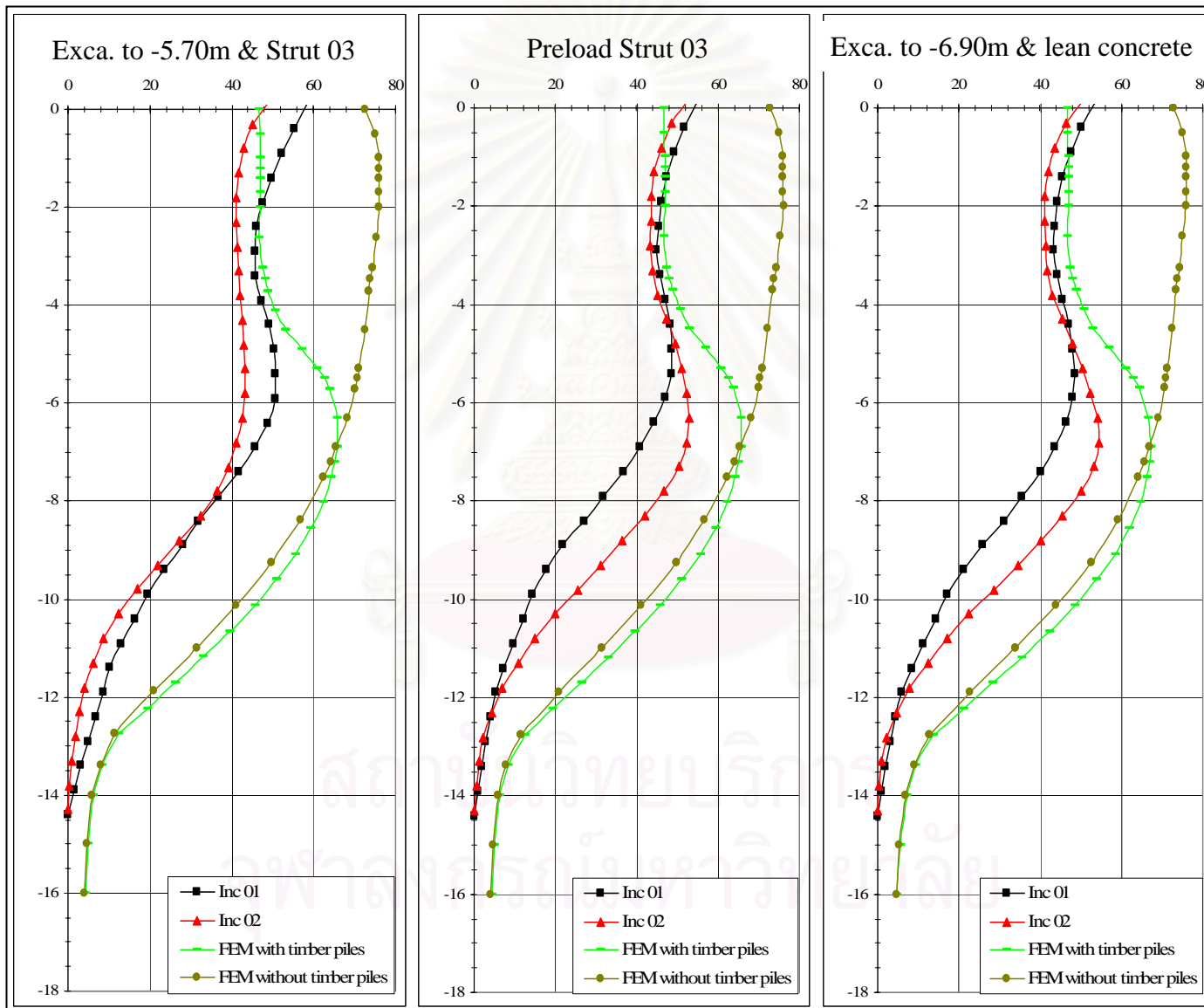
Figure 4.3 (Con't) Effect of timber piles on lateral wall movements in FEM analysis
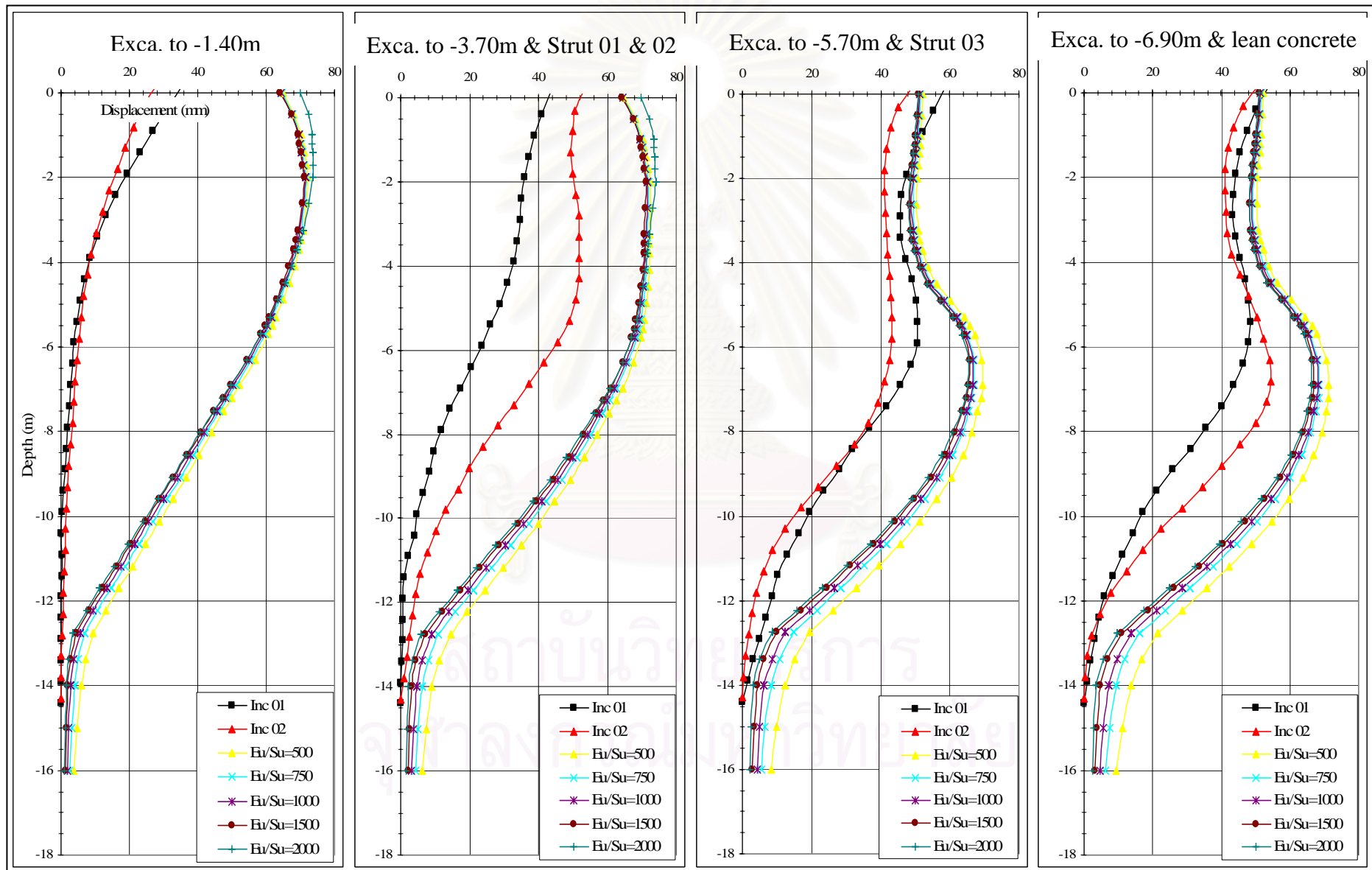
Figure 4.4 Comparison between field inclinometer data and FEM using different soil stiffness for stiff to very stiff clay

4.3 Anatomy of FEM analysis of all stages of construction

        The anatomy of the FEM analysis of all stages of construction is shown as follows:

4.3.1 Excavation to level -1.40m and no strut-layer-01 installation

        Due to high shear strain, the ratio Eu/Su for the weathered crust is low (since it is in the cantilever mode). Therefore, the value Eu/Su for the crust was initially estimated to be 150. The inclinometer data for this stage of construction was observed the relatively large deformation at the top of the sheet pile walls. Since the first struts were not placed until the excavation reached the level -3.70m instead of -1.40m, the walls behaved as a cantilever mode.

The values Eu/Su for soft clay layer 01 and layer 02 were searched and analyzed as shown in Table 4.1 and the graphs of comparison between FEM analysis and field data is shown in figure 4.5.

Table 4.1 Values Eu/Su for the whole soil profile in FEM analysis for the first stage of construction

Eu/Su Soil layers	FEM 01	FEM 02	FEM 03	FEM 04	FEM 05	FEM 06
Weathered crust	150	150	150	150	150	150
Soft clay layer 01	150	300	500	750	1000	1500
Soft clay layer 02	150	300	500	750	1000	1500
Stiff silty clay	2000	2000	2000	2000	2000	2000
Very stiff silty clay	2000	2000	2000	2000	2000	2000
Very stiff to hard silty clay	2000	2000	2000	2000	2000	2000

It is found, from figure 4.5, that the values $Eu/Su = 1500$ for soft clay layer 01 and layer 02 well fitted with the field data of inclinometers No 01 and No 02.
Then, the value Eu/Su for weathered crust was iterated to be 100, 150, 200, and 300.
The FEM analysis and its comparison with the field data is shown in figure 4.6.
From the figure, the best fitted value Eu/Su for the crust is 100.
The above-mentioned analyses were performed without inserting the adjacent building's timber piles. The inclusion of timber piles with the same parameters as

FEM 06 in table 4.1, except Eu/Su for weathered crust equals 100, FEM analysis was again analyzed and its results are shown in figure 4.7.
From figure 4.7, FEM analysis for the case without timber piles well fit than that for the case with timber piles.

Therefore, at this stage of construction, no effect of timber piles on the behavior of sheet pile lateral wall movements. The reasons for no effect of the timber pile on wall movements may come from the shallow depth of excavation (-1.40m).
Again, using the best values Eu/Su for the weathered crust and the two layers of soft clay to verify again values Eu/Su =2000 for the stiff to very stiff silty clays. Keeping constant Eu/Su for the weathered crust and the two layers of soft clays, and varying Eu/Su for stiff to very stiff silty clay to 500, 1000, 2000. The results of FEM analysis is shown in figure 4.8.

Figure 4.5 Comparison between field data and FEM wall
displacements by varying Eu/Su for soft clay layer 01 & 02

Figure 4.6 Comparison between field data and FEM wall
displacements by varying Eu/Su for weathered crust
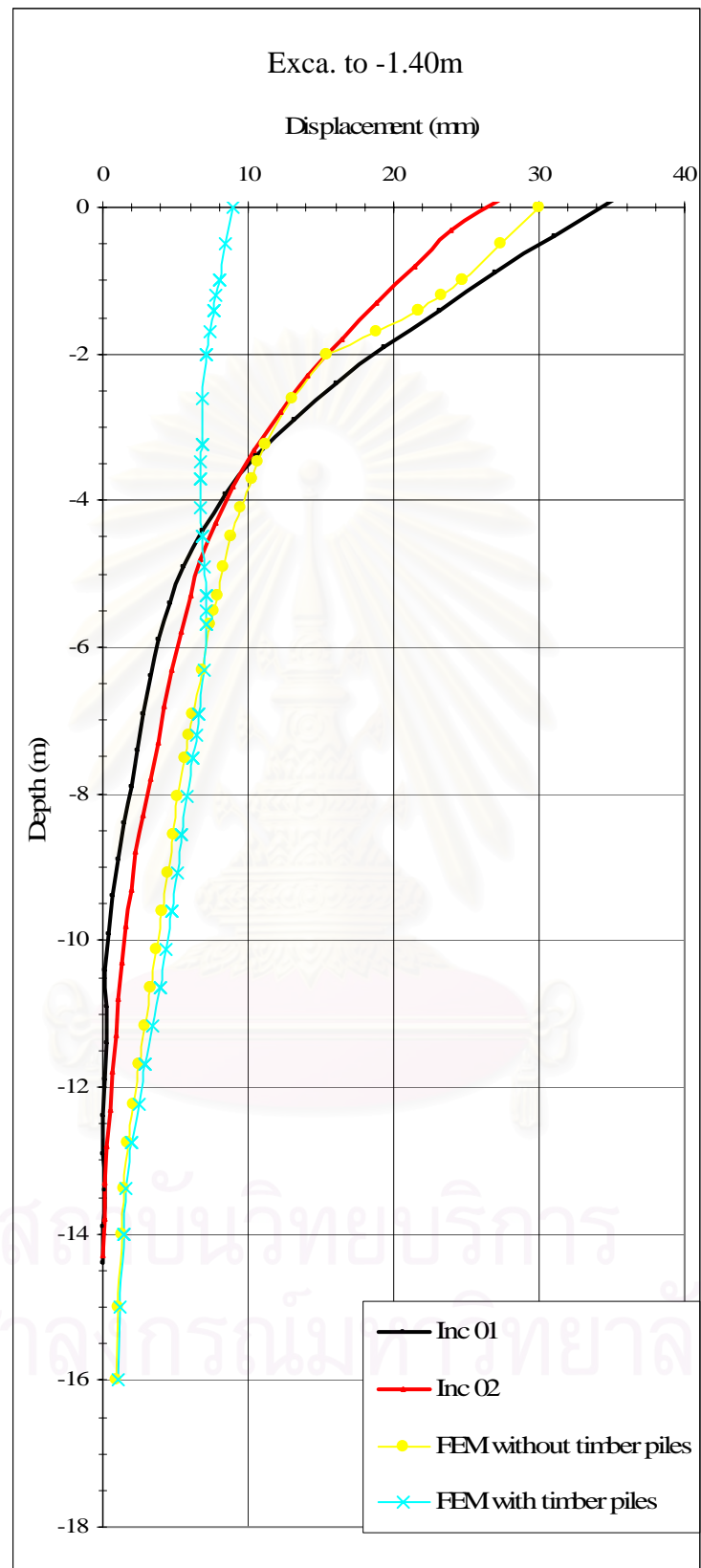
Figure 4.7 Effect of timber piles on lateral sheet pile
wall movements
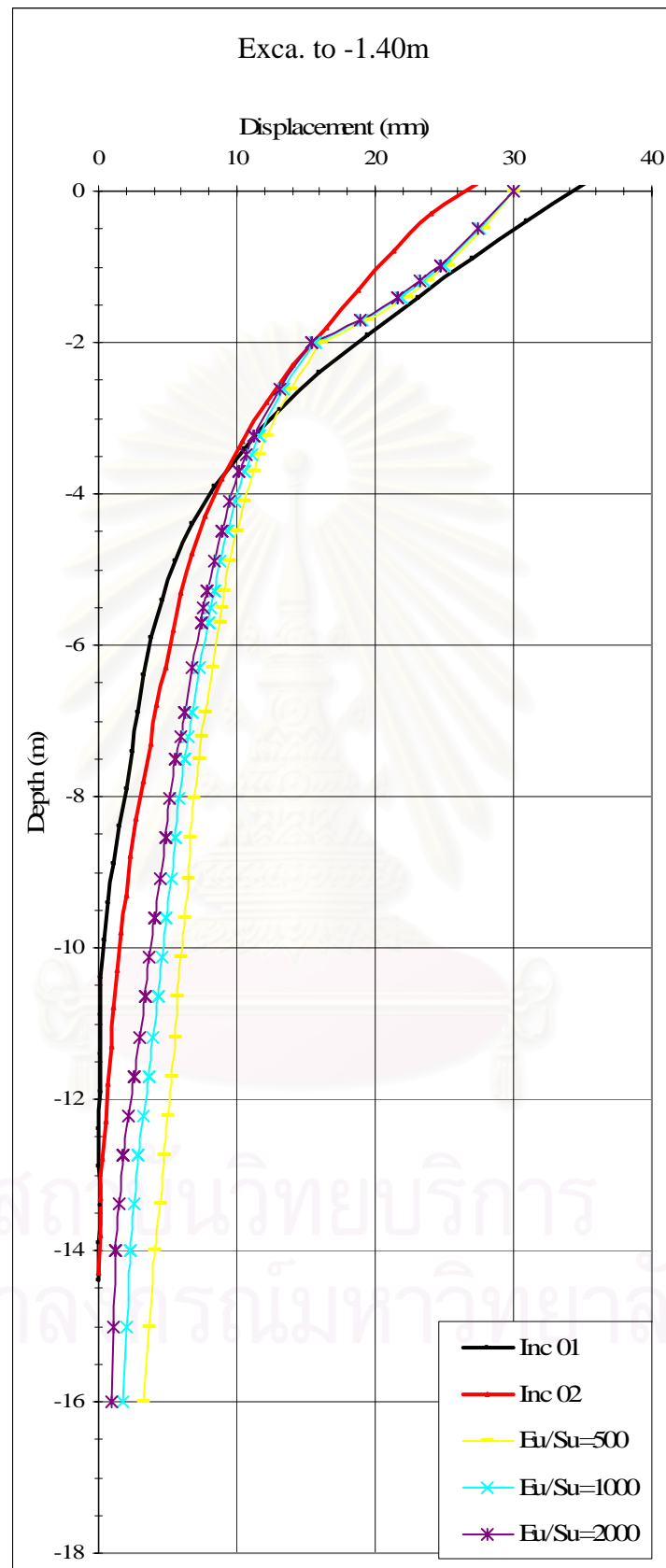
Figure 4.8 Comparison between field data and FEM wall
displacements by varying Eu/Su for stiff to very stiff clays

In summary, the best-fitted values of Eu/Su for this stage of construction are:

Table 4.2 The best-fitted values of Eu/Su for the first stage of construction

Soil Layers	Weathered crust	Soft clay layer 01	Soft clay layer 02	Stiff silty clay	Very stiff silty clay	very stiff to hard silty clay
Eu/Su	100	1500	1500	2000	2000	2000

* Note that no effect of timber piles on lateral sheet pile wall movements exists in this stage of construction.

4.3.2 Excavation to level -3.70m & strut-layer- 01 & layer-02 installation and preloading of struts layer 02

The same process was conducted as FEM analysis for the first stage of construction. The values of Eu/Su for stiff to very stiff silty clay were kept 2000. Observation from the field inclinometer data, the level of shear strain for soft clay layers in these stages ε_s =0.75%, which is higher than the first stage (ε_s =0.45%). So lower values of Eu/Su for the soft clay would be expected. Keeping constant the values Eu/Su =100 and 2000 for weathered crust and stiff to very stiff silty clays, respectively, the values Eu/Su for the soft clays could be analyzed by trials and errors as shown in table 4.3.

Table 4.3 Values Eu/Su for the whole soil profile in FEM analysis for the second and third stages of construction

Soil layers \ Eu/Su	FEM 01	FEM 02	FEM 03	FEM 04	FEM 05	FEM 06
Weathered crust	100	100	100	100	100	100
Soft clay layer 01	150	300	500	1000	500	300
Soft clay layer 02	150	300	500	1000	750	750
Stiff silty clay	2000	2000	2000	2000	2000	2000
Very stiff silty clay	2000	2000	2000	2000	2000	2000
Very stiff to hard silty clay	2000	2000	2000	2000	2000	2000

The FEM analyses compared with the field data are shown in figure 4.9.

The back-analysis for the weathered crust was searched as well by keeping the best values Eu/Su in table 4.3 except varying Eu/Su of the crust.

The timber piles from the nearby building were also inserted in the analysis. The best values Eu/Su from table 4.3 and from weathered crust FEM analysis were used to analyze the effect of the timber piles.

The results of the FEM analyses of Eu/Su for weathered crust and the effect of timber piles on lateral wall movements were plotted in figures 4.10, and 4.11, respectively.

From figures 4.9 and 4.10, it is found that the curves of FEM lateral sheet pile wall movements best fit the field data in the FEM 06 in table 4.3 except the Eu/Su =150 for the weathered crust.

The graph of FEM lateral sheet pile wall movements with timber piles has different shape compared with the field data. It cannot well fit with the field data whatsoever. But the graph of FEM lateral sheet pile wall movements without timber piles well fits with the field data.

In summary, the best-suited values of Eu/Su for all soil layers are shown in table 4.4:

Table 4.4 The best-fitted values of Eu/Su for the second
and third stages of construction

Soil Layers	Weathered crust	Soft clay layer 01	Soft clay layer 02	Stiff silty clay	Very stiff silty clay	very stiff to hard silty clay
Eu/Su	150	300	750	2000	2000	2000

* Note that no effect of timber piles on lateral sheet pile wall movements, as the first stage of construction, exists in these two stages of construction.
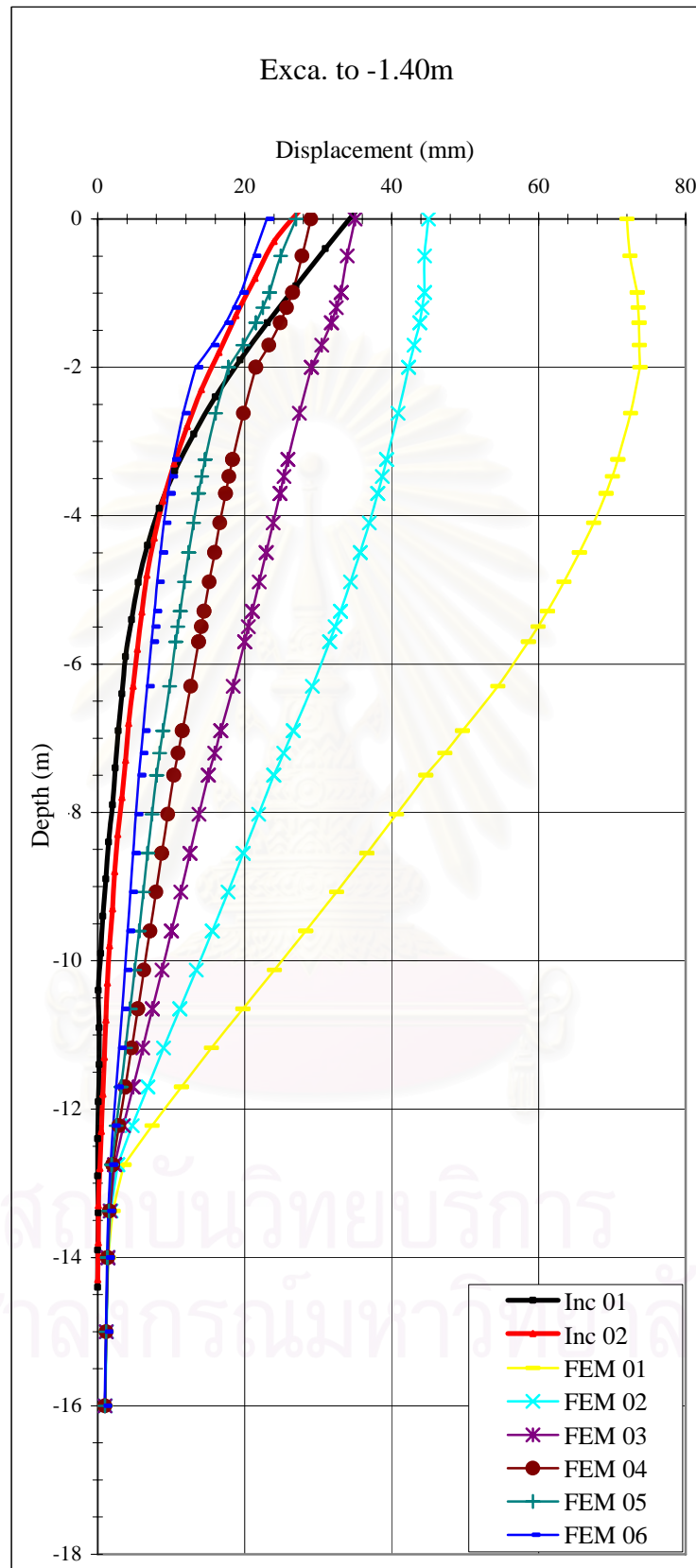
Figure 4.9 Comparison between field data and FEM wall displacements
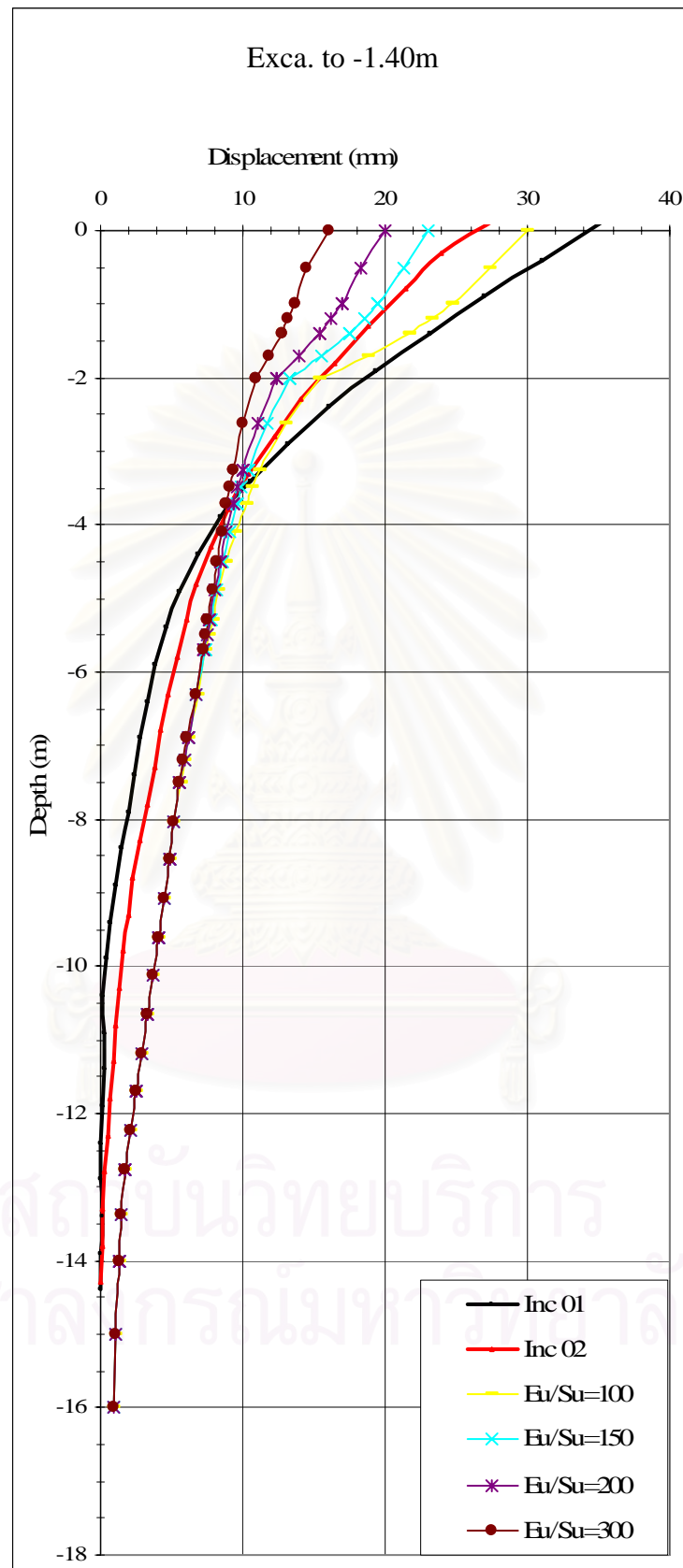by varying Eu/Su for soft clay layer 01 & 02

Figure 4.10 Comparison between field data and FEM wall displacements
by varying Eu/Su for weathered crust
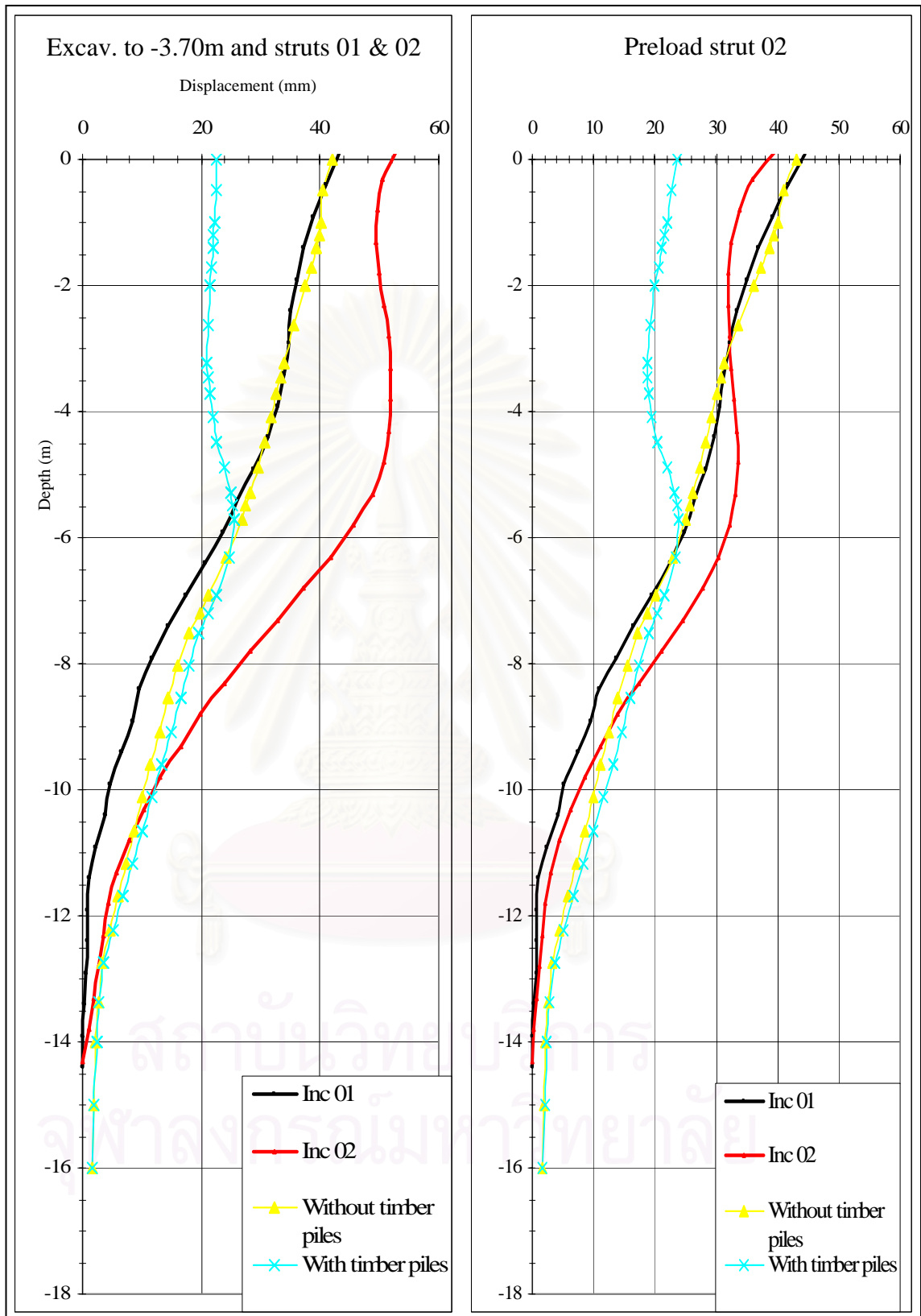
Figure 4.11 Effect of timber piles on lateral wall movements

4.3.3 Excavation to level -5.70m & struts-layer-03 installation, preloading of struts layer 03, and final excavation -6.90m & lean concrete

Similar FEM analysis was simulated as the previous stages of construction. The field inclinometer data were observed to change their behaviors from cantilevered mode to cantilevered and bulging mode inward the excavation side. The level of shear strain for soft clay layers was noticed to increase its value as deeper excavations were continued. The average shear strains of the two layers of soft clays are 1.3% and 1.4% for excavation depths to level -5.70m and -6.90m, respectively. These high shear strains for the stages of construction lead to less values of Eu/Su. The ratio Eu/Su =150 and 2000 were first kept constant for weathered crust and stiff to very stiff silty clays, respectively. The values Eu/Su for the two layers of soft clays were conducted by trials and errors as shown in table 4.5.

Table 4.5 Values Eu/Su for the whole soil profile in FEM analysis for the fourth, fifth, and final stages of construction

Eu/Su ⟍ Soil layers	FEM 01	FEM 02	FEM 03	FEM 04	FEM 05	FEM 06
Weathered crust	150	150	150	150	150	150
Soft clay layer 01	750	500	300	150	150	150
Soft clay layer 02	750	500	300	150	300	250
Stiff silty clay	2000	2000	2000	2000	2000	2000
Very stiff silty clay	2000	2000	2000	2000	2000	2000
Very stiff to hard silty clay	2000	2000	2000	2000	2000	2000

The plottings of lateral wall movements from field data and FEM analyses are shown in figure 4.12.
From figure 4.12, the best-fitted values Eu/Su =150 for soft clay layer 01 and Eu/Su =250 for soft clay layer 02.
Keeping constant the best-fitted values Eu/Su for the soft clays, Eu/Su for weathered crust can be back-analyzed by varying Eu/Su =100, 150.
The same process, the three bottom soil layers can as well be numerically verified by keeping constant the best-fitted values Eu/Su for weathered crust and the soft clays and varying Eu/Su =500, 1000, 1500, 2000 for the three bottom layers of stiff to very stiff silty clays.

The results of the FEM analyses of Eu/Su for weathered crust and stiff to very stiff silty clays were plotted in figures 4.13, and 4.14, respectively.

From figures 4.13 and 4.14, the best-fitted values Eu/Su =100 and 2000 for weathered crust and the stiff to very stiff silty clays, respectively.

The case without timber piles by using the best-fitted values Eu/Su for the whole soil profile were also analyzed in FEM. Their results are shown in figure 4.15.

From the figure 4.15, in case without timber piles, the graphs of lateral sheet pile wall movements cannot be compared with the field data, since the field behaviors of lateral wall movement of sheet piles are affected by the existence of timber piles.

In summary, the best-fitted values of Eu/Su for these stages of construction are:

Table 4.6 The best-fitted values of Eu/Su for the fourth,
fifth and sixth and third stages of construction

Soil Layers	Weathered crust	Soft clay layer 01	Soft clay layer 02	Stiff silty clay	Very stiff silty clay	very stiff to hard silty clay
Eu/Su	100	150	250	2000	2000	2000

*Note that timber-pile effect significantly exerts on lateral sheet pile wall movements in these stages of construction.
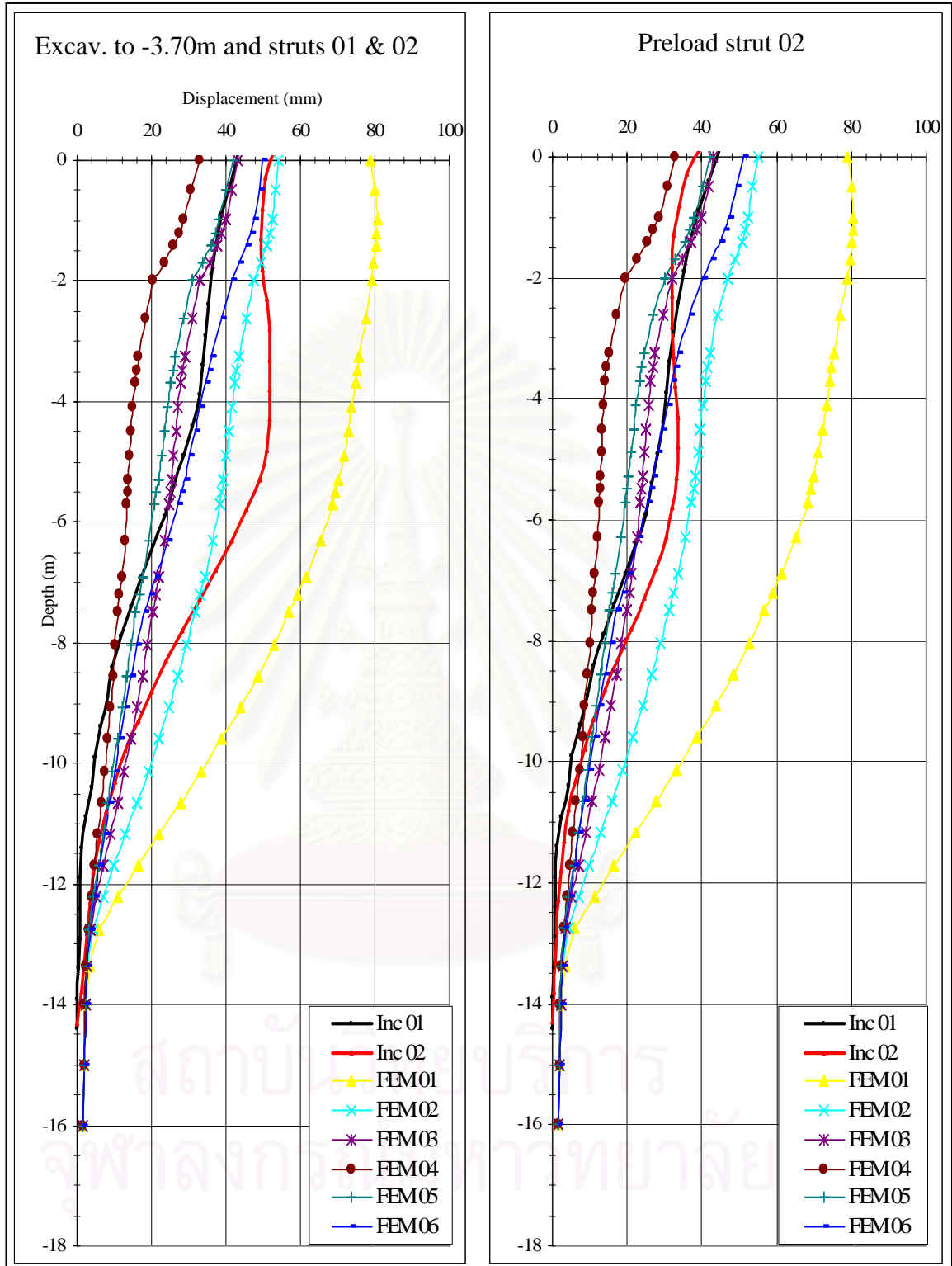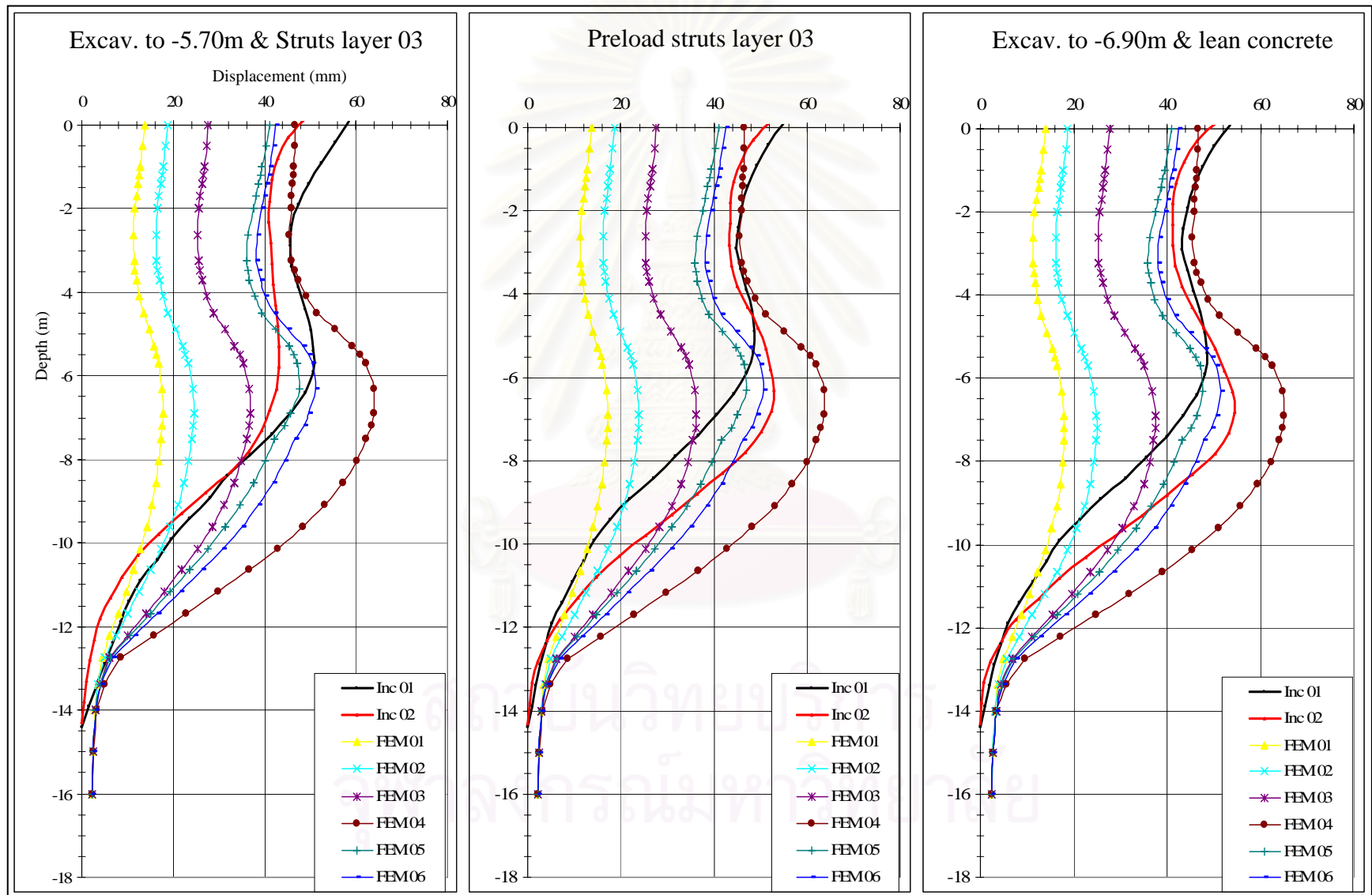
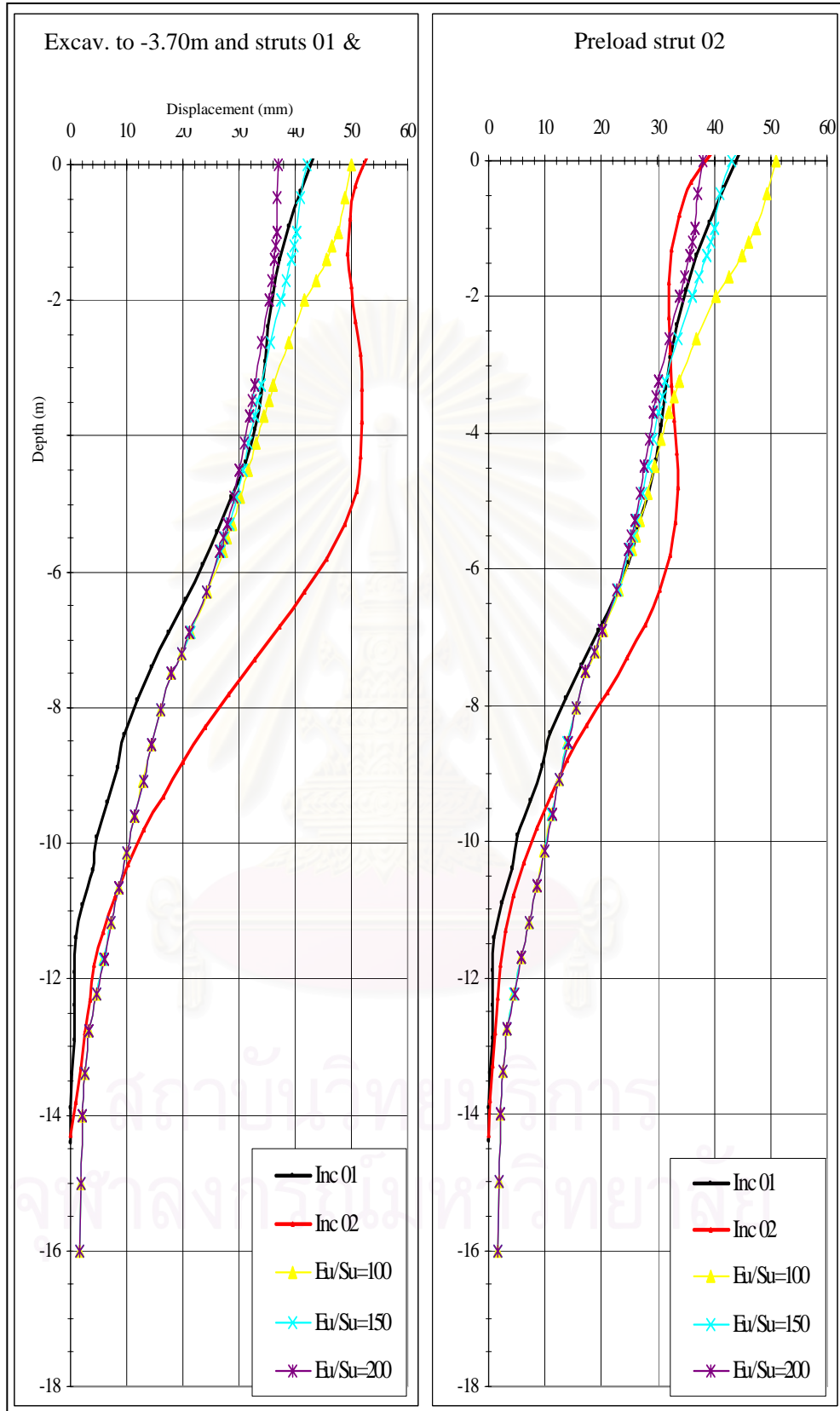Figure 4.12 Comparison between field data and FEM wall displacements by varying Eu/Su for soft clay layers 01 & 02
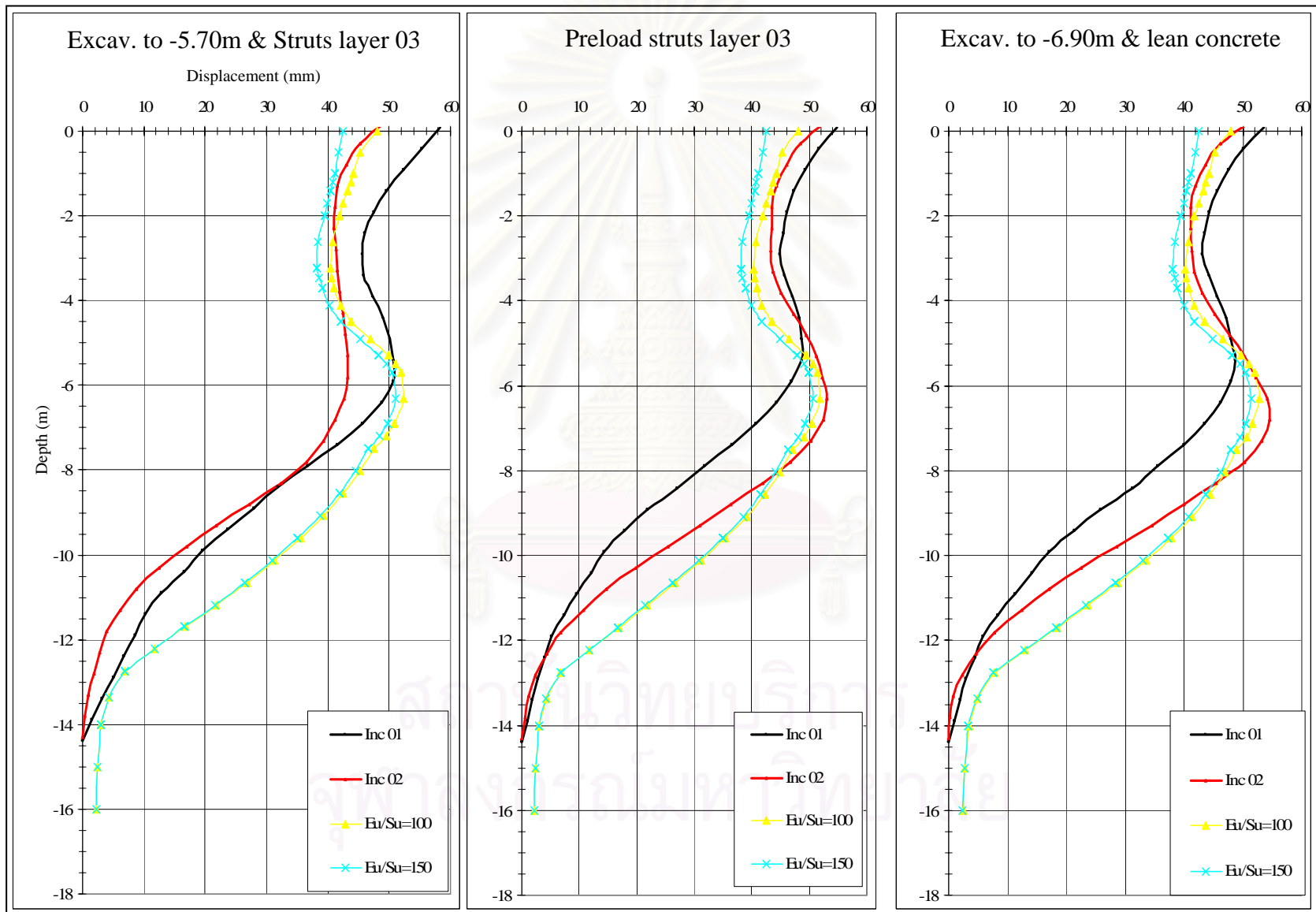
Figure 4.13 Comparison between field data and FEM wall displacements by varying Eu/Su for weathered crust
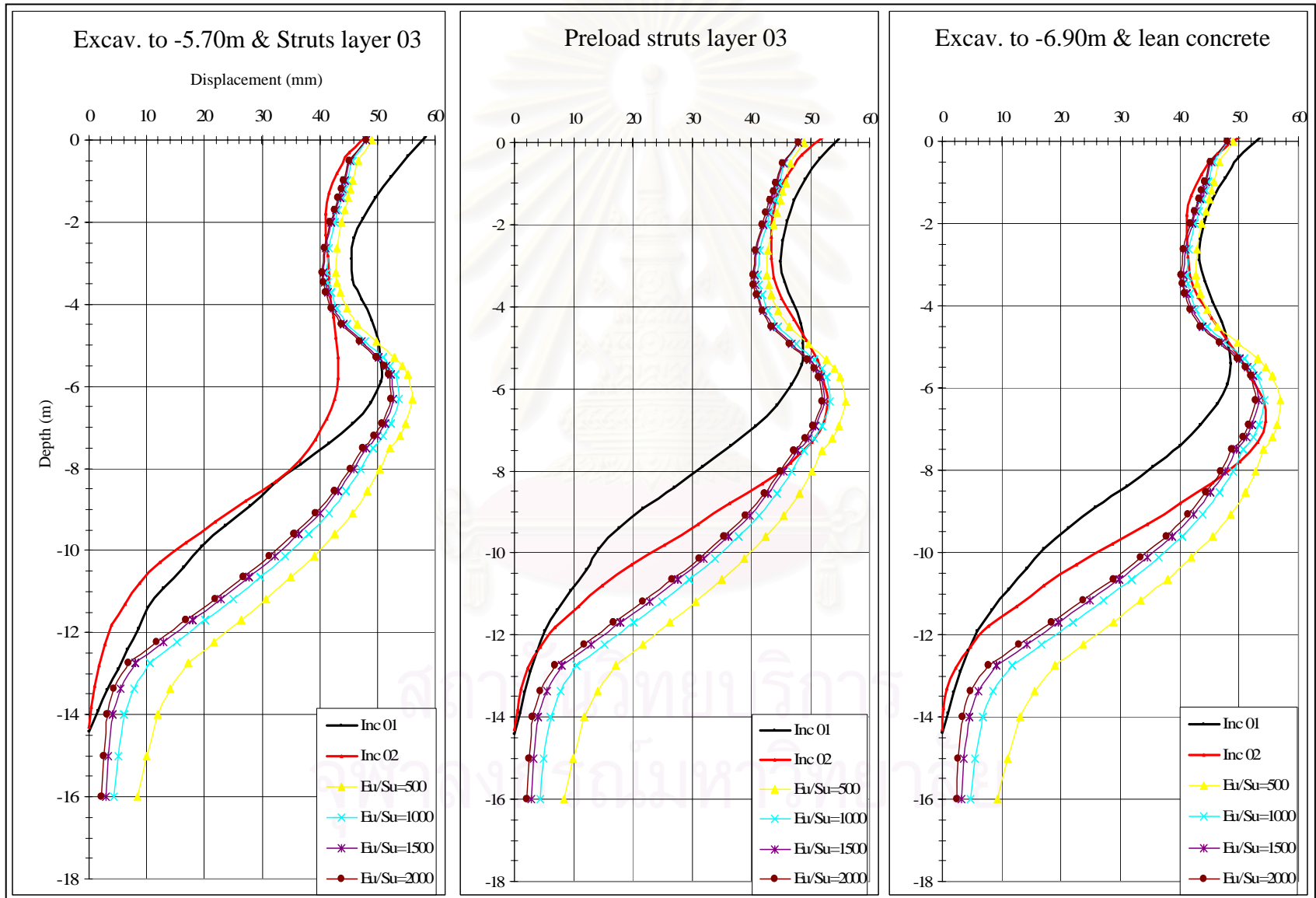
Figure 4.14 Comparison between field data and FEM wall displacements by varying Eu/Su for stiff to very stiff clays
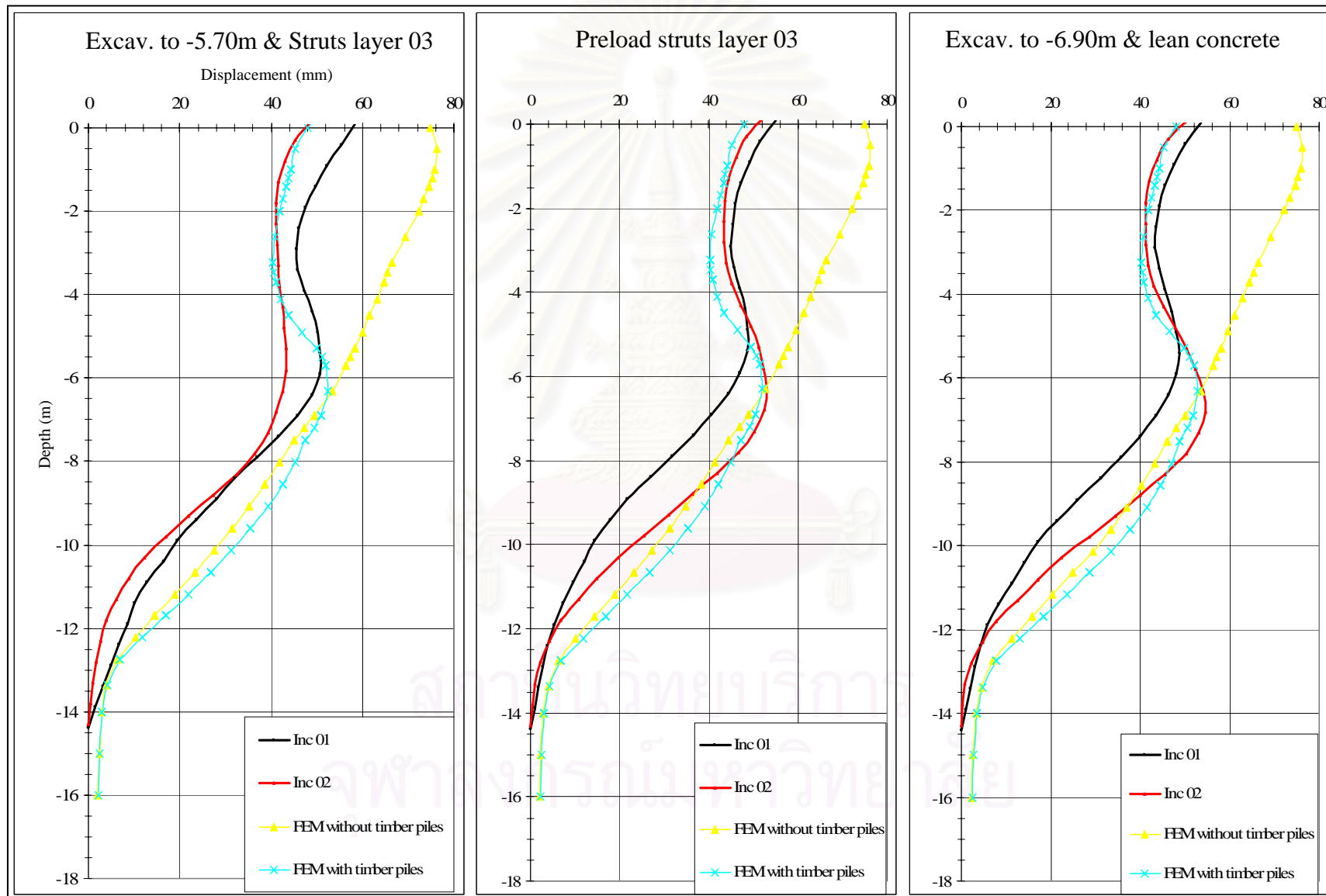
Figure 4.15 Effect of timber piles on lateral wall movements

4.3.4 Summary of back-analysis for all stages of construction

The results of best-fitted values Eu/Su from back-analysis of field data for the six soil layers according to all stages of construction can be briefed as follows:

- For excavation to level -1.40m and no strut-layer-01 installation:

Table 4.7 The best-fitted values of Eu/Su for the first stage of construction

Soil Layers	Weathered crust	Soft clay layer 01	Soft clay layer 02	Stiff silty clay	Very stiff silty clay	very stiff to hard silty clay
Eu/Su	100	1500	1500	2000	2000	2000

No effect of timber piles on lateral sheet pile wall movements exists in this stage of construction.

- For excavation to level -3.70m & strut-layer-01 & layer-02 installation and strut-layer-02 preloading:

Table 4.8 The best-fitted values of Eu/Su for, the second and third stages of construction

Soil Layers	Weathered crust	Soft clay layer 01	Soft clay layer 02	Stiff silty clay	Very stiff silty clay	very stiff to hard silty clay
Eu/Su	150	300	750	2000	2000	2000

No effect of timber piles on lateral sheet pile wall movements, as the first stage of construction, exists in these two stages of construction.

- For excavation to level -5.70m & strut-layer-03 installation, its preloading, and final depth of excavation & cast lean concrete:

Table 4.9 The best-fitted values of Eu/Su for the fourth, fifth and sixth stages of construction

Soil Layers	Weathered crust	Soft clay layer 01	Soft clay layer 02	Stiff silty clay	Very stiff silty clay	very stiff to hard silty clay
Eu/Su	100	150	250	2000	2000	2000

Timber-pile effect significantly exerts on lateral sheet pile wall movements in these stages of construction.
Best-fitted values Eu/Su from back-analysis of field data for the six soil layers according to all stages of construction are shown in figure 4.16.
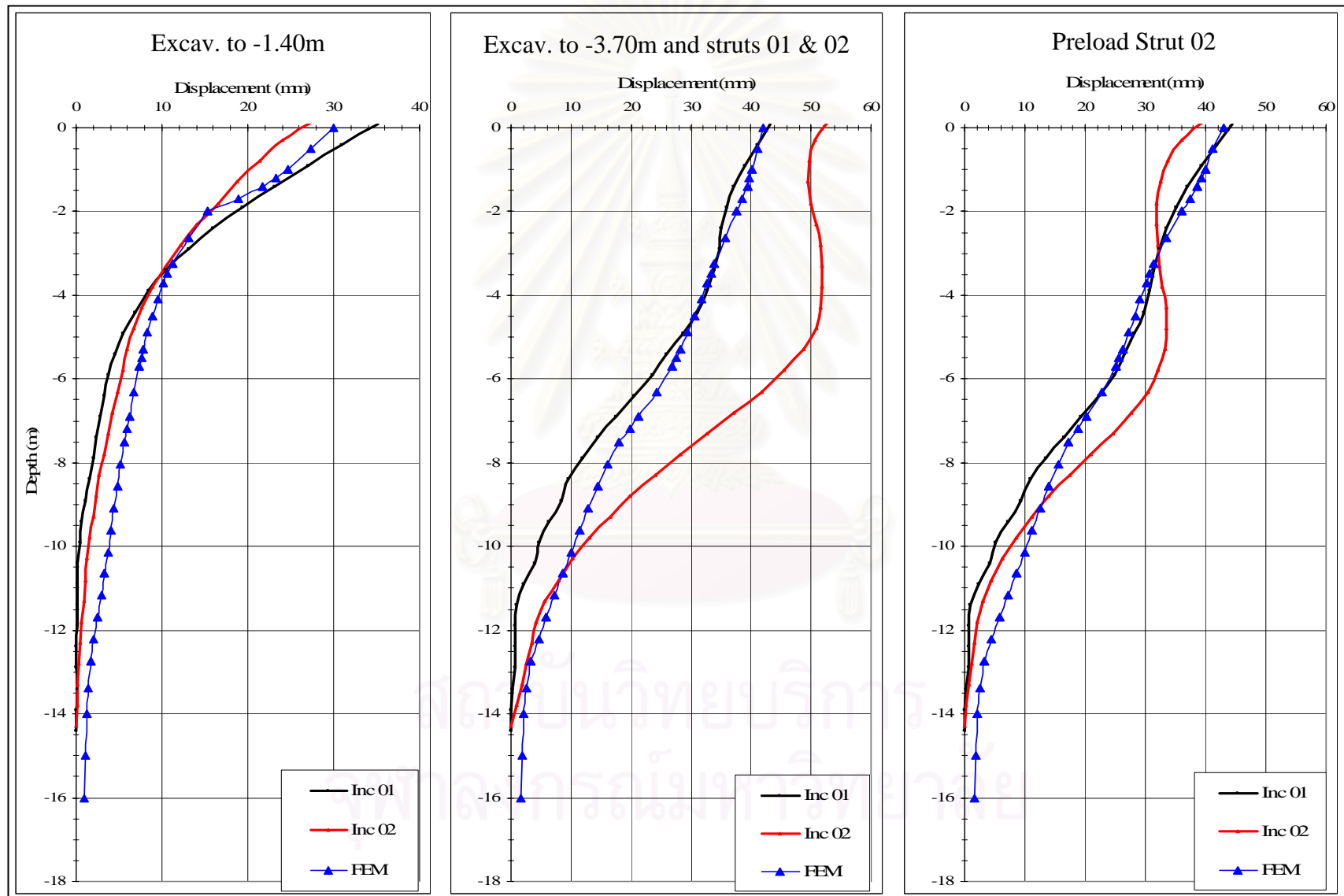
Figure 4.16 Best-fitted Eu/Su for all soil layers with sequential stages of construction
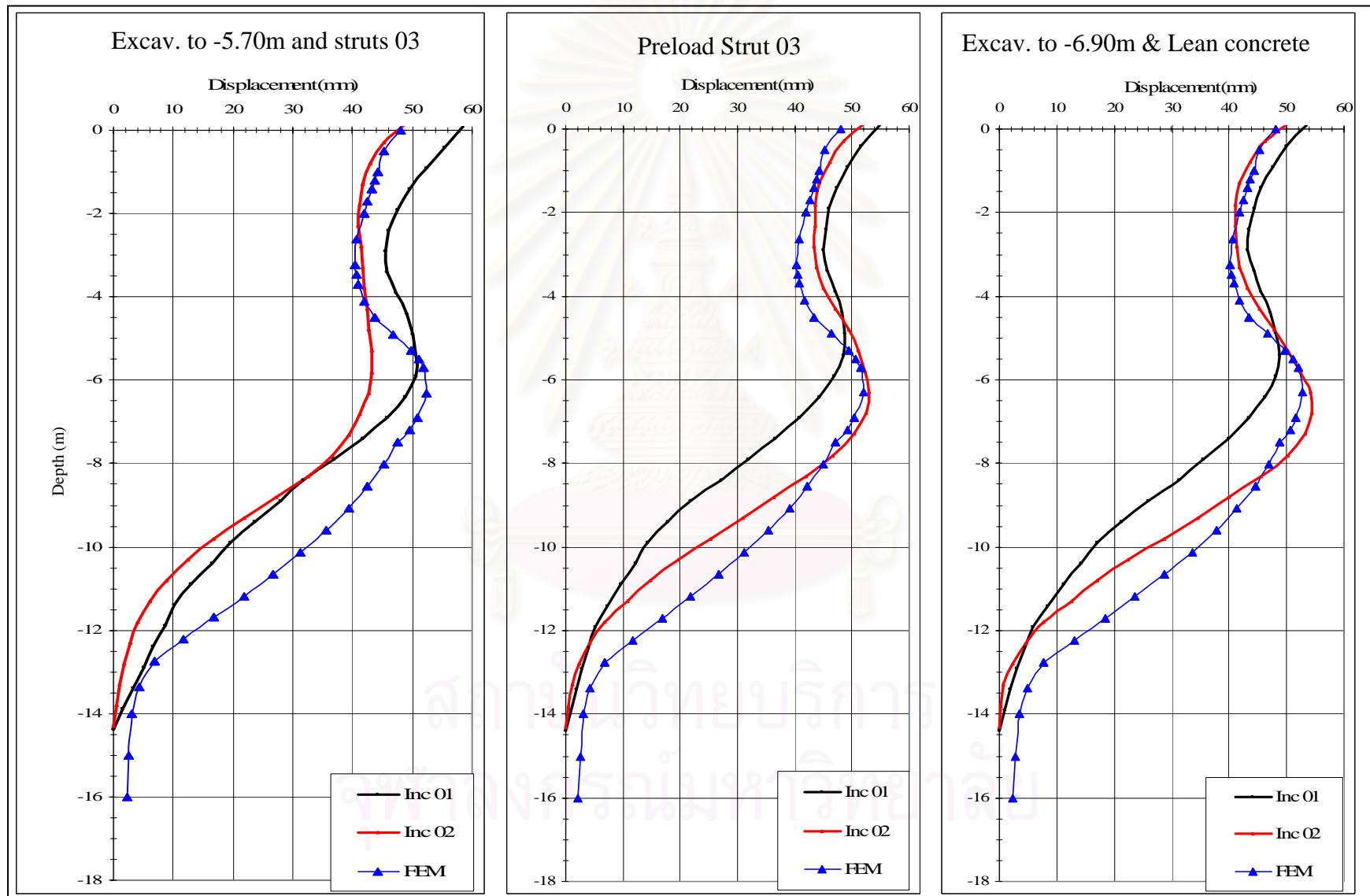
Figure 4.16 (con't) Best-fitted Eu/Su for all soil layers with sequential stages of construction

4.4 Relationship between deflection ratio and factor of safety against basal heave

The factor of safety against basal heave was calculated by the method of Terzaghi (1943). The maximum lateral sheet pile wall movements were normalized by the corresponding depths of excavation (-1.40m, -3.70m, -5.70m, and -6.90m). The values of the normalized ratio and their corresponding factors of safety were summarized in table 4.10.

Table 4.10 Values of FS and lateral wall movements of Inc No 01 and 02

Parameters / Depths(m)	FS	$\delta_{H\max}$ (Inc01) (mm)	$\delta_{H\max}$ (Inc02) (mm)
-1.40	2.77	35	28
-3.70	1.155	43	52
-5.70	0.889	51	44
-6.90	0.786	49	55
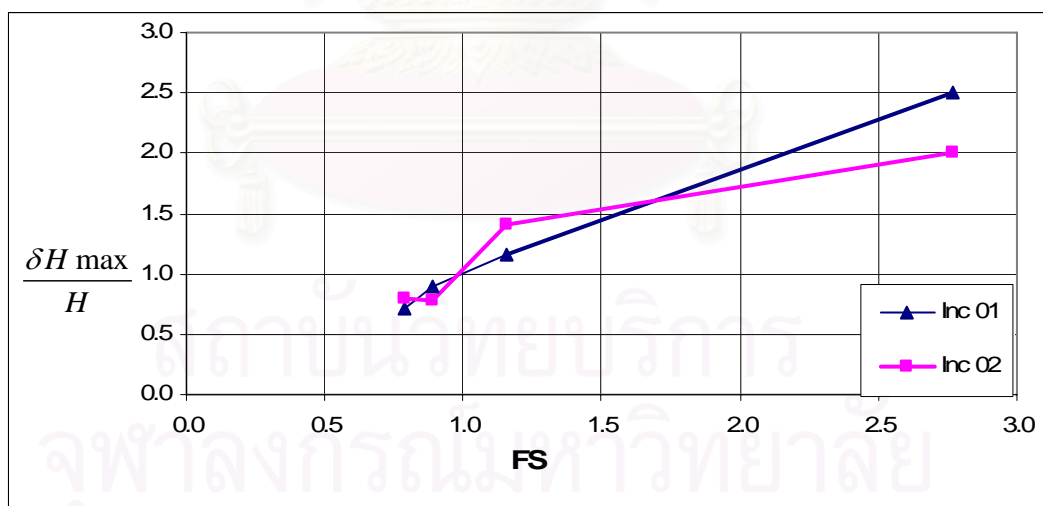
Figure 4.17 Relation between lateral wall movements and FS against basal heave

It can be seen that, for the first stage of excavation to level -1.40 m, the lateral wall movements are relatively large. The large movements were caused by the delaying of the first-strut installation. The soil mass already moved to a new state of stress

before the struts layer 01 were installed. Another graph of the relation between FS and wall deflections (data from different five projects) was also plotted as shown in figure 4.18. From the figure 4.18, the points at which excavation to -3.70m was done lie in the limits set by Mana and Clough but points at the later depths of excavation lie below the limits. This graph also shows that as the FS gets smaller, so do the deflection ratio $\dfrac{\delta_{Hmax}}{H}$. This tendency is totally opposite to what it is expected. It means, in general, that the smaller FS causes the larger deflection ratio. Some projects in Bangkok using sheet pile walls such as Baiyoke II project showed the same tendency as this project.

This phenomenon is too complicated to be analyzed. However the author believes that this may be provoked by the effects of timber piles, bored piles in front of excavation, and/or sheet pile wall stiffness. As already shown in the FEM analysis, there exists no effect of timber piles of the nearby building in the early stages of construction, but there exists the effect of timber piles when excavations were done down from level -5.70 m. Another reason may be caused by factor of safety calculated by Terzaghi (1943). This formula of FS was calculated based on short wall penetration depth. In this research project, the wall embedment depth is more than two times deeper than the final depth of excavation. Furthermore, the tip of the sheet pile walls was placed in the very stiff silty clay layer (-16 m). So the sheet piles can be considered as fixed end walls. The effectiveness of strut preloading or prestressing may be another cause.

Observations from five different projects as shown in figure 4.18, some points are below the limit curves of Mana and Clough for sheet pile bracing systems in Bangkok. So the graph was modified to well agree with the behaviors of sheet pile constructions in Bangkok. The modified curve is shown in Figure 4.19. Besides the boundary curves, another curve (middle curve) was also drawn and this curve divides into two bandwidths: A & B. If the excavation has points of the relation between FS and $\dfrac{\delta_{Hmax}}{H}$ lie outside the upper bound curve for the first excavation and then points for the second excavation lie in bandwidth B. Points of later excavation lie in bandwidth A. If the excavation has points of the relation between FS and $\dfrac{\delta_{Hmax}}{H}$ lie inside the boundary curves for the first excavation, and then points of the relation for later excavation lie in bandwidth A.
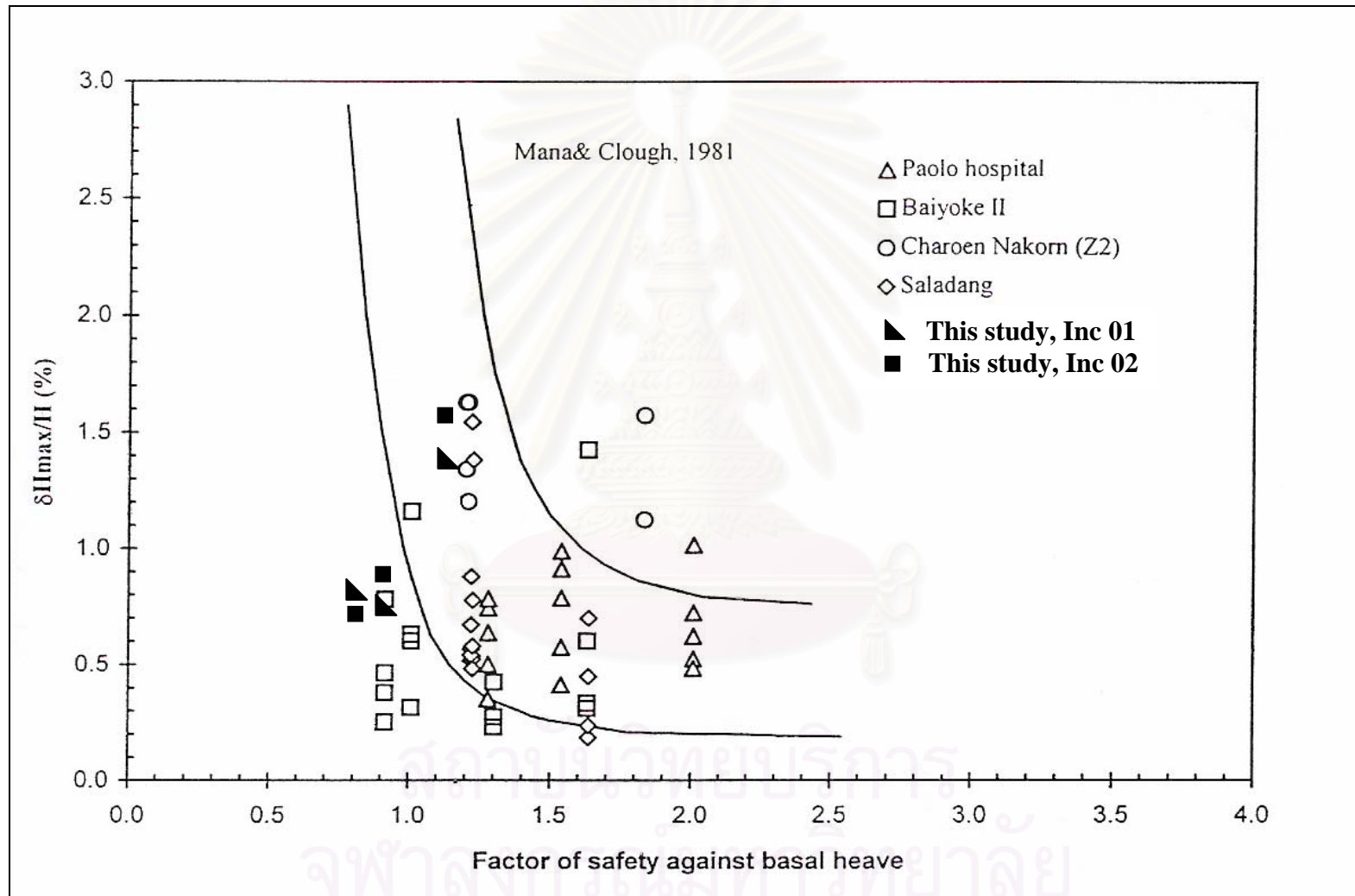
Figure 4.18 Relation between wall deflections and FS against basal heave
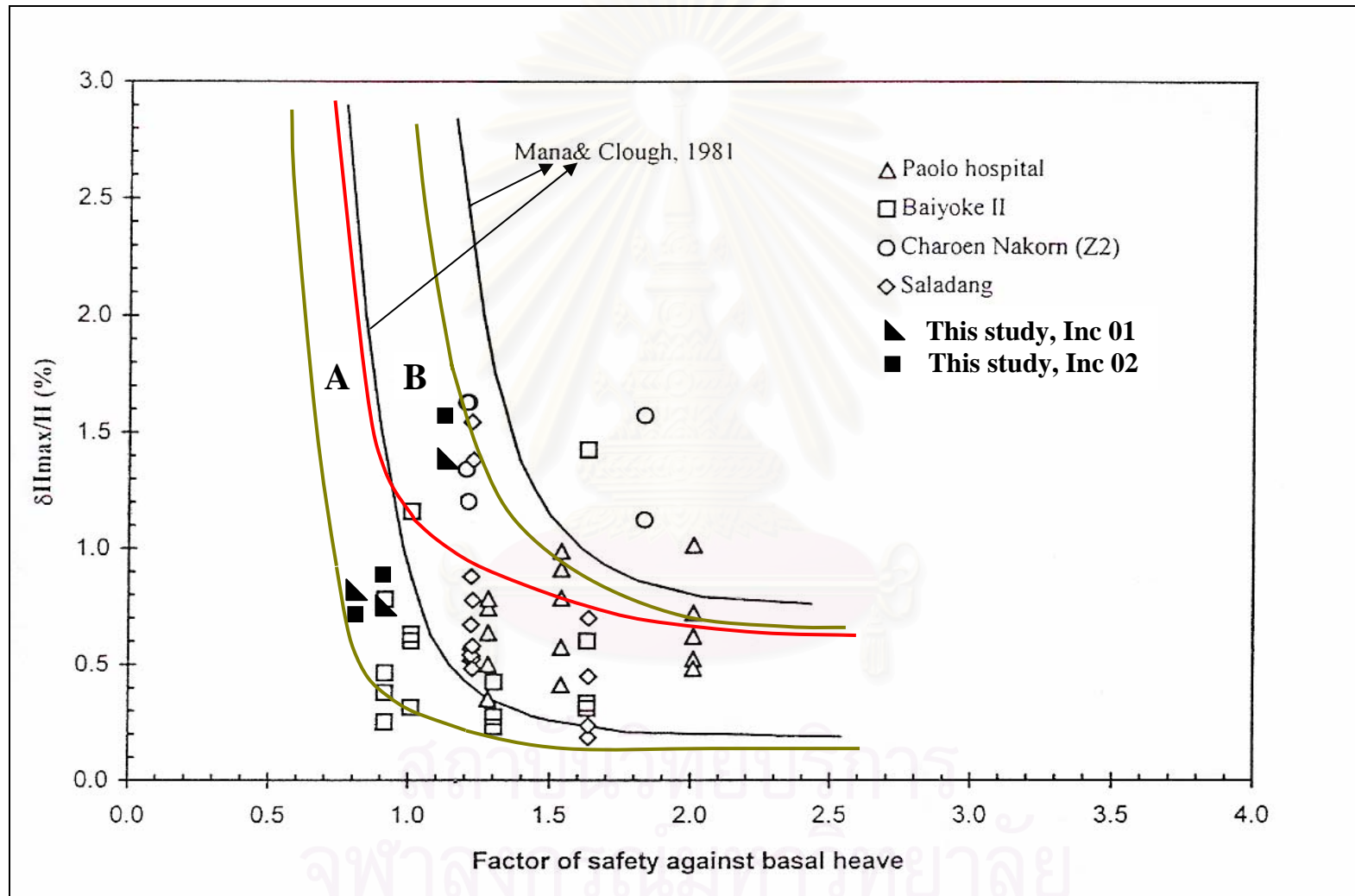
Figure 4.19 New boundaries for the relation between wall deflections and FS against basal heave

4.5 Time effect:

The construction sequence went smoothly from the beginning of excavation to the preloading of struts layer 03 without any lull of excavation. But after preloading of struts layer 03, excavations were stopped more than two months. Figure 4.20 shows the graphs of inclinometer No 01 & 02 after preloading strut 03 with 10-day time intervals. From the graphs, lateral wall displacements seem to slightly move. For over two months, the lateral wall movements are only 3mm or 4mm for both inclinometers No 01 & No 02. So time effect after strutting and preloading of strut layer 03 exerted little influences on lateral sheet pile wall movements.

4.6 In-situ sheet pile wall behaviors

Lateral wall movements for all stages of construction were observed to rotate approximately 2 m above the end tip of the sheet piles. The first stage of excavation sheet pile wall translation was not observed, but later stages of excavation, their translations steadily increased. The mode of early stages of excavation were observed to be cantilevered but after excavations were conducted to level -5.70 m, the shape of wall movements changed from cantilevered mode to cantilevered-bulging mode.

The maximum lateral wall movements occur near each depth of excavation, except the cantilevered mode. The lateral movements from three different projects as shown in figures 4.21, 4.22, and 4.23 clarified the observations.

From observations of inclinometers No 01 & 02:

Inclinometer No 01: $\delta_{H\max} = 35\text{mm} \to 51\text{mm}$

Inclinometer No 02: $\delta_{H\max} = 28\text{mm} \to 55\text{mm}$

The maximum lateral wall movements were divided by the final depth of excavation (-6.90 m):

For Inclinometer No 01: $\dfrac{\delta_{H\max}}{H_f}(\%) = 0.5\% \to 0.74\%$

For Inclinometer No 02: $\dfrac{\delta_{H\max}}{H_f}(\%) = 0.4\% \to 0.8\%$

In conclusion, the ratios of maximum lateral wall movements to the final depth of excavation range from 0.4% to 0.8%.
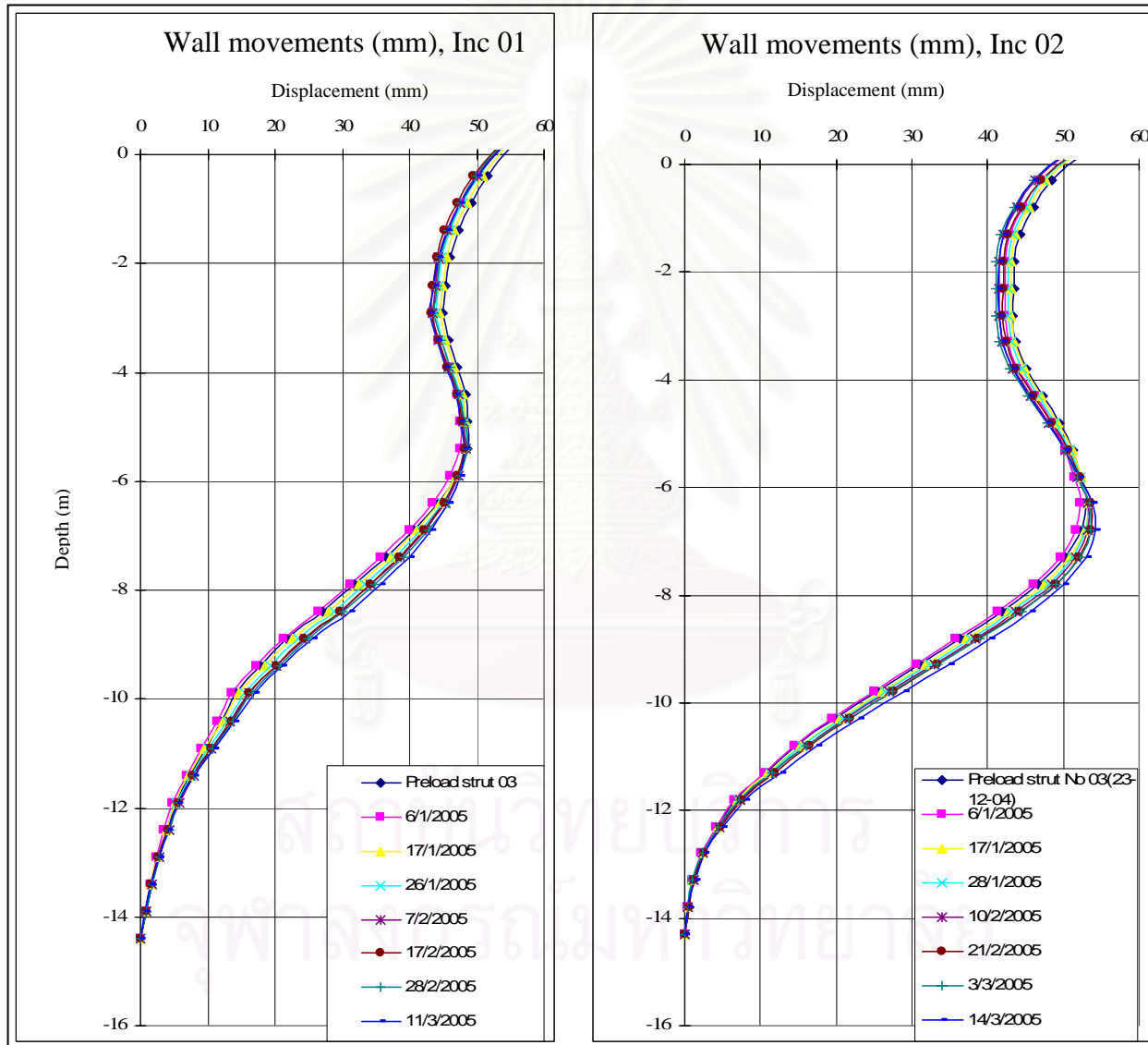
Figure 4.20 Time effect on lateral wall movements after preloading struts layer 03
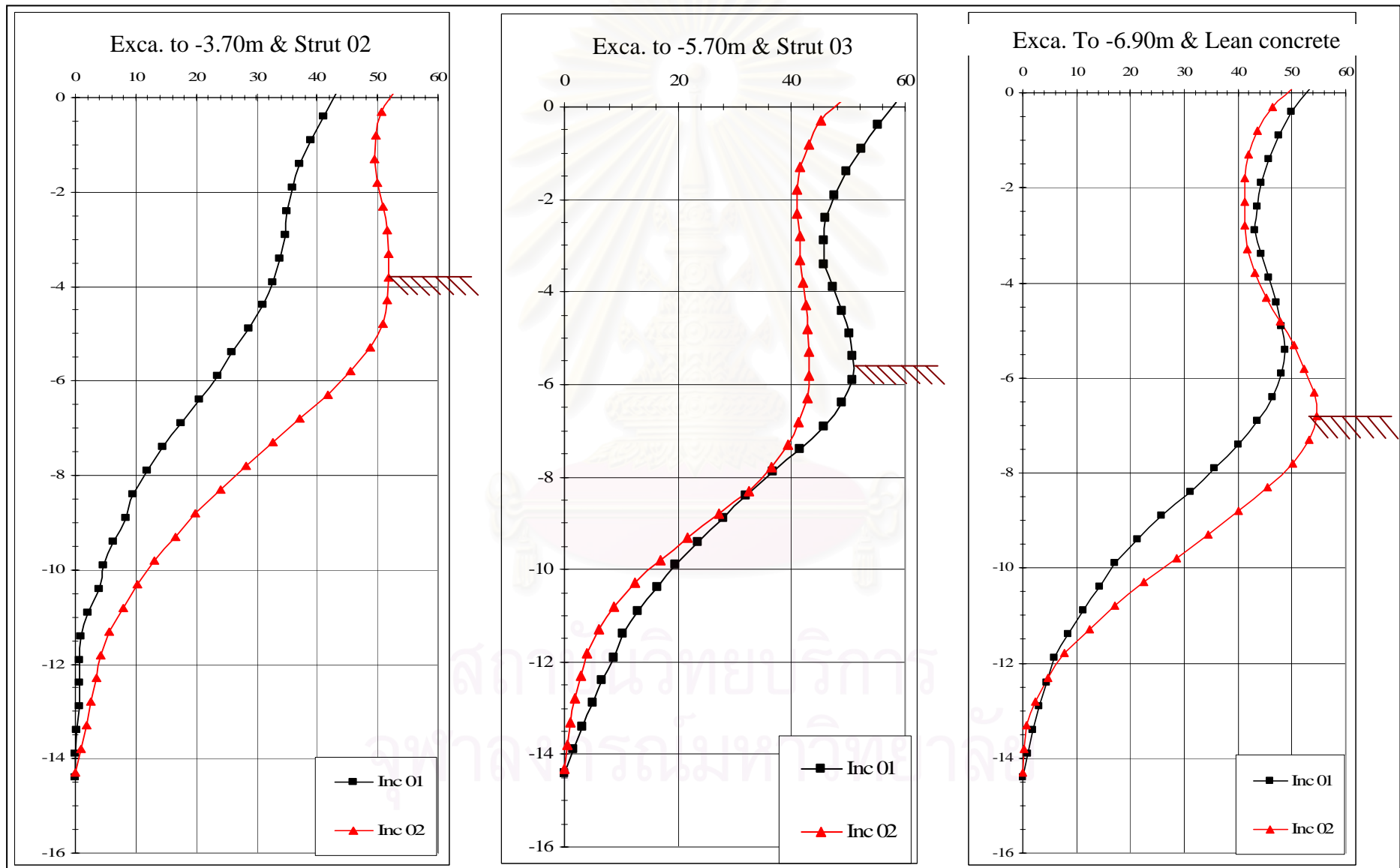
Figure 4.21 Depths at which maximum lateral wall movements occur, this research project
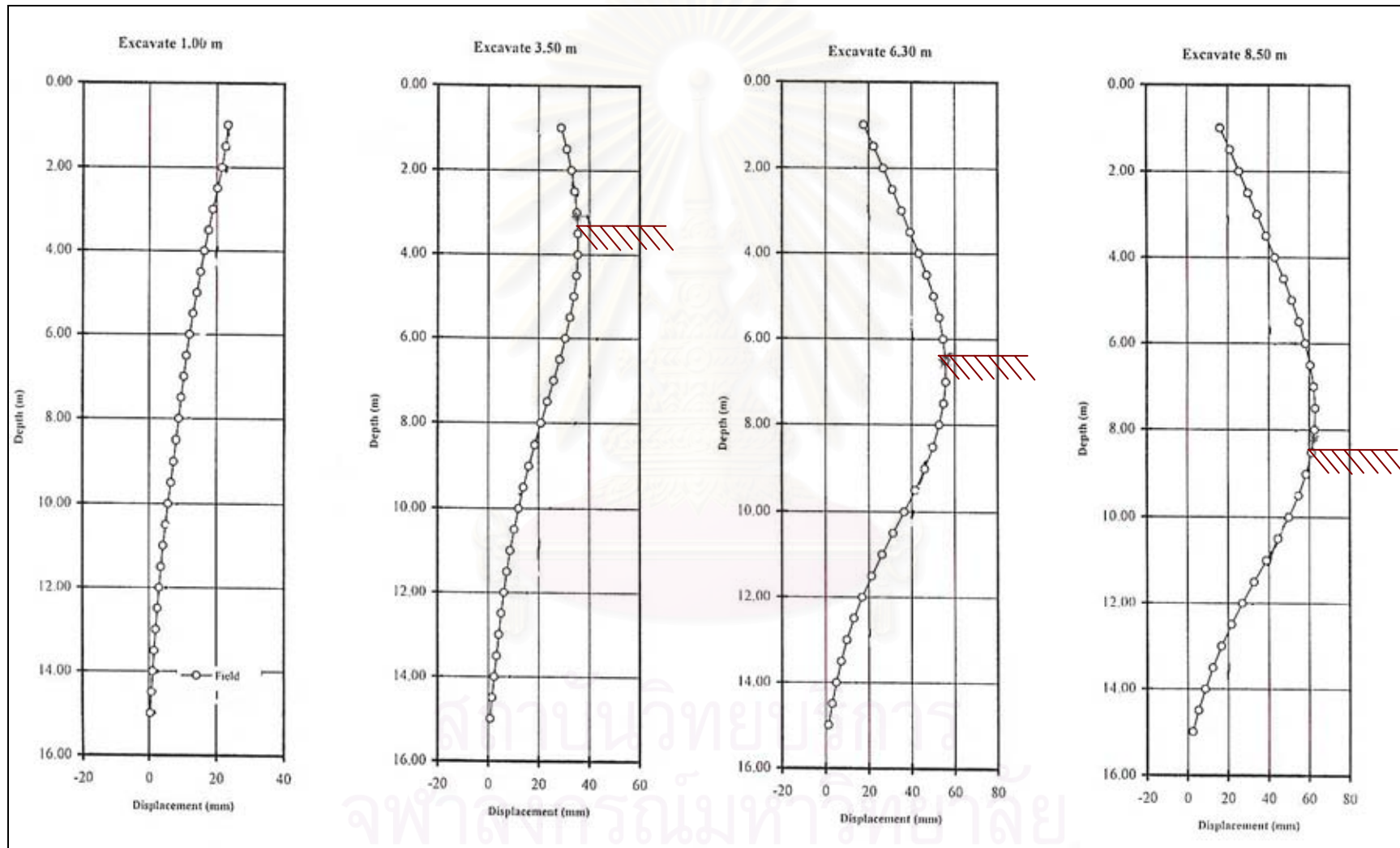
Figure 4.22 Depths at which maximum lateral wall movements occur, Paolo Hospital project
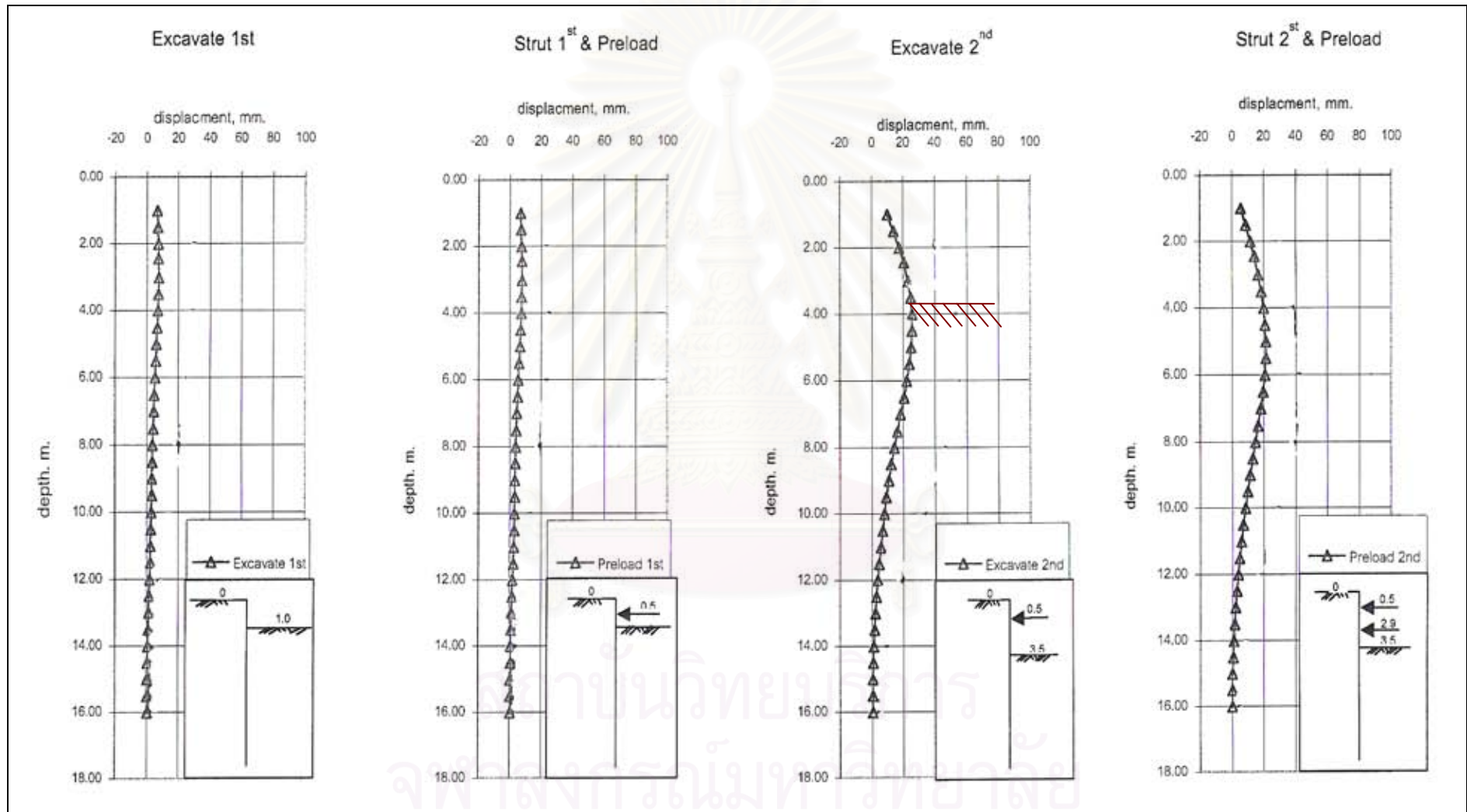
Figure 4.23 Depths at which maximum lateral wall movements occur, Saladang project
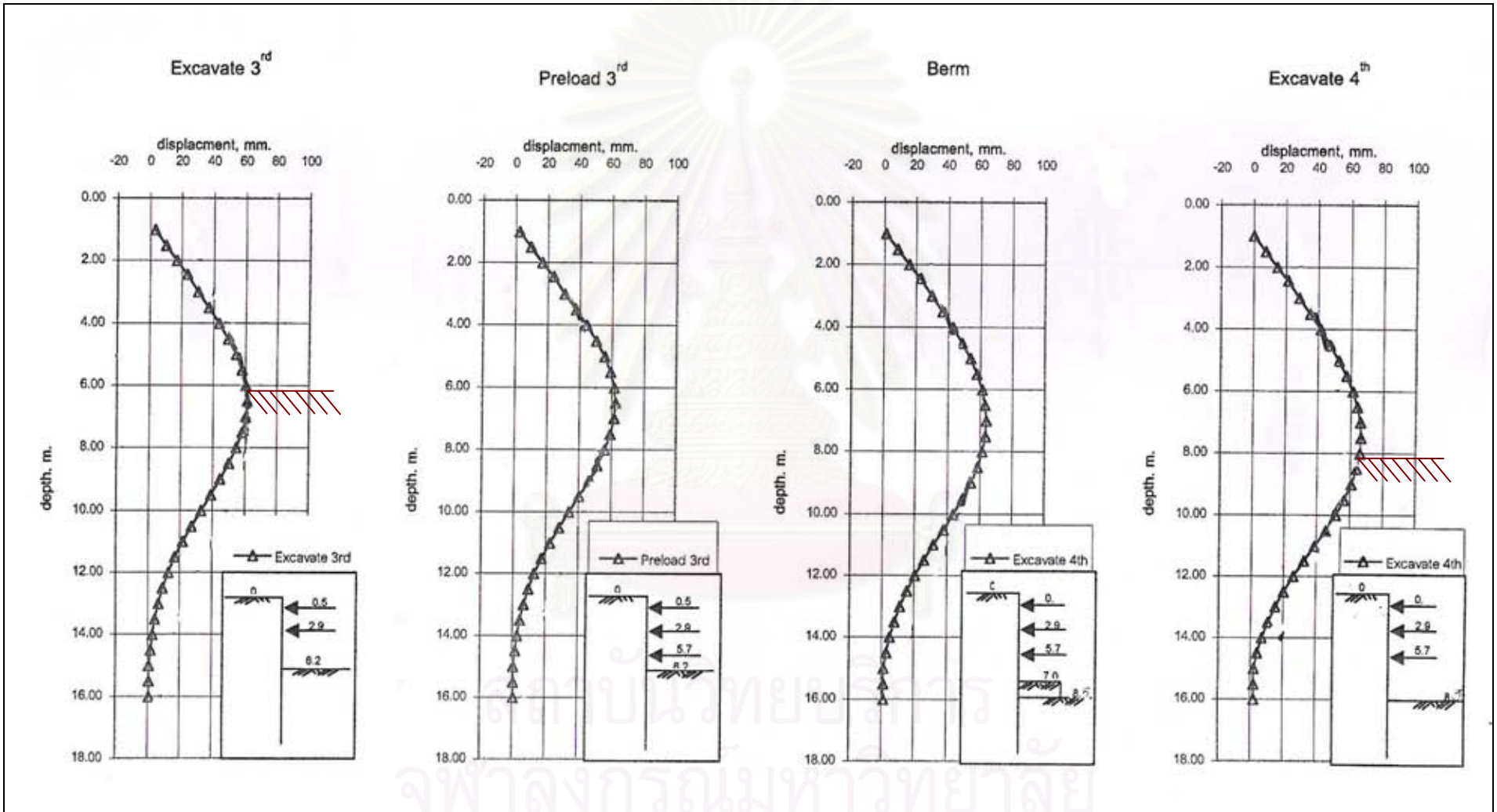
Figure 4.23 (con't) Depths at which maximum lateral wall movements occur, Saladang project

CHAPTER V

CONCLUSIONS AND RECOMMENDATIONS

5.1 Conclusions

The design and analysis of sheet pile braced excavation in Bangkok subsoils are, in general, based on the assumed values of soil stiffness or values of soil stiffness from laboratories. Those values lead to inaccurate predictions of the field behaviors of sheet piles.

Therefore, this research thesis, whose purpose is to look for the field soil stiffness, can contribute to more accurate designing and analysis. The back-analyzed soil stiffness, field behaviors of sheet piles and some influence charts can be concluded from this paper as follows:

1. The proposed values of soil stiffness E_u/S_u are:
   E_u/S_u = 100-150 for weathered crust
   E_u/S_u = 2000 for stiff to very stiff silty clays
   Owing to nonlinear stress-strain-strength behaviors of Bangkok soft clay, their values E_u/S_u vary with depths of excavation. E_u/S_u = 100-250 when excavation conducted below the depth of -6.0m. Excavations that are shallower than this depth, their values E_u/S_u are described in chapter IV (4.3.4).

2. Undrained Young's modulus is known to be dependent on the shear strain levels. The figure 5.1, which correlates soil stiffness at various strain levels for Bangkok soft clay, is proposed by the author.

3. The relation between deflection ratio and factor of safety against basal heave by Mana and Clough is reset the boundaries to adapt to sheet pile behaviors in Bangkok subsoils (Figure 4.19).

4. The mode of the first stage of excavation is observed to be cantilevered and at this stage, no sheet pile wall translation exists. But the later stages of excavation, sheet pile walls shift from cantilevered mode to cantilevered and bulging mode, and sheet pile wall translation does exist.

5. The maximum lateral wall movements occur around the depths at which excavations are undertaken.

6. The ratios of maximum lateral wall movements to the final depth of excavation $\dfrac{\delta_{H\max}}{H_f}$ for all stages of excavations range from 0.4% to 0.8%.

7. 50% to 70% of lateral sheet pile wall movements were observed in the first stage of construction (Excavation to level -1.40m) before reaching the final depth of excavation.
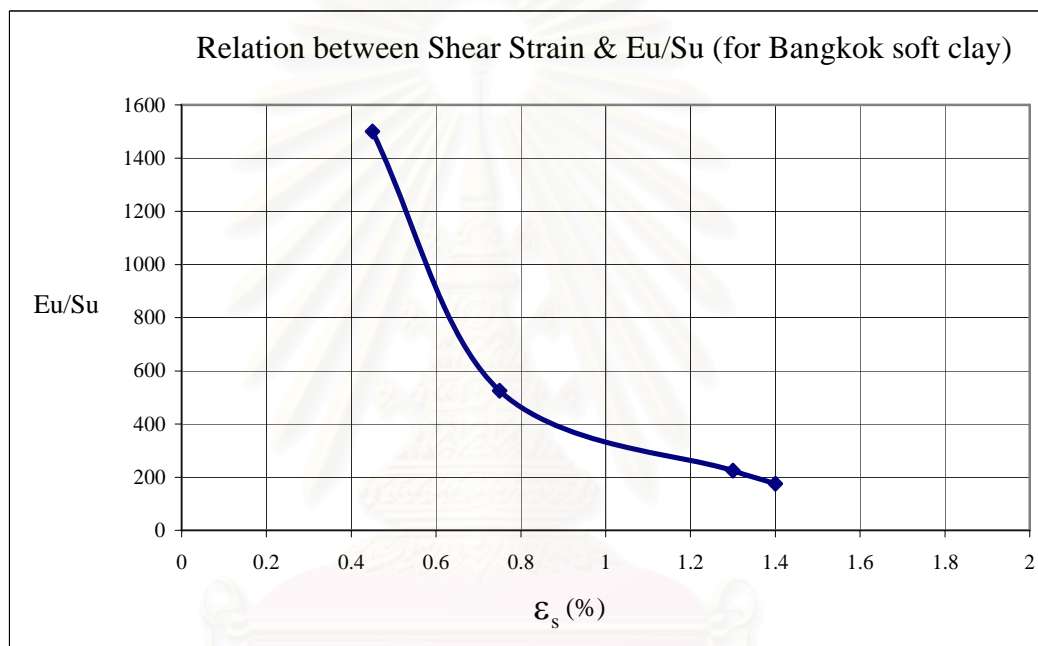
Figure 5.1 Relation between Shear Strain & Eu/Su (for Bangkok soft clay)

5.2 Recommendations:

1. The effects of sheet pile wall penetration depth, wall stiffness, and bored piles on lateral wall movements should be further researched.

2. More geotechnical instrumentations in sheet pile braced excavation such as settlements points, pressure gauges, should be further analyzed to understand more field behaviors.

REFERENCES

Akewanlop, K. (1996). Analysis of Ground Movement Data Associated with Braced Excavation in Bangkok Clay. Master's Thesis, AIT, Bangkok.

Balasubramaniann, A.S., Bergado, D.T., Chai, J.C., and Sutabutr, T. (1994). Deformation Analysis of Deep Excavations in Bangkok Subsoils, XIII ICSMFE, New Delhi, India.

Bjerrum, I. and Eide, O. (1956), Stability of Strutted Excavations in Clay. Geotechnique, Vol. 6.

Bowles, J.E. (1997), Foundation Analysis and Design. Fifth Edition. New York: McGraw-Hill.

Brinkgreve, R.B.J., and Vermeer, P.A. (2001). Reference Manual and Material Models Manual of PLAXIS. Version 7.2. A.A.BALKEMA / ROTTERDAM / BROOKFIELD.

Brooker, E.W. and Ireland, H.O. (1965). Earth Pressure at Rest Related to Stress History. Canadian Geotechnical Journal, Vol. 2.

Chaiseri, A. and Parkinson (1989). Design and Performance Monitoring of a Diaphragm Wall for 6-Level Excavation in Bangkok. EIT Annual Meeting, Theme: New Technology in Engineering.

Chang, M.F. (2000). Basal Stability Analysis of Braced Cuts in Clay. J. of Geotechnical and Geoenvironmental Engineering. ASCE, Vol. 126.

Clough, G.W. and Hansen, L.A. (1981). Clay Anisotrophy and Braced Wall Behavior. ASCE, Vol. 107.

Clough, G.W. and Reed, M. W.. Measured Behavior of Braced Wall in Very Soft Clay. ASCE, Vol. 110.

Clough, G.W. and Gordon, M.D. (1977). Stabilization Berm Design for Temporarily Wall in Clay. J. of Soil Mechanics and Foundation Engineering Division, ASCE, Vol. 103.

Das, B.M. (2004). Principles of Geotechnical Engineering: Fifth Edition: BROOKS/COLE.

Das, B.M. (2004). Foundation Engineering. Fifth Edition: BROOKS/COLE.

Finno, R.J. and Nerby, S.V. (1989). Saturated Clay Response During Braced Cut Construction. ASCE, Vol. 115.

German Society for Geotechnics (2003). Recommendations on Excavations. Ernst and Sohn.

Golberg, D.T. et al (1976). Lateral Support Systems and Underpinning, Design Fundamentals of Federal Highway Administration.

Geotechnical Aspects of Underground Construction in Soft Ground (1999). Proc. of the International Symposium on Geotechnical Aspects of Underground Construction in Soft Ground. Tokyo, Japan.

Hock, G.C., (1997). Review and Analysis of Ground Movements of Braced Excavation in Bangkok Subsoil Using Diaphragm Walls. Master's Thesis, AIT, Bangkok.

Holmberg, S. (1997). Some Engineering Properties of Soft Bangkok Clay. J. of South East Asian Geotechnical Society, Vol. 8.

Moh, Z. C. and Chung, T.C (1994). International Symposia on Underground Construction in Soft Ground. New Delhi, India.

NAVFAC DM-7.2 (1982). Foundations and Earth Structures. Department of the Nawy.

O'Rourke, T. (1981). The Ground Movements Caused by Braced Excavation. J. of Geotechnical Engineering, Vol. 34.

Peck, R.B. (1974). Foundation Engineering. Second Edition. New York: JOHN WILEY and SONS.

Phien-wej, N. (1991). Soil Movements in Braced Sheet Pile Excavation in Bangkok Clay. First Young Asian Geotechnical Engineering Conference, 1991, Bangkok, Thailand.

Pott, D.M. and Fourie, A.B. (1984). The Behavior of a Propped Retaining Wall: Results of a Numerical Experiment. Geotechnique, Vol. 34.

Puller, M. (1996). Deep Excavation. First Edition: Thomas Telford.

Salvi, G. (1991). Diaphragm Wall, Seminar on Foundation and Underground Construction. Bangkok, Thailand.

Sambandharaksa, S. (1989). The Use of In-Situ Test for Foundation Design in Bangkok Clay. Proc. of the 12th International Conference on Soil Mechanics and Foundation Engineering, Vol.3.

Satabutr, T. (1992). Deformation Analysis of Deep Excavation in Bangkok Subsoils. Master's Thesis, AIT, Bangkok.

Sirimas, V. (1998). Behaviors of Sheet Pile Deflection in Braced Excavation in Soft Bangkok Clay. Master's Thesis, Chulalongkorn University.

Smoltczyk, U.. Geotechnical Engineering Handbook (2003). Vol. 3: Elements and Structures, Ernst and Sohn.

Som, N.N. (1991). Performance Study of Braced Cut for Calcutta Metro Construction. Proc. of the 9th Asian Regional Conference on Soil Mechanics and Foundation Engineering, Vol. 2. Bangkok, Thailand.

Srichaimongkol, W. (1991). Performance of Supported and Unsupported Excavations in Bangkok Subsoils. Master's Thesis, AIT, Bangkok.

Teng, W.C (1981). Foundation Design. Eight Edition: Prentice Hall of India.

Tanseng, P. (1997). Instrumented Deep Excavations in Bangkok Subsoils. Master's Thesis, AIT, Bangkok.

Teparaksa, W. (1993). Behavior of Deep Excavation Using Sheet Pile Bracing System in Soft Bangkok Clay. Proc. of Third International Conference on Case Histories in Geotechnical Engineering. St. Louis, Missouri, Paper No. 5.21.

Teparaksa, W. (1994). Movement and Its Influence Zone of Flexible Sheet Pile Wall for Deep Basement Excavation in Soft Bangkok Clay. Conf. on Deep Foundations and Ground Improvement Schemes. 21-24 Nov., Bangkok, Thailand.

Teparaksa, W. (1999). Analysis of Lateral Wall Movements for Deep Excavation of Bangkok Subsoils. Civil and Environmental Conf. New Frontiers & Challenges. 8-12 Nov., 1999, Bangkok, Thailand.

Terzaghi, K. (1943). Theoretical Soil Mechanics. New York: JOHN WILEY and SONS.

Terzaghi, K. and Peck, R.B. (1969). Soil Mechanics in Engineering Practice. 2nd Edition: JOHN WILEY & SONS.

Vazari, H.H. and Troughton, V.M. (1992). An Efficient Three-Dimensional Soil-Structure Interaction Model for Analysis of Earth Retaining Structure. Canadian Geotechnical Journal, Vol. 29.

Wong, K.S. and Broms, B.B. (1989). Lateral Wall Deflections of Braced Excavations in Clay. ASCE, Vol.115.

Keith F. F. and Thomas G W. (1997). Wood Engineering and Construction. Third Edition: Prentice Hall,

APPENDICES

Inclinometer data

Lateral wall movements of inclinometer No 01			
Depth (m)	Excav to -1.40m and install strut 01	Preload of strut 01	Excav to -3.70m and install strut 02
0.1	35.1	35.1	43.3
-0.4	31	31.4	41
-0.9	27	27.6	38.9
-1.4	23.1	23.9	37.1
-1.9	19.4	20.3	36
-2.4	16	17.2	35.1
-2.9	13.1	14.3	34.7
-3.4	10.5	11.7	33.9
-3.9	8.4	9.8	32.8
-4.4	6.8	8.2	31.1
-4.9	5.5	7	28.7
-5.4	4.6	6.2	26
-5.9	3.8	5.3	23.6
-6.4	3.3	4.6	20.5
-6.9	2.8	3.9	17.4
-7.4	2.4	3.5	14.4
-7.9	2	3	11.8
-8.4	1.5	2.4	9.5
-8.9	1.1	2.1	8.3
-9.4	0.7	1.5	6.4
-9.9	0.4	0.9	4.7
-10.4	0.1	1.1	3.9
-10.9	0.2	0.6	2.2
-11.4	0.2	0.2	1
-11.9	0.1	0.1	0.7
-12.4	0	0	0.7
-12.9	0	0	0.6
-13.4	0.1	0.1	0.3
-13.9	0	0	0
-14.4	0	0	0

Inclinometer data

Lateral wall movements of inclinometer No 01			
Depth (m)	Preload of strut 02	Excav to -5.70m and install strut 03	Preload of strut 03
0.1	44.5	58.4	54.9
-0.4	41.8	55.3	51.6
-0.9	39.2	52.3	49.2
-1.4	36.9	49.6	47.3
-1.9	35	47.5	46
-2.4	33.4	46	45.4
-2.9	32.3	45.6	44.9
-3.4	31.3	45.8	45.7
-3.9	30.6	47.3	47
-4.4	29.7	49	48.3
-4.9	28.2	50.2	48.7
-5.4	26.5	50.7	48.6
-5.9	24.9	50.7	46.9
-6.4	22.4	48.9	44.3
-6.9	19.4	45.7	40.7
-7.4	16.5	41.6	36.6
-7.9	13.6	36.8	31.8
-8.4	11	31.9	27.1
-8.9	9.4	28	21.8
-9.4	7.3	23.6	17.8
-9.9	5.2	19.5	14.3
-10.4	4.2	16.5	12.1
-10.9	2.3	12.9	9.6
-11.4	1	10.2	7.3
-11.9	0.7	8.6	5.2
-12.4	0.7	6.7	3.9
-12.9	0.6	5	2.7
-13.4	0.3	3.2	1.8
-13.9	0	1.5	0.9
-14.4	0	0	0

Inclinometer data

Lateral wall movements of inclinometer No 01				
Depth(m)	Final depth of excavation (-6.90m)	Remove strut 03	Remove strut 02	Remove strut 01
0.1	53.5	53.8	53.3	54.4
-0.4	50	50.1	50.2	51.6
-0.9	47.6	47.5	48.2	49.6
-1.4	45.6	45.4	46.9	48.2
-1.9	44.3	44.2	46.3	47.9
-2.4	43.5	43.6	46.2	47.8
-2.9	43.2	43.5	46.3	47.6
-3.4	44.3	45.2	47.2	48.2
-3.9	45.6	47.4	49.1	49.8
-4.4	47.1	49.9	51.4	51.9
-4.9	48	51.8	53.1	53.4
-5.4	48.7	52.7	54	54
-5.9	48	52	53.2	52.9
-6.4	46.3	50.2	51.5	50.9
-6.9	43.5	47.4	48.8	48.1
-7.4	40	44	44.9	44.5
-7.9	35.6	39.7	40.1	40.2
-8.4	31.2	35.1	35.6	35.6
-8.9	25.8	29.6	30	30
-9.4	21.3	24.8	25.4	25.4
-9.9	17	20.2	20.7	20.9
-10.4	14.2	16.8	17.4	17.6
-10.9	11.2	13.2	13.7	14.1
-11.4	8.4	9.7	10.3	10.7
-11.9	5.8	7	7.6	7.9
-12.4	4.4	5.2	5.5	5.6
-12.9	3	3.4	3.5	3.8
-13.4	1.9	2.1	2.4	2.1
-13.9	0.9	1.1	1.2	1
-14.4	0	0	0	0

Inclinometer data

Lateral wall movements of inclinometer No 02			
Depth(m)	Excav to -1.40m and install strut 01	Preload strut 01	Excav to -3.70m and install strut 02
0.2	28.2	27.8	53.3
-0.3	24	23.1	50.6
-0.8	21.4	20.3	49.8
-1.3	18.8	17.9	49.4
-1.8	16.5	16.1	50
-2.3	14.1	14.5	50.8
-2.8	12.2	13.2	51.7
-3.3	10.4	12	51.9
-3.8	8.9	11	51.9
-4.3	7.7	10.1	51.7
-4.8	6.7	9.1	50.9
-5.3	6	8.7	48.9
-5.8	5.4	7.8	45.5
-6.3	4.8	6.8	41.7
-6.8	4.2	6.1	37.2
-7.3	3.8	5.3	32.8
-7.8	3.3	4.4	28.2
-8.3	2.7	3.7	24
-8.8	2.3	3.1	19.9
-9.3	2	2.6	16.6
-9.8	1.6	2.2	13.1
-10.3	1.3	1.8	10.3
-10.8	1.1	1.4	7.9
-11.3	0.9	1.1	5.7
-11.8	0.7	0.7	4.3
-12.3	0.5	0.5	3.4
-12.8	0.3	0.2	2.6
-13.3	0.1	0.1	1.9
-13.8	0.1	0	1
-14.3	0	0	0

Inclinometer data

Lateral wall movements of inclinometer No 02			
Depth(m)	Preload strut 02	Excav to -5.70m and install strut 03	Preload strut 03
0.2	40.2	49.3	52.9
-0.3	36	45.2	48.5
-0.8	33.8	43	46.1
-1.3	32.5	41.6	44.3
-1.8	31.9	41.1	43.6
-2.3	31.9	41	43.5
-2.8	32.2	41.4	43.4
-3.3	32.4	41.6	43.8
-3.8	32.8	41.9	45.1
-4.3	33.4	42.5	47.2
-4.8	33.6	42.8	49.4
-5.3	33.2	43.2	51.2
-5.8	32.1	43.2	52.2
-6.3	30.4	42.7	53
-6.8	27.7	41.2	52.4
-7.3	24.6	39.3	50.3
-7.8	21	36.5	46.7
-8.3	17.4	32.5	41.9
-8.8	14	27.2	36.4
-9.3	11.1	21.8	31
-9.8	8.6	16.9	25.4
-10.3	6.3	12.4	19.8
-10.8	4.4	8.8	14.8
-11.3	3	6.2	10.8
-11.8	2.2	4	6.8
-12.3	1.7	2.8	4.3
-12.8	1.1	1.8	2.3
-13.3	0.6	1	1.1
-13.8	0.3	0.4	0.5
-14.3	0	0	0

Inclinometer data

Lateral wall movements of inclinometer No 02				
Depth(m)	Final depth of excavation (-6.90m)	Remove strut 03	Remove strut 02	Remove strut 01
0.2	51.2	52.9	50.9	54.2
-0.3	46.3	48.1	46.8	50.9
-0.8	43.7	45.5	45	49.3
-1.3	41.9	43.7	43.9	47.8
-1.8	41.2	43.1	44.2	47.5
-2.3	41.2	43.4	45.1	47.8
-2.8	41.3	43.9	46	48.2
-3.3	41.8	45.3	47.1	48.7
-3.8	43.1	47.9	49.1	50.1
-4.3	45.3	51.5	52.5	52.9
-4.8	47.8	55.1	56	55.8
-5.3	50.3	58	58.3	58.1
-5.8	52.3	59.4	59.9	59.3
-6.3	54.1	60.4	61	60
-6.8	54.5	60.1	60.6	59.5
-7.3	53.2	58.2	58.9	57.4
-7.8	50.2	54.8	54.8	53.9
-8.3	45.5	50	50.2	48.9
-8.8	40	44.3	44.7	43.1
-9.3	34.5	38.5	39.1	37.2
-9.8	28.6	32.2	32.7	31
-10.3	22.5	25.8	26.2	24.7
-10.8	17	19.7	20	18.8
-11.3	12.5	14.6	14.9	13.9
-11.8	7.7	9.5	9.7	9
-12.3	4.7	6.1	6.2	5.8
-12.8	2.3	3.4	3.6	3.2
-13.3	0.8	1.6	1.4	1.5
-13.8	0.2	0.6	-0.1	0.5
-14.3	0	0	0	0

Inclinometer data

Lateral wall movements of inclinometer No 01 after preloading of strut 03 (18/12/04)			
Depth (m)	6/1/2005	17/1/2005	26/1/2005
0.1	53.1	54	53.6
-0.4	49.8	50.9	50.3
-0.9	47.5	48.6	47.9
-1.4	45.6	46.7	46
-1.9	44.4	45.5	44.8
-2.4	43.8	44.9	44.2
-2.9	43.4	44.5	43.8
-3.4	44.3	45.3	44.7
-3.9	45.7	46.6	46.1
-4.4	47	47.9	47.5
-4.9	47.6	48.4	48.1
-5.4	47.6	48.4	48.3
-5.9	46	46.9	47.1
-6.4	43.4	44.5	44.9
-6.9	39.9	41.1	41.8
-7.4	35.8	37.1	37.9
-7.9	31.1	32.5	33.4
-8.4	26.4	27.9	28.9
-8.9	21.2	22.6	23.5
-9.4	17.2	18.4	19.3
-9.9	13.6	14.7	15.4
-10.4	11.5	12.2	12.9
-10.9	9	9.5	10.1
-11.4	6.8	7.1	7.5
-11.9	4.8	5.1	5.4
-12.4	3.5	3.8	4.2
-12.9	2.4	2.5	2.8
-13.4	1.5	1.6	1.8
-13.9	0.8	0.8	0.9
-14.4	0	0	0

Inclinometer data

Lateral wall movements of inclinometer No 01 after preloading of strut 03 (18/12/04)				
Depth (m)	7/2/2005	17/2/2005	28/2/2005	11/3/2005
0.1	53.4	52.8	53.1	53.6
-0.4	50	49.4	49.8	50.1
-0.9	47.5	47	47.5	47.6
-1.4	45.6	45.1	45.7	45.6
-1.9	44.4	44	44.6	44.3
-2.4	43.8	43.5	44	43.6
-2.9	43.5	43.2	43.7	43.1
-3.4	44.4	44.2	44.7	44
-3.9	45.9	45.6	46.1	45.4
-4.4	47.3	47	47.4	46.8
-4.9	48	47.7	48.1	47.5
-5.4	48.4	48.1	48.6	48.1
-5.9	47.3	47.1	47.6	47.5
-6.4	45.3	45.1	45.7	45.9
-6.9	42.4	42.2	42.8	43.3
-7.4	38.7	38.6	39.2	39.9
-7.9	34.3	34.2	34.8	35.6
-8.4	29.8	29.7	30.2	31.1
-8.9	24.5	24.4	24.9	25.6
-9.4	20.2	20.2	20.6	21.1
-9.9	16.1	16.2	16.5	16.9
-10.4	13.4	13.5	13.8	14
-10.9	10.5	10.6	10.8	10.9
-11.4	7.9	7.8	7.9	8
-11.9	5.7	5.6	5.6	5.6
-12.4	4.3	4	4.2	4.1
-12.9	2.9	2.6	2.8	2.7
-13.4	1.8	1.6	1.7	1.6
-13.9	0.9	0.8	0.9	0.7
-14.4	0	0	0	0

Inclinometer data

Lateral wall movements of inclinometer No 02 after preloading of strut 03 (23/12/04)			
Depth (m)	6/1/2005	17/1/2005	28/1/2005
0.2	51.5	51.9	51.6
-0.3	47.1	47.7	47.3
-0.8	44.8	45.4	45.1
-1.3	43	43.7	43.4
-1.8	42.4	43.2	42.8
-2.3	42.3	43.1	42.7
-2.8	42.3	43.1	42.8
-3.3	42.7	43.5	43.2
-3.8	44	44.9	44.5
-4.3	46.2	47	46.6
-4.8	48.4	49.3	48.9
-5.3	50.3	51.2	50.9
-5.8	51.4	52.4	52.2
-6.3	52.2	53.3	53.3
-6.8	51.6	52.9	53.1
-7.3	49.6	50.9	51.3
-7.8	46.1	47.5	48
-8.3	41.3	42.7	43.2
-8.8	35.8	37.2	37.7
-9.3	30.5	31.8	32.3
-9.8	25	26.1	26.5
-10.3	19.4	20.4	20.8
-10.8	14.5	15.2	15.5
-11.3	10.5	11	11.3
-11.8	6.5	6.9	7.1
-12.3	4.1	4.3	4.5
-12.8	2.2	2.3	2.4
-13.3	0.9	1	1
-13.8	0.4	0.4	0.4
-14.3	0	0	0

Inclinometer data

Lateral wall movements of inclinometer No 02 after preloading of strut 03 (23/12/04)				
Depth (m)	10/2/2005	21/2/2005	3/3/2005	14/3/2005
0.2	50.6	51.4	50.4	50.4
-0.3	46.2	47	46	46
-0.8	43.9	44.6	43.6	43.8
-1.3	42.1	42.8	41.8	42.1
-1.8	41.5	42.2	41.1	41.5
-2.3	41.5	42.1	41.1	41.4
-2.8	41.5	42	41.2	41.5
-3.3	42	42.5	41.6	42
-3.8	43.3	43.8	43	43.3
-4.3	45.6	46	45.3	45.5
-4.8	48	48.4	47.8	47.9
-5.3	50.2	50.6	50.2	50.2
-5.8	51.8	52.2	51.9	52
-6.3	53.2	53.7	53.5	53.8
-6.8	53.2	53.7	53.7	54.2
-7.3	51.6	52.1	52.2	53
-7.8	48.4	49	49.1	50.1
-8.3	43.8	44.3	44.5	45.7
-8.8	38.3	38.8	38.9	40.4
-9.3	32.9	33.4	33.4	34.9
-9.8	27.1	27.6	27.5	29
-10.3	21.3	21.9	21.6	23
-10.8	16	16.4	16	17.4
-11.3	11.6	12	11.6	12.7
-11.8	7.3	7.6	7.1	8
-12.3	4.6	4.7	4.4	5
-12.8	2.4	2.5	2.3	2.6
-13.3	1.1	1.2	0.9	1.3
-13.8	0.4	0.5	0.3	0.4
-14.3	0	0	0	0

BIOGRAPHY

Vuthy Horng was born in Saang District, Kandal Province, Cambodia on March 13, 1980. He got his Bachelor's Degree, in 2003, from Division of Geotechnical Engineering and Geology, Institute of Technology of Cambodia. In April, 2004, he got scholarship from AUN/SEED-Net-JICA to pursue his Master's Degree at Chulalongkorn University, Bangkok City, Thailand. His field of study is Geotechnical Engineering.